

1  
2  
3  
4  
5  
6  
7  
8  
9  
10  
11  
12  
13  
14  
15  
16  
17  
18  
19  
20  
21  
22  
23  
24  
25  
26  
27  
28  
29  
30

# **Global Sea Level Budget 1993-Present**

WCRP Global Sea Level Budget Group\*

\*A full list of authors and their affiliations appears at the end of the paper

**Revised version**  
**23 July 2018**

Corresponding author: Anny Cazenave, LEGOS, 18 Avenue Edouard Belin, 31401 Toulouse,  
Cedex 9, France; anny.cazenave@legos.obs-mip.fr

31 **Abstract**

32

33 Global mean sea level is an integral of changes occurring in the climate system in response to  
34 unforced climate variability as well as natural and anthropogenic forcing factors. Its temporal  
35 evolution allows detecting changes (e.g., acceleration) in one or more components. Study of  
36 the sea level budget provides constraints on missing or poorly known contributions, such as  
37 the unsurveyed deep ocean or the still uncertain land water component. In the context of the  
38 World Climate Research Programme Grand Challenge entitled “Regional Sea Level and  
39 Coastal Impacts”, an international effort involving the sea level community worldwide has  
40 been recently initiated with the objective of assessing the various data sets used to estimate  
41 components of the sea level budget during the altimetry era (1993 to present). These data sets  
42 are based on the combination of a broad range of space-based and in situ observations, model  
43 estimates and algorithms. Evaluating their quality, quantifying uncertainties and identifying  
44 sources of discrepancies between component estimates is extremely useful for various  
45 applications in climate research. This effort involves several tens of scientists from about fifty  
46 research teams/institutions worldwide ([www.wcrp-climate.org/grand-challenges/gc-sea-](http://www.wcrp-climate.org/grand-challenges/gc-sea-level)  
47 [level](http://www.wcrp-climate.org/grand-challenges/gc-sea-level)). The results presented in this paper are a synthesis of the first assessment performed  
48 during 2017-2018. We present estimates of the altimetry-based global mean sea level (average  
49 rate of  $3.1 \pm 0.3$  mm/yr and acceleration of  $0.1$  mm/yr<sup>2</sup> over 1993-present), as well as of the  
50 different components of the sea level budget (<http://doi.org/10.17882/54854>). We further  
51 examine closure of the sea level budget, comparing the observed global mean sea level with  
52 the sum of components. Ocean thermal expansion, glaciers, Greenland and Antarctica  
53 contribute by 42%, 21%, 15% and 8% to the global mean sea level over the 1993-present. We  
54 also study the sea level budget over 2005-present, using GRACE-based ocean mass estimates  
55 instead of sum of individual mass components. Our results demonstrate that the global mean  
56 sea level can be closed to within 0.3 mm/yr (one sigma). Substantial uncertainty remains for  
57 the land water storage component, as shown in examining individual mass contributions to  
58 sea level.

59

60

61

62

63

64

65

## 66 **1. Introduction**

67  
68 Global warming has already several visible consequences, in particular increase of the Earth's  
69 mean surface temperature and ocean heat content (Rhein et al., 2013, Stocker et al., 2013),  
70 melting of sea ice, loss of mass of glaciers (Gardner et al., 2013), and ice mass loss from the  
71 Greenland and Antarctica ice sheets (Rignot et al., 2011, Shepherd et al., 2012). On average  
72 over the last 50 years, about 93% of heat excess accumulated in the climate system because of  
73 greenhouse gas emissions has been stored in the ocean, and the remaining 7% has been  
74 warming the atmosphere and continents, and melting sea and land ice (von Schuckmann et al.,  
75 2016). Because of ocean warming and land ice mass loss, sea level rises. Since the end of the  
76 last deglaciation about 3000 years ago, sea level remained nearly constant (e.g., Lambeck et  
77 al., 2010, Kemp et al., 2011, Kopp et al. 2014). However, direct observations from in situ tide  
78 gauges available since the mid-to-late 19<sup>th</sup> century show that the 20<sup>th</sup> century global mean sea  
79 level has started to rise again at a rate of 1.2 mm/yr to 1.9 mm/yr (Church and White, 2011,  
80 Jevrejeva et al., 2014a, Hay et al., 2015, Dangendorf et al., 2017). Since the early 1990s sea  
81 level rise is measured by high-precision altimeter satellites and the rate has increased to ~3  
82 mm/yr on average (Legeais et al., 2018, Nerem et al., 2018).

83 Accurate assessment of present-day global mean sea level variations and its components  
84 (ocean thermal expansion, ice sheet mass loss, glaciers mass change, changes in land water  
85 storage, etc.) is important for many reasons. The global mean sea level is an integral of  
86 changes occurring in the Earth's climate system in response to unforced climate variability as  
87 well as natural and anthropogenic forcing factors e.g., net contribution of ocean warming,  
88 land ice mass loss, and changes in water storage in continental river basins. Temporal changes  
89 of the components are directly reflected in the global mean sea level curve. If accurate  
90 enough, study of the sea level budget provides constraints on missing or poorly known  
91 contributions, e.g., the deep ocean or polar regions under sampled by current observing  
92 systems, or still uncertain changes in water storage on land due to human activities (e.g.  
93 ground water depletion in aquifers). Global mean sea level corrected for ocean mass change in  
94 principle allows one to independently estimate temporal changes in total ocean heat content,  
95 from which the Earth's energy imbalance can be deduced (von Schuckmann et al., 2016). The  
96 sea level and/or ocean mass budget approach can also be used to constrain models of Glacial  
97 Isostatic Adjustment (GIA). The GIA phenomenon has significant impact on the  
98 interpretation of GRACE-based space gravimetry data over the oceans (for ocean mass  
99 change) and over Antarctica (for ice sheet mass balance). However, there is still incomplete

100 consensus on best estimates, a result of uncertainties in deglaciation models and mantle  
101 viscosity structure. Finally, observed changes of the global mean sea level and its components  
102 are fundamental for validating climate models used for projections.

103 In the context of the Grand Challenge entitled “Regional Sea Level and Coastal Impacts” of  
104 the World Climate Research Programme (WCRP), an international effort involving the sea  
105 level community worldwide has been recently initiated with the objective of assessing the sea  
106 level budget during the altimetry era (1993 to present). To estimate the different components  
107 of the sea level budget, different data sets are used. These are based on the combination of a  
108 broad range of space-based and in situ observations. Evaluating their quality, quantifying their  
109 uncertainties, and identifying the sources of discrepancies between component estimates,  
110 including the altimetry-based sea level time series, are extremely useful for various  
111 applications in climate research.

112 Several previous studies have addressed the sea level budget over different time spans and  
113 using different data sets. For example, Munk (2002) found that the 20<sup>th</sup> century sea-level rise  
114 could not be closed with the data available at that time and showed that if the missing  
115 contribution were due to polar ice melt, this would be in conflict with external astronomical  
116 constraints. The enigma has been resolved in two ways. Firstly, an improved theory of  
117 rotational stability of the Earth (Mitrovica et al., 2006) effectively removed the constraints  
118 proposed by Munk (2002), and allows a polar ice sheet contribution to 20<sup>th</sup> century sea-level  
119 rise of as much as ~1.1 mm/yr, with about 0.8 mm/yr beginning in the 20<sup>th</sup> century. In  
120 addition, more recent studies by Gregory et al. (2013) and Slangen et al. (2017), combining  
121 observations with model estimates, showed that it was possible to effectively close the 20<sup>th</sup>  
122 century sea level budget within uncertainties. For the altimetry era, many studies have  
123 investigated closure of the sea level budget (e.g., Cazenave et al., 2009, Leuliette and Willis,  
124 2010, Church and White, 2011, Chambers et al., 2017, Dieng et al., 2017, Chen et al., 2017,  
125 Nerem et al., 2018). Assessments of the published literature have also been performed in past  
126 IPCC (Intergovernmental Panel on Climate Change) reports (e.g., Church et al., 2013).  
127 Building on these previous works, here we intend to provide a collective update of the global  
128 mean sea level budget, involving the many groups worldwide interested in present-day sea  
129 level rise and its components. We focus on observations rather than model-based estimates  
130 and consider the high-precision altimetry era starting in 1993 that includes the period since  
131 the mid-2000s where new observing systems, like the Argo float project (Roemmich et al.,  
132 2012) and the GRACE space gravimetry mission (Tapley et al., 2004) that provide improved

133 data sets of high value for such a study. Only the global mean budget is considered here.  
 134 Regional budget will be the focus of a future assessment.

135 Section 2 describes for each component of the sea level budget equation the different data sets  
 136 used to estimate the corresponding contribution to sea level, discusses associated errors and  
 137 provides trend estimates for the two periods. Section 3 addresses the mass and sea level  
 138 budgets over the study periods. A discussion is provided in Section 4, followed by a  
 139 conclusion.

140

## 141 **2. Methods and Data**

142 In this section, we briefly present the global mean sea level budget (sub section 2.1), then  
 143 provide, for each term of the budget equation, an assessment of the most up-to-date published  
 144 results. Multiple organizations and research groups routinely generate the basic measurements  
 145 as well as the derived data sets and products used to study the sea level budget. Sub-sections  
 146 2.2 to 2.7 summarize the measurements and methodologies used to derive observed sea level,  
 147 as well as steric and mass components. In most cases, we focus on observations but in some  
 148 instances (e.g., for GIA corrections applied to the data), model-based estimates are the only  
 149 available information.

150

### 151 **2.1 Sea level budget equation**

152 Global mean sea level (GMSL) change as a function of time  $t$  is usually expressed by the sea  
 153 level budget equation:

$$154 \quad \text{GMSL}(t) = \text{GMSL}(t)_{\text{steric}} + \text{GMSL}(t)_{\text{ocean mass}} \quad (1)$$

155 where  $\text{GMSL}(t)_{\text{steric}}$  refers to the contributions of ocean thermal expansion and salinity to sea  
 156 level change, and  $\text{GMSL}(t)_{\text{oceanmass}}$  refers to the change in mass of the oceans. Due to water  
 157 conservation in the climate system, the ocean mass term (also noted as  $M(t)_{\text{ocean}}$ ) can further  
 158 be expressed as:

159

$$160 \quad \text{M}(t)_{\text{ocean}} + \text{M}(t)_{\text{glaciers}} + \text{M}(t)_{\text{Greenland}} + \text{M}(t)_{\text{Antarctica}} + \text{M}(t)_{\text{TWS}} + \text{M}(t)_{\text{WV}} + \text{M}(t)_{\text{Snow}} \\ 161 \quad + \text{uncertainty} = 0 \quad (2)$$

162

163 where  $M(t)_{\text{glaciers}}$ ,  $M(t)_{\text{Greenland}}$ ,  $M(t)_{\text{Antarctica}}$ ,  $M(t)_{\text{TWS}}$ ,  $M(t)_{\text{WV}}$ ,  $M(t)_{\text{Snow}}$  represent temporal  
 164 changes in mass of glaciers, Greenland and Antarctica ice sheets, terrestrial water storage  
 165 (TWS), atmospheric water vapor (WV), and snow mass changes. The uncertainty is a result of

166 uncertainties in all of the estimates and potentially missing mass terms, for example,  
 167 permafrost melting.

168

169 From equation (2), we deduce:

170

$$\begin{aligned}
 171 \quad \text{GMSL}(t)_{\text{ocean mass}} = & - [M(t)_{\text{glaciers}} + M(t)_{\text{Greenland}} + M(t)_{\text{Antarctica}} + M(t)_{\text{TWS}} + M(t)_{\text{WV}} + M(t)_{\text{Snow}} \\
 172 \quad & + \text{missing mass terms}] \quad (3)
 \end{aligned}$$

173

174 In the next subsections, we successively discuss the different terms of the budget (equations 1  
 175 and 2) and how they are estimated from observations. We do not consider the atmospheric  
 176 water vapor and snow components, assumed to be small. Two periods are considered: (1)  
 177 1993-present (i.e. the entire altimetry era), and (2) 2005-present (i.e. the period covered by  
 178 both Argo and GRACE).

179

## 180 **2.2 Altimetry-based global mean sea level over 1993-present**

181 The launch of the TOPEX/Poseidon (T/P) altimeter satellite in 1992 led to a new paradigm for  
 182 measuring sea level from space, providing for the first time precise and globally distributed  
 183 sea level measurements at 10-day intervals. At the time of the launch of T/P, the  
 184 measurements were not expected to have sufficient accuracy for measuring GMSL changes.  
 185 However, as the radial orbit error decreased from ~10 cm at launch to ~1 cm presently, and  
 186 other instrumental and geophysical corrections applied to altimetry system improved (e.g.,  
 187 Stammer and Cazenave, 2017), several groups regularly provided an altimetry-based GMSL  
 188 time series (e.g., Nerem et al. 2010, Church et al. 2011, Ablain et al., 2015, Legeais et al.,  
 189 2018). The initial T/P GMSL time series was extended with the launch of Jason-1 (2001),  
 190 Jason-2 (2008) and Jason-3 (2016). By design, each of these missions has an overlap period  
 191 with the previous one in order to inter-compare the sea level measurements and estimate  
 192 instrument biases (e.g., Nerem et al., 2010; Ablain et al., 2015). This has allowed the  
 193 construction of an uninterrupted GMSL time series that is currently 25-year long.

194

### 195 **2.2.1 Global mean sea level datasets**

196 Six groups (AVISO/CNES, SL\_cci/ESA, University of Colorado, CSIRO, NASA/GSFC,  
 197 NOAA) provide altimetry-based GMSL time series. All of them use 1-Hz altimetry  
 198 measurements derived from T/P, Jason-1, Jason-2 and Jason-3 as reference missions. These

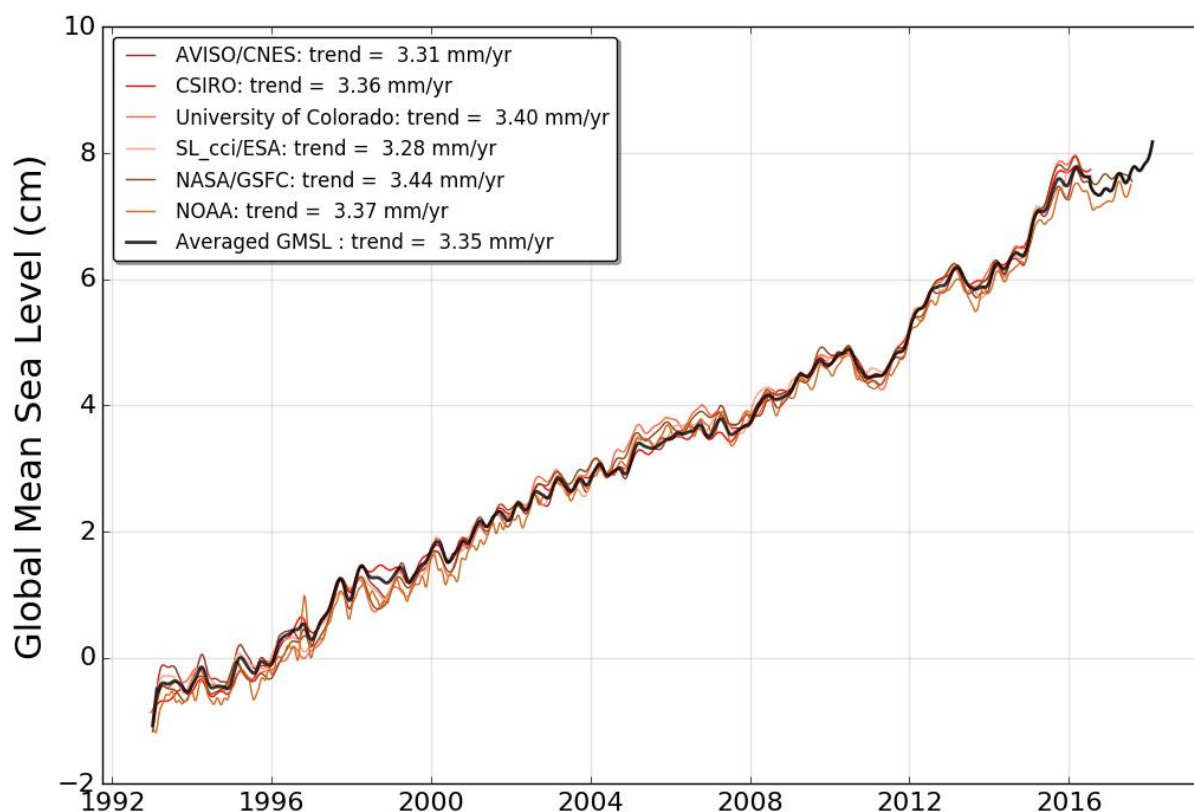
199 missions provide the most accurate long-term stability at global and regional scales (Ablain et  
200 al. 2009, 2017a), and are all on the same historical T/P ground track. This allows computation  
201 of a long-term record of the GMSL from 1993 to present. In addition, complementary  
202 missions (ERS-1, ERS-2, Envisat, Geosat Follow-on, CryoSat-2, SARAL/AltiKa and  
203 Sentinel-3A) provide increased spatial resolution and coverage of high latitude ocean areas,  
204 pole-ward of  $66^{\circ}$ N/S latitude (e.g. the European Space Agency/ESA Climate Change  
205 Initiative/CCI sea level data set; Legeais et al. 2018).

206 The above groups adopt different approaches when processing satellite altimetry data. The  
207 most important differences concern the geophysical corrections needed to account for various  
208 physical phenomena such as atmospheric propagation delays, sea state bias, ocean tides, and  
209 the ocean response to atmospheric wind and pressure forcing. Other differences come from  
210 data editing, methods to spatially average individual measurements during orbital cycles and  
211 link between successive missions (Masters et al. 2012; Henry et al. 2014).

212 Overall, the quality of the different GMSL time series is similar. Long-term trends agree well  
213 to within 6% of the signal, approximately 0.2 mm/yr (see Figure 1) within the GMSL trend  
214 uncertainty range ( $\sim 0.3$  mm/yr; see next section). The largest differences are observed at  
215 interannual time scales and during the first years (before 1999; see below). Here we use an  
216 ensemble mean GMSL based on averaging all individual GMSL time series.

217

218



219  
220

221 *Figure 1: Evolution of GMSL time series from 6 different groups (AVISO/CNES, SL\_cci/ESA,*  
 222 *University of Colorado, CSIRO, NASA/GSFC, NOAA) products. Annual signals are removed*  
 223 *and 6-month smoothing applied. All GMSL time series are centered in 1993 with zero mean.*  
 224 *A GIA correction of -0.3 mm/yr has been subtracted to each data set.*

### 225 **2.2.2 Global mean sea level uncertainties and TOPEX-A drift**

226 Based on an assessment of all sources or uncertainties affecting satellite altimetry (Ablain et  
 227 al. 2017), the GMSL trend uncertainty (90% confidence interval) is estimated as ~0.4 mm/yr  
 228 over the whole altimetry era (1993-2017). The main contribution to the uncertainty is the wet  
 229 tropospheric correction with a drift uncertainty in the range of 0.2-0.3 mm/yr (Legeais et al.  
 230 2018) over a 10-year period. To a lesser extent, the orbit error (Couhert et al. 2015; Escudier  
 231 et al., 2017) and the altimeter parameters' (range, sigma-0 and significant wave height/SWH)  
 232 instability (Ablain et al., 2012) also contribute to the GMSL trend uncertainty, at the level of  
 233 0.1 mm/yr. Furthermore, imperfect links between successive altimetry missions lead to  
 234 another trend uncertainty of about 0.15 mm/yr over the 1993-2017 period (Zawadzki and  
 235 Ablain, 2016).

236 Uncertainties are higher during the first decade (1993-2002) where T/P measurements display  
 237 larger errors at climatic scales. For instance, the orbit solutions are much more uncertain due



238 to gravity field solutions calculated without GRACE data. Furthermore, the switch from  
 239 TOPEX-A to TOPEX-B in February 1999 (with no overlap between the two instrumental  
 240 observations) leads to an error of  $\sim 3$  mm in the GMSL time series (Escudier et al., 2017).

241 However, the most significant error that affects the first 6 years (January-1993 to February  
 242 1999) of the T/P GMSL measurements is due to an instrumental drift of the TOPEX-A  
 243 altimeter, not included in the formal uncertainty estimates discussed above. This effect on the  
 244 GMSL time series was recently highlighted via comparisons with tide gauges (Valladeau et  
 245 al. 2012; Watson et al. 2015; Chen et al. 2017; Ablain et al. 2017), via a sea level budget  
 246 approach (i.e., comparison with the sum of mass and steric components; Dieng et al., 2017)  
 247 and by comparing with Poseidon-1 measurements (Zawadsky, personal communication). In a  
 248 recent study, Beckley et al. (2017) asserted that the corresponding error on the 1993-1998  
 249 GMSL resulted from incorrect onboard calibration parameters.

250 All three approaches conclude that during the period January 1993 to February 1999, the  
 251 altimetry-based GMSL was overestimated. TOPEX-A drift correction was estimated close to  
 252 1.5 mm/yr (in terms of sea level trend) with an uncertainty of  $\pm 0.5$  to  $\pm 1.0$  mm/yr (Watson et  
 253 al. 2015; Chen et al. 2017; Dieng et al. 2017). Beckley et al. (2017) proposed to not apply the  
 254 suspect onboard calibration correction on TOPEX-A measurements. The impact of this  
 255 approach is similar to the TOPEX-A drift correction estimated by Dieng et al. (2017) and  
 256 Ablain et al. (2017b). In the latter study, accurate comparison between TOPEX A-based  
 257 GMSL and tide gauge measurements leads to a drift correction to about -1.0 mm/yr between  
 258 January 1993 and July 1995, and +3.0 mm/yr between August 1995 and February 1999, with  
 259 an uncertainty of 1.0 mm/yr (with a 68% confidence level, see Table 1).

260

<b>TOPEX-A drift correction</b>	<b>to be subtracted from the first 6-years (Jan. 1993 to Feb. 1999) of the uncorrected GMSL record</b>
Watson et al. (2015)	1.5 +/- 0.5 mm/yr over Jan.1993/ Feb.1999
Chen et al. (2017); Dieng et al. (2017)	1.5 +/- 0.5 mm/yr over Jan.1993/ Feb.1999
Beckley et al. (2017)	No onboard calibration applied
Ablain et al. (2017b)	-1.0 +/- 1.0 mm/yr over Jan.1993/ Jul.1995

	+3.0 +/-1.0 mm/yr over Aug.1995- Feb.1999
--	---

261 *Table 1. TOPEX-A GMSL drift corrections proposed by different studies*

262

263 **2.2.3 Global Mean Sea Level variations**

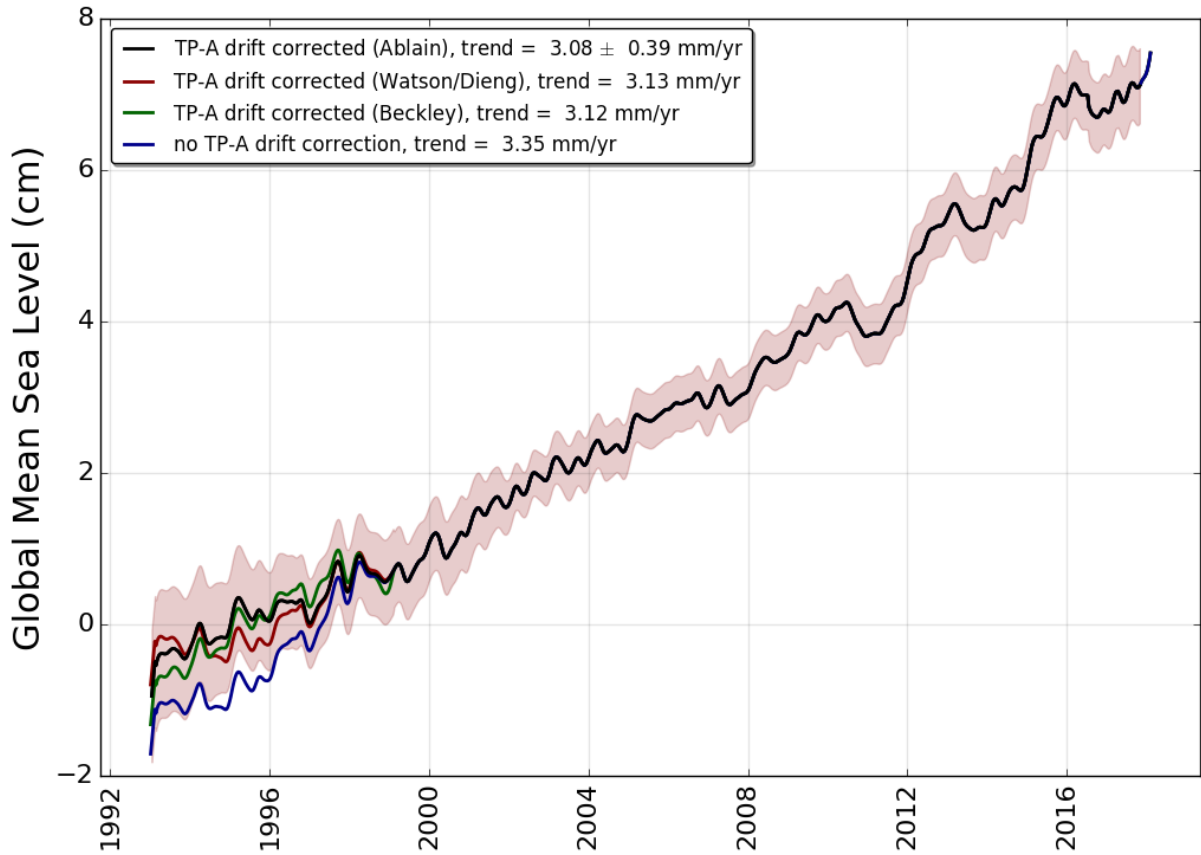
264

265 The ensemble mean GMSL rate after correcting for the TOPEX-A drift (for all of the  
 266 proposed corrections) amounts to 3.1 mm/yr over 1993-2017 (Figure 2). This corresponds to a  
 267 mean sea level rise of about 7.5 cm over the whole altimetry period. More importantly, the  
 268 GMSL curve shows a net acceleration, estimated at 0.08 mm/yr<sup>2</sup> (Chen et al. 2017; Dieng et  
 269 al. 2017) and 0.084 +/- 0.025 mm/yr<sup>2</sup> (Nerem et al., 2018) (Note Watson et al. found a smaller  
 270 acceleration after correcting for the instrumental bias over a shorter period up to the end of  
 271 2014.). GMSL trends calculated over 10-year moving windows illustrate this acceleration  
 272 (Figure 3). GMSL trends are close to 2.5 mm/yr over 1993-2002 and 3.0 mm/yr over 1996-  
 273 2005. After a slightly smaller trend over 2002-2011, the 2008-2017 trend reaches 4.2 mm/yr.  
 274 Uncertainties (90% confidence interval) associated to these 10-year trends regularly decrease  
 275 through time from 1.3 mm/yr over 1993-2002 (corresponding to T/P data) to 0.65 mm/yr for  
 276 2008-2017 (corresponding to Jason-2 and Jason-3 data).

277 Removing the trend from the GMSL time series highlights inter-annual variations (not  
 278 shown). Their magnitudes depend on the period (+3 mm in 1998-1999, -5 mm in 2011-2012,  
 279 and +10 mm in 2015-2016) and are well correlated in time with El Niño and La Niña events  
 280 (Nerem et al. 2010; Cazenave et al. 2014, Nerem et al., 2018). However, substantial  
 281 differences (of 1-3 mm) exist between the six de-trended GMSL time series. This issue needs  
 282 further investigation.

283

284



285

286

287 *Figure 2: Evolution of ensemble mean GMSL time series (average of the 6 GMSL products*  
 288 *from AVISO/CNES, SL\_cci/ESA, University of Colorado, CSIRO, NASA/GSFC, and NOAA).*

289 *On the black, red and green curves, the TOPEX-A drift correction is applied respectively*  
 290 *based on (Ablain et al, 2017b), (Watson et al. 2015; Dieng et al. 2017) and Beckley et al.,*  
 291 *2017). Annual signal removed and 6-month smoothing applied; GIA correction also applied.*

292 *Uncertainties (90% confidence interval) of correlated errors over a 1-year period are*  
 293 *superimposed for each individual measurement (shaded area).*

294

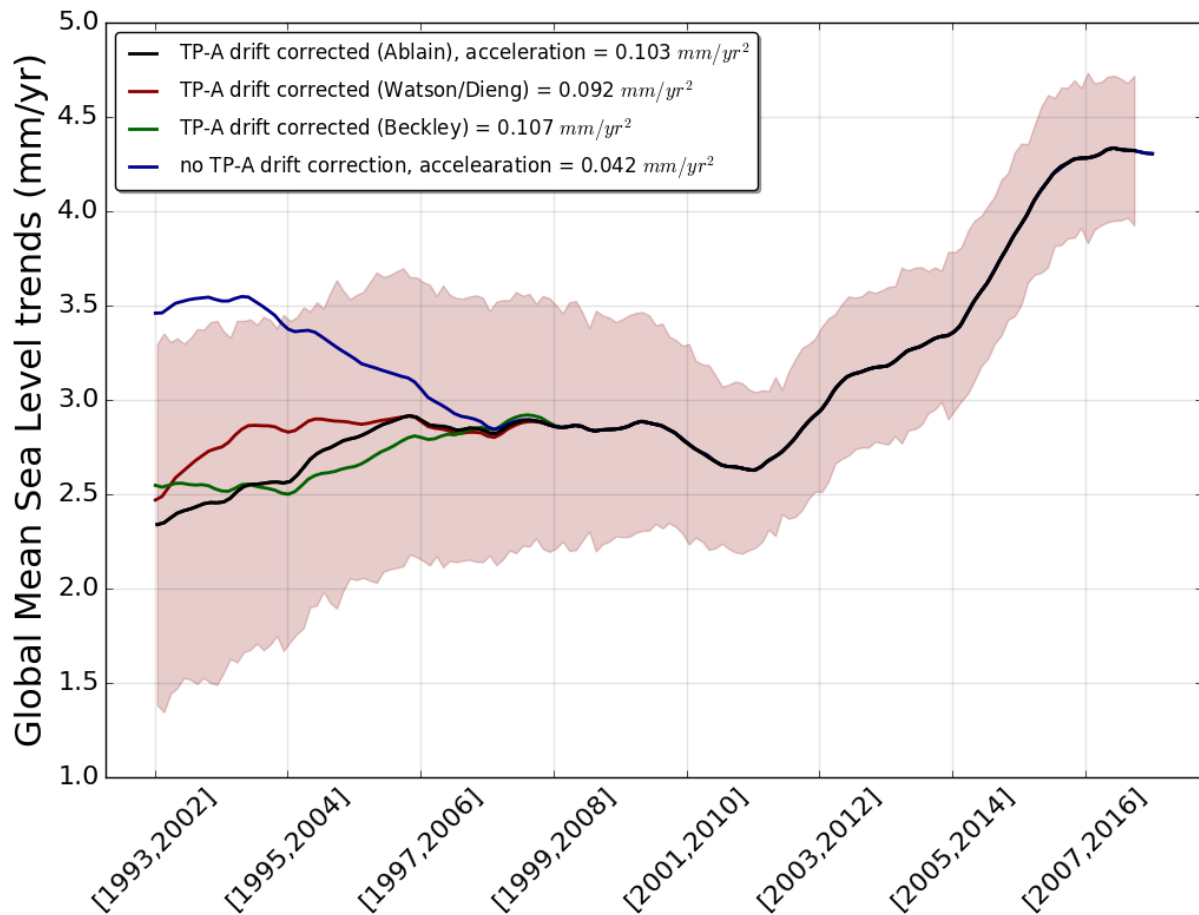
295

296

297

298

299



300

301

302 *Figure 3: Ensemble mean GMSL trends calculated over 10-year moving windows. On the*  
 303 *black, red and green curves, the TOPEX-A drift correction is applied respectively based on*  
 304 *(Ablain et al, 2017b), and Beckley et al., 2017). Uncorrected GMSL trends are shown by the*  
 305 *blue curve. The shaded area represents trend uncertainty over 10-year periods (90%*  
 306 *confidence interval).*

307

308 For the sea level budget assessment (section 3), we will use the ensemble mean GMSL time  
 309 series corrected for the TOPEX A drift using the Ablain et al. (2017b) correction.

310

### 311 **2.2.4. Comparison with tide gauges**

312

313 Prior to 1992 global sea level rise estimates rely on the tide gauge measurements, and it is  
 314 worth mentioning past attempts to produce global sea level reconstructions utilizing these  
 315 measurements (e.g. Gornitz et al. 1982; Barnett 1984; Douglas 1991, 1997, 2001). Here we  
 316 focus on global sea level reconstructions that overlap with satellite altimetry data over a  
 317 substantial common time span. Some of these reconstructions rely on tide gauge data only

318 (Jevrejeva et al. 2006, 2014; Merrifield et al. 2009; Wenzel and Schroter 2010; Ray and  
319 Douglas 2011; Hamlington et al. 2011, Spada and Galassi 2012; Thompson and Merrifield  
320 2014; Dangendorf et al. 2017; Frederikse et al. 2017). In addition, there are reconstructions  
321 that jointly use satellite altimetry and tide gauge records (Church and White 2006, 2011) and  
322 reconstructions which combines tide gauge records with ocean models (Meysignac et al.  
323 2011) or physics-based and model-derived geometries of the contributing processes (Hay et  
324 al. 2015).

325 For the period since 1993, with most of the world coastlines densely sampled, the rates of sea  
326 level rise from all tide gauge based reconstructions and estimates from satellite altimetry  
327 agree within their specific uncertainties, e.g., rates of  $3.0 \pm 0.7 \text{ mm} \cdot \text{yr}^{-1}$  (Hay et al. 2015);  $2.8$   
328  $\pm 0.5 \text{ mm} \cdot \text{yr}^{-1}$  (Church and White 2011; Rhein et al. 2013);  $3.1 \pm 0.6 \text{ mm} \cdot \text{yr}^{-1}$  (Jevrejeva et  
329 al, 2014);  $3.1 \pm 1.4 \text{ mm} \cdot \text{yr}^{-1}$  (Dangendorf et al. 2017) and the estimate from satellite altimetry  
330  $3.2 \pm 0.4 \text{ mm} \cdot \text{yr}^{-1}$  (Nerem et al. 2010; Rhein et al. 2013). However, classical tide gauge-  
331 based reconstructions still tend to overestimate the inter-annual to decadal variability of  
332 global mean sea level (e.g. Calafat et al., 2012; Dangendorf et al. 2015; Natarov et al. 2017)  
333 compared to global mean sea level from satellite altimetry, due to limited and uneven spatial  
334 sampling of the global ocean afforded by the tide gauge network. Sea level rise being non  
335 uniform, spatial variability of sea-level measured at tide gauges is evidenced by 2D  
336 reconstruction methods. The most widely used approach is the use of empirical orthogonal  
337 functions (EOF) calibrated with the satellite altimetry data (e.g. Church and White, 2004).  
338 Alternatively, Choblet et al. (2014) implemented a Bayesian inference method based on a  
339 Voronoi tessellation of the Earth's surface to reconstruct sea level during the twentieth  
340 century. Considerable uncertainties remain however in long term assessments due to poorly  
341 sampled ocean basins such as the South Atlantic, or regions which are significantly influenced  
342 by open-ocean circulation (e.g. Subtropical North Atlantic) (Frederikse et al. 2017).  
343 Uncertainties involved in specifying vertical land motion corrections at tide gauges also  
344 impact tide gauge reconstructions (Jevrejeva et al. 2014; Woppelmann and Marcos 2016;  
345 Hamlington et al. 2016). Frederikse et al. (2017) recently also demonstrated that both global  
346 mean sea level reconstructed from tide gauges and the sum of steric and mass contributors  
347 show a good agreement with altimetry estimates for the overlapping period 1993-2014.

348

### 349 **2.3 Steric sea level**

350 Steric sea level variations result from temperature (T) and salinity (S) related density changes  
351 of sea water associated to volume expansion and contraction. These are referred to as  
352 thermosteric and halosteric components. Despite clear detection of regional salinity changes  
353 and the dominance of the salinity effect on density changes at high latitudes (Rhein et al.,  
354 2013), the halosteric contribution to present-day global mean steric sea level rise is negligible,  
355 as the ocean's total salt content is essentially constant over multidecadal timescales (Gregory  
356 and Lowe, 2000). Hence in this study, we essentially consider the thermosteric sea level  
357 component.

358 Averaged over the 20<sup>th</sup> century, ocean thermal expansion associated with ocean warming has  
359 been the largest contribution to global mean sea level rise (Church et al., 2013). This remains  
360 true for the altimetry period starting in the year 1993 (e.g., Chen et al. 2017; Dieng et al.,  
361 2017, Nerem et al., 2018). But total land ice mass loss (from glaciers, Greenland and  
362 Antarctica) during this period, now dominates the sea level budget (see section 3).

363 Until the mid-2000s, the majority of ocean temperature data have been retrieved from  
364 shipboard measurements. These include vertical temperature profiles along research cruise  
365 tracks from the surface sometimes all the way down to the bottom layer (e.g. Purkey and  
366 Johnson, 2010) and upper-ocean broad-scale measurements from ships of opportunity  
367 (Abraham et al., 2013). These upper-ocean in situ temperature measurements however are  
368 limited to the upper 700 m depth due to common use of expandable bathy thermographs  
369 (XBTs). Although the coverage has been improved through time, large regions characterized  
370 by difficult meteorological conditions remained under-sampled, in particular the southern  
371 hemisphere oceans and the Arctic area.

372

### 373 *2.3.1 Thermosteric data sets*

374 Over the altimetry era, several research groups have produced gridded time series of  
375 temperature data for different depth levels, based on XBTs (with additional data from  
376 mechanical bathythermographs -MBTs- and conductivity-temperature-depth (CTD) devices  
377 and moorings) and Argo float measurements. The temperature data have further been used to  
378 provide thermosteric sea level products. These differ because of different strategies adopted  
379 for data editing, temporal and spatial data gaps filling, mapping methods, baseline  
380 climatology and instrument bias corrections (in particular the time-to-depth correction for  
381 XBT data, Boyer et al., 2016).

382 The global ocean in situ observing system has been dramatically improved through the  
383 implementation of the international Argo program of autonomous floats, delivering a unique

384 insight of the interior ocean from the surface down to 2000 m depth of the ice-free global  
 385 ocean (Roemmich et al., 2012, Riser et al., 2016). More than 80% of initially planned full  
 386 deployment of Argo float program was achieved during the year 2005, with quasi- global  
 387 coverage of the ice-free ocean by the start of 2006. At present, more than 3800 floats provide  
 388 systematic T/S data, with quasi (60°S-60°N latitude) global coverage down to 2000 m depth.  
 389 A full overview on in situ ocean temperature measurements is given for example in Abraham  
 390 et al. (2013).

391 In this section, we consider a set of 11 direct (in situ) estimates, publically available over the  
 392 entire altimetry era, to review global mean thermosteric sea level rise and, ultimately, to  
 393 construct an ensemble mean time series. These data sets are:

- 394 1. CORA = Coriolis Ocean database for ReAnalysis, Copernicus Service, France  
 395 marine.copernicus.eu/, product name :  
 396 INSITU\_GLO\_TS\_OA\_REP\_OBSERVATIONS\_013\_002\_b
- 397 2. CSIRO (RSOI) = Commonwealth Scientific and Industrial Research  
 398 Organisation/Reduced-Space Optimal Interpolation, Australia
- 399 3. ACECRC/IMAS-UTAS = Antarctic Climate and Ecosystem Cooperative Research  
 400 Centre/Institute for Marine and Antarctic Studies-University of Tasmania, Australia  
 401 [http://www.cmar.csiro.au/sealevel/thermal\\_expansion\\_ocean\\_heat\\_timeseries.html](http://www.cmar.csiro.au/sealevel/thermal_expansion_ocean_heat_timeseries.html)
- 402 4. ICCES = International Center for Climate and Environment Sciences, Institute of  
 403 Atmospheric Physics, China  
 404 <http://ddl.escience.cn/f/PKFR>
- 405 5. ICDC = Integrated Climate Data Center, Universit of Hamburg, Germany
- 406 6. IPRC = International Pacific Research Center, University of Hawaii, USA  
 407 [http://apdrc.soest.hawaii.edu/projects/Argo/data/gridded/On\\_standard\\_levels/index-1.html](http://apdrc.soest.hawaii.edu/projects/Argo/data/gridded/On_standard_levels/index-1.html)  
 408
- 409 7. JAMSTEC = Japan Agency for Marine-Earth Science and Technology, Japan  
 410 [ftp://ftp2.jamstec.go.jp/pub/argo/MOAA\\_GPV/Glb\\_PRS/OI/](ftp://ftp2.jamstec.go.jp/pub/argo/MOAA_GPV/Glb_PRS/OI/)
- 411 8. MRI/JMA = Meteorological Resarch Institute/Japan Meteorological Agency, Japan  
 412 <https://climate.mri-jma.go.jp/~ishii/.wcrp/>
- 413 9. NCEI/NOAA = National Centers for Environmental Information/National Oceanic  
 414 and Atmospheric Adinistration, USA
- 415 10. SIO = Scripps Institution of Oceanography, USA  
 416 Deep/abyssal: <https://cchdo.ucsd.edu/>
- 417 11. SIO = Scripps Institution of Oceanography, USA  
 418 Deep/abyssal: <https://cchdo.ucsd.edu/> (for the abyssal ocean)

419

420 Their characteristics are presented in Table 2.

421

422

423

424  
425  
426  
427

Product/Institution	Period	Depth-integration (m)				Temporal resolution / Latitudinal range	Reference
		0-700	700 - 2000	0-2000	≥2000		
1 CORA	1993-2016	Y	Y	Y	---	Monthly 60°S-60°N	<a href="http://marine.copernicus.eu/services-portfolio/access-to-products/">http://marine.copernicus.eu/services-portfolio/access-to-products/</a>
2 CSIRO (RSOI)	2004-2017	Y/E (0-300)	Y/E	Y/E	---	Monthly 65°S-65°N	Roemmich et al. (2015); Wijffels et al. (2016)
3 CSIRO/ACE CRC/IMAS-UTAS	1970-2017	Y/E (0-300)	---	---	---	Yearly (3-yr run. mean) 65°S-65°N	Domingues et al. (2008); Church et al. (2011)
4 ICCES	1970-2016	Y/E (0-300)	Y/E	Y/E	---	Yearly 89°S-89°N	Cheng and Zhu (2016); Cheng et al. (2017)
5 ICDC	1993-2016	Y (1993)	---	Y (2005)	---	Monthly	Gouretzki and Koltermann (2007)
6 IPRC	2005-2016	---	---	Y	---	Monthly	<a href="http://apdrc.soest.hawaii.edu/projects/argo">http://apdrc.soest.hawaii.edu/projects/argo</a>
7 JAMSTEC	2005-2016	---	---	Y	---	Monthly	Hosoda et al. (2008)
8 MRI/JMA	1970-2016 (rel. to 1961-1990 averages)	Y/E (0-300)	Y/E	Y/E	---	Yearly 89°S-89°N	Ishii et al. (2017)
9 NCEI/NOAA	1970-2016	Y/E	Y/E	Y/E	---	Yearly 89°S-89°N	Antonov et al. (2005)
10 SIO	2005-2016	---	---	Y	---	Monthly	Roemmich and Gilson (2009)
1 SIO	1990-2010	---	---	---	Y/E	Linear	Purkey and



1	(Deep/abyssal)	(as of 01/2018)					trend 89°S-89°N, as an aggregation of 32 deep ocean basins	Johnson (2010)
---	----------------	-----------------	--	--	--	--	--	----------------

428 *Table 2: Compilation of available in situ datasets from different originators and/or*  
429 *contributors. The table indicates the time span covered by the data, the depth of integration, as*  
430 *well as the temporal resolution and latitude coverage.*

431

432

### 433 **2.3.2 Individual estimates**

434

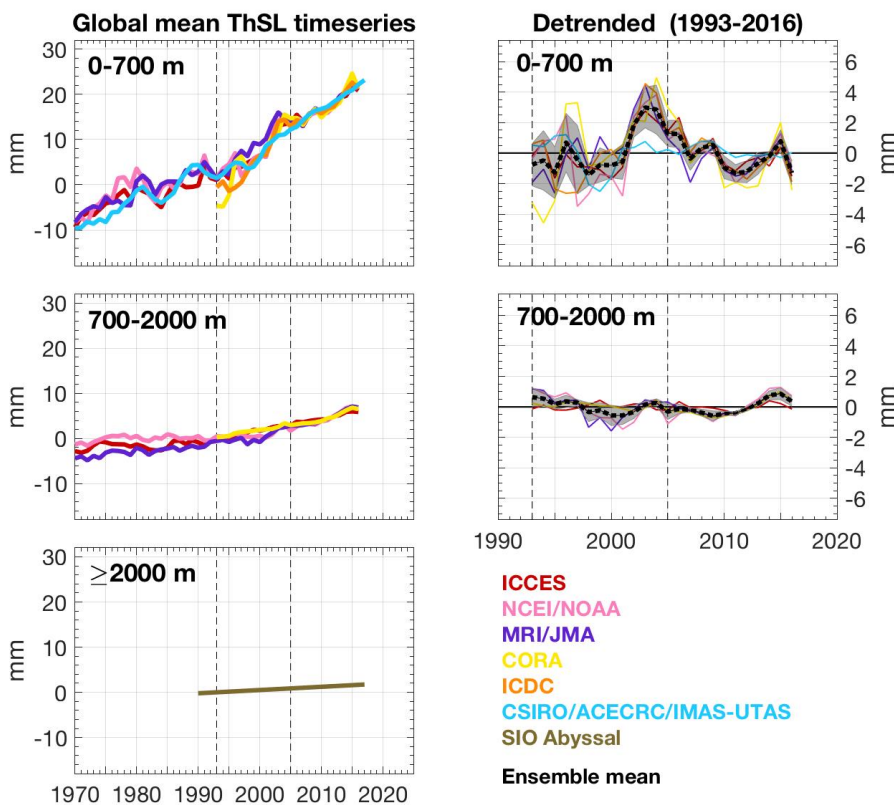
435 All in situ estimates compiled in this study show a steady rise in global mean thermosteric sea  
436 level, independent of depth-integration and decadal/multidecadal periods (Figure 4 and 5, left  
437 panels). As the deep/abyssal ocean estimate only illustrates the updated version of the linear  
438 trend from Purkey and Johnson (2010) for 1990-2010 extrapolated to 2016, it does not have  
439 any variability superimposed.

440 Interannual to decadal variability during the Altimeter era (since 1993) is similar for both 0-  
441 700 m and 700-2000 m, with larger amplitude in the upper ocean (Figure 4 and 5, right  
442 panels). For the 0-700 m, there is an apparent change in amplitude before/after the Argo era  
443 (since 2005), mostly due to a maximum (2-4 mm) around 2001-2004, except for one estimate.  
444 Higher amplitude and larger spread in variability between estimates before the Argo era is a  
445 symptom of the much sparser in situ coverage of the global ocean. Interannual variability over  
446 the Argo era (Figures 4 and 5, right panels) is mainly modulated by El Niño Southern  
447 Oscillation (ENSO) phases in the upper 500 m ocean, particularly for the Pacific, the largest  
448 ocean basin (Roemmich et al., 2011; Johnson and Birnbaum, 2017).

449 In terms of depth contribution, on average, the upper 300 m explains the same percentage  
450 (almost 70%) of the 0-700 m linear rate over both altimetry and Argo eras, but the  
451 contribution from the 0-700 m to 0-2000 m varies: about 75% for 1993-2016 and 65% for  
452 2005-2016. Thus, the 700-2000 m contribution increases by 10% during the Argo decade,  
453 when the number of observations within 700-2000 m has significantly increased.

454

455

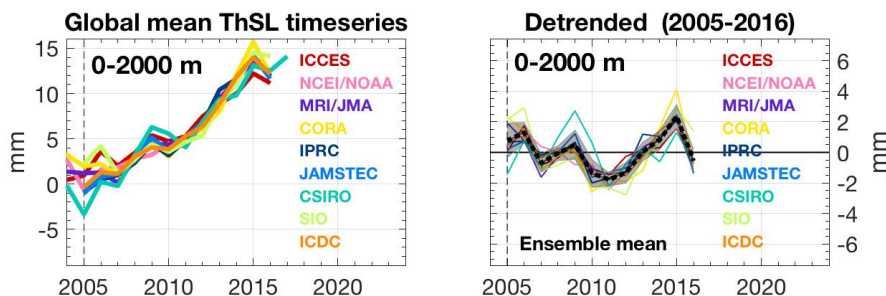


456

457 Figure 4. Left- panels. Annual mean global mean thermosteric anomaly Time-series since  
 458 1970, from various research groups (color) and for three depth-integrations: 0-700 m (top),  
 459 700-2000 m (middle), and below 2000 m (bottom). Vertical dashed lines are plotted along  
 460 1993 and 2005. For comparison, all time-series were offset arbitrarily. Right panels.  
 461 Respective linearly de-trended time-series for 1993-2016. Black bold dashed line is the  
 462 ensemble mean and gray shadow bar the ensemble spread (1-standard deviation). Units are  
 463 mm.

464

465



466

467 Figure 5. Left- panel. Annual mean global mean thermosteric anomaly time-series since 2004,  
 468 from various research groups (color) in the upper 2000 m. A vertical dashed line is plotted  
 469 along 2005. For comparison, all time-series were offset arbitrarily. Right panel. Respective  
 470 linearly de-trended time series for 2005-2016. Black bold dashed line is the ensemble mean  
 471 and gray shadow bar the ensemble spread (1-standard deviation). Units are mm.

472  
473  
474  
475  
476  
477  
478  
479  
480  
481  
482  
483  
484  
485  
486  
487  
488  
489  
490  
491  
492  
493  
494  
495  
496  
497  
498  
499  
500  
501  
502  
503  
504  
505  
506  
507  
508

### *2.3.3. Ensemble mean thermosteric sea level*

Given that the global mean thermosteric sea level anomaly estimates compiled for this study are not necessarily referenced to the same baseline climatology, they cannot be directly averaged together to create an ensemble mean. To circumvent this limitation, we created an ensemble mean in three steps, as explained below.

Firstly, we de-trended the individual time-series by removing a linear trend for 1993-2016 and averaged together to obtain an “ensemble mean variability time-series”. Secondly, we averaged together the corresponding linear trends of the individual estimates to obtain an “ensemble mean linear rate”. Thirdly, we combined this “ensemble mean linear rate” with the “ensemble mean variability time-series” to obtain the final ensemble mean time-series. We applied the same steps for the Argo era (2005-2016).

To maximise the number of individual estimates used in the final full-depth ensemble mean time-series, the three steps above were actually divided into depth-integrations and then summed. For the Argo era, we summed 0-2000 m (9 estimates) and  $\geq 2000$  m (1 estimate). For the altimetry era, we summed 0-700 m (6 estimates), 700-2000 (4 estimates) and  $\geq 2000$  m (1 estimate), although there is no statistical difference if the calculation was only based on the sum of 0-2000 m (4 estimates) and  $\geq 2000$  m (1 estimate). There is also no statistical difference between the full-depth ensemble mean time-series created for the Altimeter and Argo eras during their overlapping years (since 2005).

Figure 6 shows the full-depth ensemble mean time series over 1993-2016 and 2005-2016. It reveals a global mean thermosteric sea level rise of about 30 mm over 1993-2016 (24 years) or about 18 mm over 2005-2016 (12 years) , with a record high in 2015. These thermosteric changes are equivalent to a linear rate of  $1.32 \pm 0.4$  mm/yr and  $1.31 \pm 0.4$  mm/yr respectively.

509  
510  
511  
512  
513  
514  
515  
516  
517  
518  
519  
520  
521  
522  
523  
524  
525  
526  
527  
528  
529  
530  
531  
532  
533  
534  
535  
536  
537

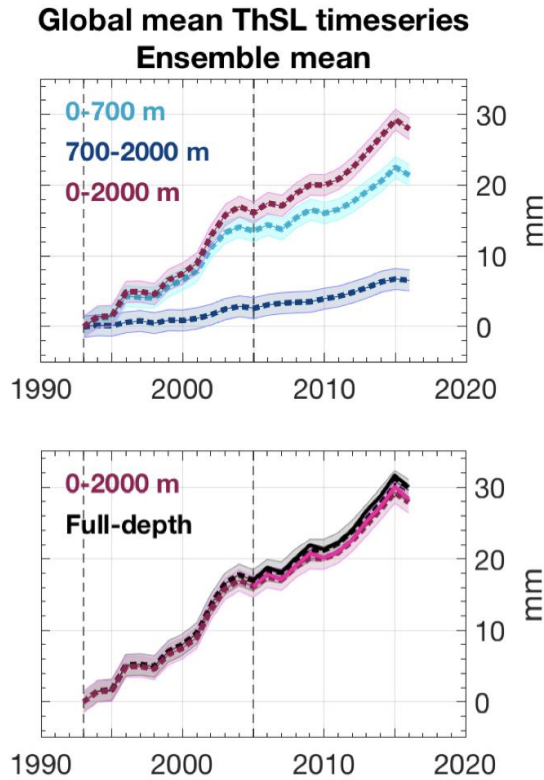
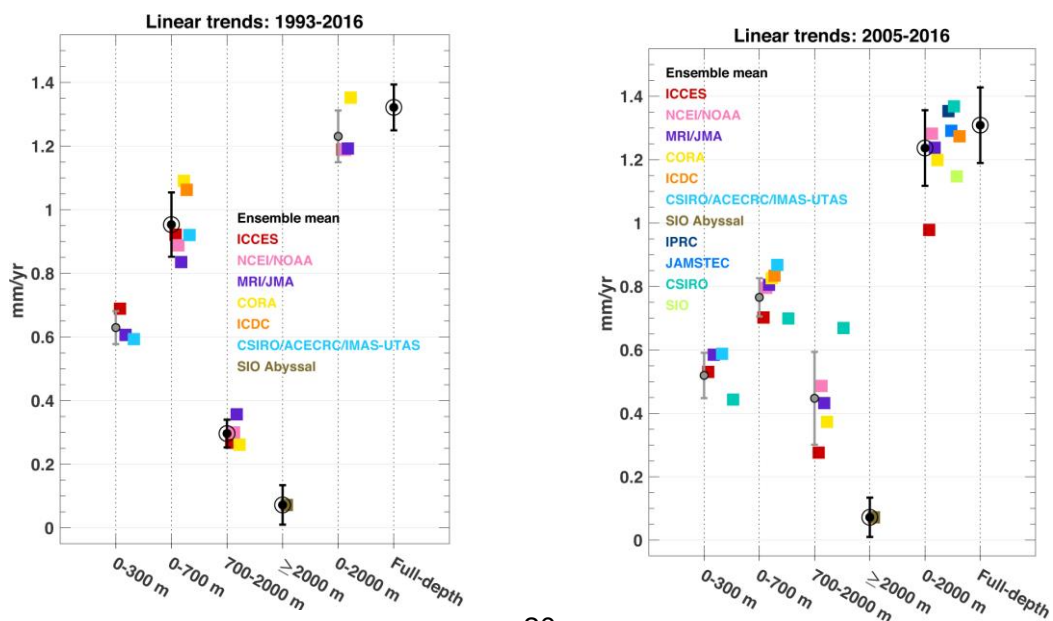


**Figure 6:** Ensemble mean time-series for global mean thermosteric anomaly, for three-depth integrations (top) and for 0-2000 m and full-depth (bottom). In the bottom panel, dashed lines are for the 1993-2016 period whereas solid lines are for 2005-2016. Error bars represent the ensemble spread (standard deviation). Units are mm.

538 Figure 7 shows thermosteric sea level trends for each of the data sets used over the 1993-2016  
539 (left panel) and 2005-2016 (right panel) time spans and different depth ranges (including full  
540 depth), as well as associated ensemble mean trends. The full depth ensemble mean trend  
541 amounts to 1.3 +/- 0.4 mm/yr over 2005-2016. It is similar to the 1993-2016 ensemble mean  
542 trend, suggesting negligible acceleration of the thermosteric component over the altimetry era.

543  
544  
545  
546  
547  
548  
549  
550  
551  
552  
553  
554



555  
 556 *Figure 7: Linear rates of global mean thermosteric sea level for depth-integrations (x-axis), for*  
 557 *individual estimates and ensemble means, over 1993-2016 (left) and 2005-2016 (right). Ensemble*  
 558 *mean rates with a black circle were used in the estimation of the time-series described in Section*  
 559 *2.3.4. Error bars are standard deviation due to spread of the estimates except for  $\geq 2000$  m. Units are*  
 560 *mm/yr.*

561  
 562

## 563 **2.4 Glaciers**

564 Glaciers have strongly contributed to sea-level rise during the 20<sup>th</sup> century – around 40% -  
 565 and will continue to be an important part of the projected sea-level change during the 21<sup>st</sup>  
 566 century – around 30% (Kaser et al., 2006, Church et al., 2013, Gardner et al., 2013, Marzeion  
 567 et al., 2014, Zemp et al., 2015; Huss and Hock, 2015). Because glaciers are time-integrated  
 568 dynamic systems, a response lag of at least 10 years to a few hundred years is observed  
 569 between changes in climate forcing and glacier shape, mainly depending on glacier length and  
 570 slope (Johannesson et al., 1989, Bahr et al., 1998). Today, glaciers are globally (a notable  
 571 exception is the Karakoram/Kunlun Shan region, e.g. Brun et al., 2017) in a strong  
 572 disequilibrium with the current climate and are losing mass, due essentially to the global  
 573 warming in the second half of the 20<sup>th</sup> century (Marzeion et al., 2018).

574 Global glacier mass changes are derived from in situ measurements of glacier mass changes  
 575 or glacier length changes. Remote sensing methods measure elevation changes over entire  
 576 glaciers based on differencing digital elevation models (DEMs) from satellite imagery  
 577 between two epochs (or at points from repeat altimetry), surface flow velocities for  
 578 determination of mass fluxes, and glacier mass changes from space-based gravimetry. Mass  
 579 balance modeling driven by climate observations is also used (Marzeion et al., 2017 provide a  
 580 review of these different methods).

581 Glacier contribution to sea level is primarily the result of their surface mass balance and  
 582 dynamic adjustment, plus iceberg discharge and frontal ablation (below sea level) in the case  
 583 of marine-terminating glaciers. The sum of worldwide glacier mass balances (MBs) does not  
 584 correspond to the total glacier contribution to sea-level change for the following reasons:

585 - Glacier ice below sea level does not contribute to sea-level change, apart from a  
 586 small lowering when replacing ice with seawater of a higher density. Total volume of glacier  
 587 ice below sea level is estimated to be 10 – 60 mm sea-level equivalent (SLE, Huss and  
 588 Farinotti, 2012, Haeberli and Linsbauer, 2013, Huss and Hock, 2015).

589 - Incomplete transfer of melting ice from glaciers to the ocean: meltwater stored in  
 590 lakes or wetlands, meltwater intercepted by natural processes and human activities (e.g.

591 drainage to lakes and aquifers in endorheic basins, impoundment in reservoirs, agriculture use  
592 of freshwater, Loriaux and Casassa, 2013, Käab et al., 2015).

593 Despite considerable progress in observing methods and spatial coverage (Marzeion et al.,  
594 2017), estimating glacier contribution to sea-level change remains challenging due to the  
595 following reasons:

596 - Number of regularly observed glaciers (in the field) remains very low (0.25% of the  
597 200 000 glaciers of the world have at least one observation and only 37 glaciers have multi  
598 decade-long observations, Zemp et al. 2015).

599 - Uncertainty of the total glacier ice mass remains high (Figure 8, Grinsted et al., 2013,  
600 Pfeffer et al., 2014, Farinotti et al., 2017, Frey et al. 2014).

601 - Uncertainties in glacier inventories and DEMs are not negligible. Sources of  
602 uncertainties include debris-covered glaciers, disappearance of small glaciers, positional  
603 uncertainties, wrongly mapped seasonal snow, rock glaciers, voids and artifacts in DEMs  
604 (Paul et al., 2004, Bahr and Radić, 2012).

605 - Uncertainties of satellite retrieval algorithms from space-based gravimetry and  
606 regional DEM differencing are still high, especially for global estimates (Gardner et al. 2013,  
607 Marzeion et al., 2017, Chambers et al., 2017).

608 - Uncertainties of global glacier modeling (e.g. initial conditions, model assumptions  
609 and simplifications, local climate conditions, Marzeion et al., 2012).

610 - Knowledge about some processes governing mass balance (e.g. wind redistribution  
611 and metamorphism, sublimation, refreezing, basal melting) and dynamic processes (e.g. basal  
612 hydrology, fracking, surging) remains limited (Farinotti et al., 2017).

613 An annual assessment of glacier contribution to sea-level change is difficult to perform from  
614 ground-based or space-based observations except space-based gravimetry, due to the sparse  
615 and irregular observation of glaciers, and the difficulty of assessing accurately the annual  
616 mass balance variability. Global annual averages are highly uncertain because of the sparse  
617 coverage, but successive annual balances are uncorrelated and therefore averages over several  
618 years are known with greater confidence.

619

#### 620 **2.4.1 Glacier datasets**

621 The following datasets are considered, with a focus on the trends of annual mass changes:

622 1. Update of Gardner et al., 2013 (Reager et al., 2016), from satellite gravimetry and  
623 altimetry, and glaciological records, called G16.

624 2. Update of Marzeion et al, 2012 (Marzeion et al., 2017), from global glacier  
625 modeling and mass balance observations, called M17.

626 3. Update of Cogley (2009) (Marzeion et al., 2017), from geodetic and direct mass-  
627 balance measurements, called C17.

628 4. Update of Leclercq et al., 2011 (Marzeion et al., 2017), from glacier length changes,  
629 called L17.

630 5. Average of GRACE-based estimates of Marzeion et al. (2017), from spatial  
631 gravimetry measurements, called M17-G.

632 In general it is not possible to align measurements of glacier mass balance with the calendar.  
633 Most in-situ measurements are for glaciological years that extend between successive annual  
634 minima of the glacier mass at the end of the summer melt season. Geodetic measurements  
635 have start and end dates several years apart and are distributed irregularly through the  
636 calendar year; some are corrected to align with annual mass minima but most are not.  
637 Consequently, measurements discussed here for 1993-2016 (the altimetry era) and 2005-2016  
638 (the GRACE and Argo era) are offset by up to a few months from the nominal calendar years.  
639 Peripheral glaciers around the Greenland and Antarctic ice sheets are not treated in detail in  
640 this section (see sections 2.5 and 2.6 for mass-change estimates that combine the peripheral  
641 glaciers with the Greenland Ice Sheet and Antarctic Ice Sheet respectively). This is primarily  
642 because of the lack of observations (especially ground-based measurements) and also because  
643 of the high spatial variability of mass balance in those regions, and the slightly different  
644 climate (e.g. precipitation regime) and processes (e.g. refreezing). In the past, these regions  
645 have often been neglected. However, Radić and Hock (2010) estimated the total ice mass of  
646 peripheral glaciers around Greenland and Antarctica as  $191 \pm 70$  mm SLE, with an actual  
647 contribution to sea-level rise of around  $0.23 \pm 0.04$  mm/yr (Radić and Hock, 2011). Gardner  
648 et al. (2013) found a contribution from Greenland and Antarctic peripheral glaciers equal to  
649  $0.12 \pm 0.05$  mm/yr.

650 Note that some new or updated datasets for peripheral glaciers surrounding polar ice sheets  
651 are under development and would hopefully be available in coming years in order to  
652 incorporate Greenland and Antarctic peripheral glaciers in the estimates of global glacier  
653 mass changes.

654

#### 655 **2.4.2 Methods**

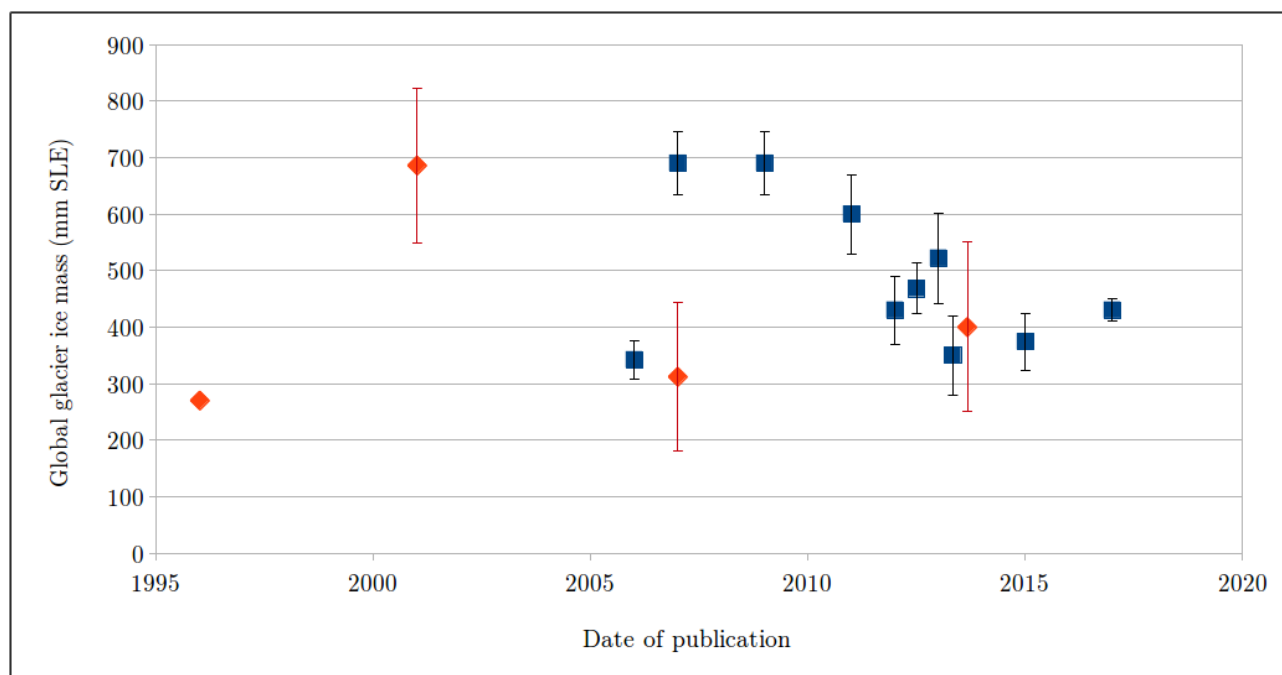
656 No globally complete observational dataset exists for glacier mass changes (except GRACE  
657 estimates, see below). Any calculation of the global glacier contribution to sea-level change

658 has to rely on spatial interpolation or extrapolation or both, or to consider limited knowledge  
659 of responses to climate change (due to the heterogeneous spatial distribution of glaciers  
660 around the world). Consequently, most observational methods to derive glacier sea-level  
661 contribution must extend local observations (in situ or satellite) to a larger region. Thanks to  
662 the recent global glacier outline inventory (Randolph Glacier Inventory – RGI – first release  
663 in 2012) as well as global climate observations, glacier modeling can now also be used to  
664 estimate the contribution of glaciers to sea level (Marzeion et al., 2012, Huss and Hock, 2015,  
665 Maussion et al., 2018, *subm.*). Still, those global modeling methods need to globalize local  
666 observations and glacier processes which require fundamental assumptions and  
667 simplifications. Only GRACE-based gravimetric estimates are global but they suffer from  
668 large uncertainties in retrieval algorithms (signal leakage from hydrology, GIA correction)  
669 and coarse spatial resolution, not resolving smaller glaciated mountain ranges or those  
670 peripheral to the Greenland ice sheet.

671 DEM differencing method is not yet global, but regional, and can hopefully in the near future  
672 be applied globally. This method needs also to convert elevation changes to mass changes  
673 (using assumptions on snow and ice densities). In contrast, very detailed glacier surface mass  
674 balance and glacier dynamic models are today far from being applicable globally, mainly due  
675 to the lack of crucial observations (e.g., meteorological data, glacier surface velocity and  
676 thickness) and of computational power for the more demanding theoretical models. However,  
677 somewhat simplified approaches are currently developed to make best use of the steadily  
678 increasing datasets. Modeling-based estimates suffer also from the large spread in estimates of  
679 the actual global glacier ice mass (Figure 8). The mean value is 469 +/- 146 mm SLE, with  
680 recent studies converging towards a range of values between 400 and 500 mm SLE global  
681 glacier ice mass. But as mentioned above, a part of this ice mass will not contribute to sea  
682 level.

683





684 *Fig 8. Evolution of global glacier ice mass estimates from different studies published over the*  
 685 *past two decades, based on different observations and methods. The red marks correspond to*  
 686 *IPCC reports. We clearly see the most recent publications lead to less scattered results. Note*  
 687 *that Antarctica and Greenland peripheral glaciers are taken into account in this figure.*

688

### 689 **2.4.3 Results (trends)**

690 Table 3 presents most recent estimates of trends in global glacier mass balances.

691

	<b>1993 – 2016 mm/yr SLE</b>	<b>2005 – 2016 mm/yr SLE</b>
G16		0.70 +- 0.070 <sup>a</sup>
M17	0.68 +- 0.032	0.80 +- 0.048
C17	0.63 +- 0.070	0.75 +- 0.070 <sup>b</sup>
L17		0.84 +- 0.640 <sup>c</sup>
M17-G		0.61 +- 0.070 <sup>d</sup>

692

693 *Table 3: All data are in mm/yr SLE. <sup>a</sup> The time period of G16 is 2002 – 2014. <sup>b</sup> The time*  
 694 *period of C17 is 2003 – 2009. <sup>c</sup> The time period of L17 is 2003 – 2009. <sup>d</sup> The time period of*  
 695 *M17-G is 2002/2005 – 2013/2015 because this value is an average of different estimates.*

696

697 The ensemble mean contribution of glaciers to sea-level rise for the time period 1993 – 2016  
698 is 0.65 +/- 0.051 mm/yr SLE and 0.74 +/- 0.18 mm/yr for the time period 2005 – 2016  
699 (uncertainties are averaged). Different studies refer to different time periods. However,  
700 because of the probable low variability of global annual glacier changes, compared to other  
701 components of the sea-level budget, averaging trends for slightly different time periods is  
702 appropriate.

703 The main source of uncertainty is that the vast majority of glaciers are unmeasured, which  
704 makes interpolation or extrapolation necessary, whether for in situ or satellite measurements,  
705 and for glacier modeling. Other main contributions to uncertainty in the ensemble mean stem  
706 from methodological differences, such as the downscaling of atmospheric forcing required for  
707 glacier modeling, the separation of glacier mass change to other mass change in the spatial  
708 gravimetry signal and the derivation of observational estimates of mass change from different  
709 raw measurements (e.g. length and volume changes, mass balance measurements and geodetic  
710 methods) all with their specific uncertainties.

711

## 712 **2.5 Greenland**

713 Ice sheets are the largest potential source of future sea level rise (SLR) and represent the  
714 largest uncertainty in projections of future sea level. Almost all land ice (~99.5%) is locked in  
715 the ice sheets, with a volume in sea level equivalent/SLE terms of 7.4 m for Greenland, and  
716 58.3 m for Antarctica. It has been estimated that approximately 25% to 30% of the total land  
717 ice contribution to sea level rise over the last decade came from the Greenland ice sheet (e.g.  
718 Dieng et al., 2017, Box and Colgan, 2017).

719 There are three main methods that can be used to estimate the mass balance of the Greenland  
720 ice sheet: (1) measurement of changes in elevation of the ice surface over time ( $dh/dt$ ) either  
721 from imagery or altimetry; (2) the mass budget or Input-Output Method (IOM) which  
722 involves estimating the difference between the surface mass balance and ice discharge; and  
723 (3) consideration of the redistribution of mass via gravity anomaly measurements which only  
724 became viable with the launch of GRACE in 2002. Uncertainties due to the GIA correction  
725 are small in Greenland compared to Antarctica: on the order of  $\pm 20$  Gt/yr mass equivalent  
726 (Khan et al., 2016). Prior to 2003, mass trends are reliant on IOM and altimetry. Both  
727 techniques have limited sampling in time and/or space for parts of the satellite era (1992-  
728 2002) and errors for this earlier period are, therefore, higher (van den Broeke et al., 2016,  
729 Hurkmans et al., 2014).

730 The consistency between the three methods mentioned above was demonstrated for Greenland  
 731 by Sasgen et al. (2012) for the period 2003-2009. Ice sheet wide estimates showed excellent  
 732 agreement although there was less consistency at a basin scale. We have, therefore, high  
 733 confidence and relatively low uncertainties in the mass rates for the Greenland ice sheet in the  
 734 satellite era (see also Bamber et al., 2018).

735

### 736 **2.5.1 Datasets considered for the assessment**

737 This assessment of sea level budget contribution from the Greenland ice sheet considers the  
 738 following datasets:

<b>Reference</b>	<b>Time period</b>	<b>Method</b>
Update from Barletta et al. (2013)	2003-2016	GRACE
Groh and Horwath (2016)	2003-2015	GRACE
Update from Luthcke et al. (2013)	2003-2015	GRACE
Update from Sasgen et al. (2012)	2003-2016	GRACE
Update from Schrama et al. (2014)	2003-2016	GRACE
Update from (van den Broeke et al., 2016)	1993-2016	Input/output Method (IOM)
Wiese et al. (2016)	2003-2016	GRACE
Update from Wouters et al. (2008)	2003-2016	GRACE

739 *Table 4. Datasets considered in the Greenland mass balance assessment, as well as covered*  
 740 *time span and type of observations.*

741

### 742 **2.5.2. Methods and analyses**

743 All but one of these datasets are based on GRACE data and therefore provide annual time  
 744 series from ~2002 onwards. The one exception uses IOM (van den Broeke et al., 2016) to  
 745 give an annual mass time series for a longer time period (1993 onwards).

746 Notwithstanding this, each group has chosen their own approach to estimate mass balance  
 747 from GRACE observations. As the aim of this Global Sea Level Budget assessment is to  
 748 compile existing results (rather than undertake new analyses), we have not imposed a specific  
 749 methodology. Instead, we asked for the contributed datasets to reflect each group's 'best  
 750 estimate' of annual trends for Greenland using the method(s) they have published.

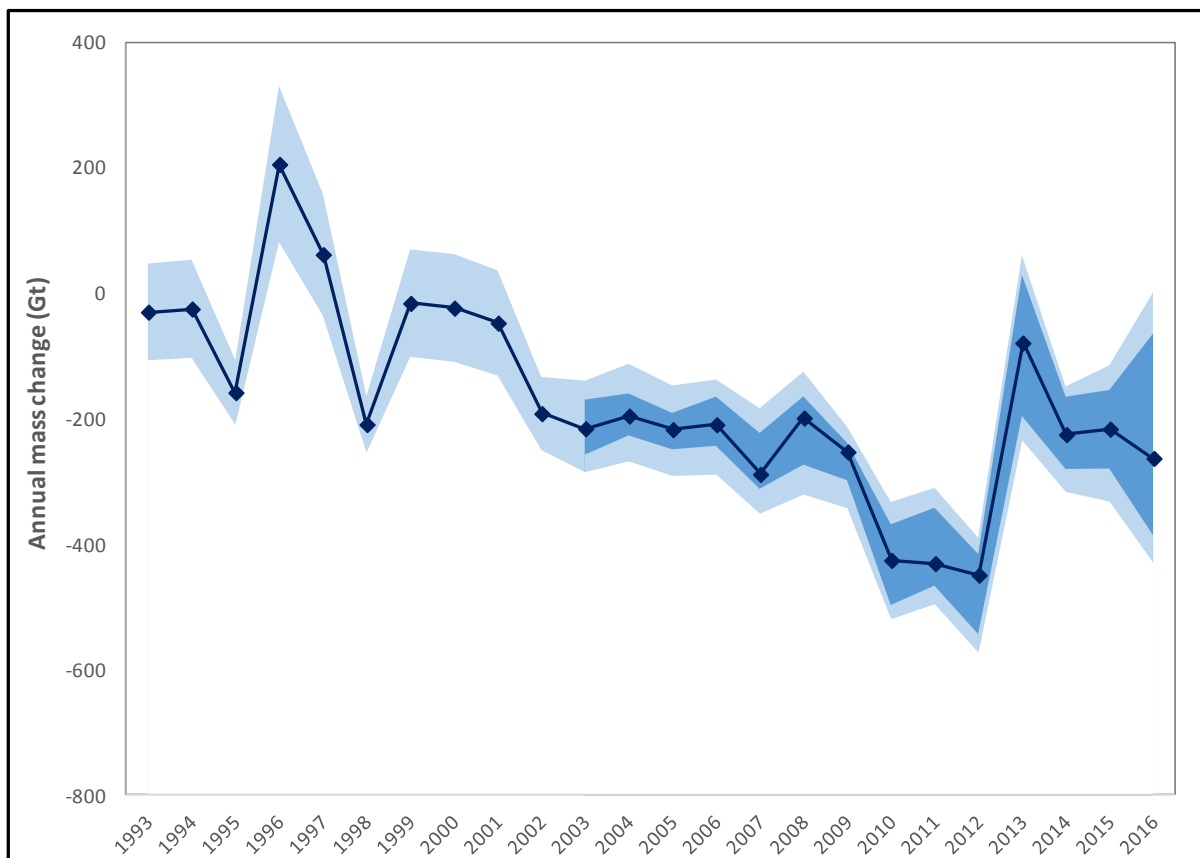
751 Greenland contains glaciers and ice caps around the margins of the main ice sheet, often  
 752 referred to as peripheral GIC (PGIC), which are a significant proportion of the total mass  
 753 imbalance (circa 15-20%) (Bolch et al., 2013). Some studies consider the mass balance of the  
 754 ice sheets and the PGIC separately but there has been, in general, no consistency in the  
 755 treatment of PGIC and many studies do not specify if they are included or excluded from the  
 756 total. The GRACE satellites have an approximate spatial resolution of 300 km and the large  
 757 number of studies that use GRACE, by default, include all land ice within the domain of  
 758 interest. For this reason, the results below for Greenland mass trends all include PGIC.

759 From these datasets, for each year from 1993 to 2015 (and 2016 where available), we have  
 760 calculated an average change in mass (calculated as the weighted mean based on the stated  
 761 error value for each year) and an error term. Prior to 2003, the results are based on just one  
 762 dataset (van den Broeke et al., 2016).

763

### 764 2.5.3 Results

765



766

767 *Figure 9. Greenland annual mass change from 1993 to 2016. The medium blue region shows*  
 768 *the range of estimates from the datasets listed in Table 1. The lighter blue region shows the*

769 *range of estimates when stated errors are included, to provide upper and lower bounds. The*  
 770 *dark blue line shows the mean mass trend.*

771

772

773

774

<b>Year</b>	<b><math>\Delta</math> mass (Gt/yr)</b>	<b>Error (Gt/yr)</b>	<b><math>\sigma</math> (Gt)</b>
1993	-30	76	
1994	-25	77	
1995	-159	51	
1996	205	123	
1997	61	97	
1998	-209	45	
1999	-16	85	
2000	-24	85	
2001	-48	83	
2002	-192	58	
2003	-216	13	28
2004	-196	12	24
2005	-218	13	21
2006	-210	12	29
2007	-289	10	31
2008	-199	11	39
2009	-253	11	21
2010	-426	9	42
2011	-431	9	47
2012	-450	10	41
2013	-80	13	76
2014	-225	13	38
2015	-217	13	48
2016	-263	23	123
Average estimate 1993-2015	-167	54	

Average estimate 1993-2016	-171	53	
Average estimate 2005-2015	-272	11	
Average estimate 2005-2016	-272	13	

775

776 *Table 5. Annual time series of Greenland mass change (GT/yr, negative values mean*  
777 *decreasing mass).  $\Delta$  mass is calculated as the weighted mean based on the stated error value*  
778 *for each year. The error for each year is calculated as the mean of all stated 1-sigma errors*  
779 *divided by  $\sqrt{N}$  where  $N$  is the number of datasets available for that year, assuming that*  
780 *the errors are uncorrelated. The standard deviation ( $\sigma$ ) is also given to illustrate the level of*  
781 *agreement between datasets for each year when multiple datasets are available (2003*  
782 *onwards).*

783

784 There is generally a good level of agreement between the datasets (Figure 9), and taken  
785 together they provide an average estimate of 171 Gt/yr of ice mass loss (or sea level budget  
786 contribution) from Greenland for the period 1993 to 2016, increasing to 272 Gt/yr for the  
787 period 2005 to 2016 (Table 5).

788 All the datasets illustrate the previously documented accelerating mass loss up to 2012  
789 (Rignot et al., 2011, Velicogna, 2009) . In 2012, the ice sheet experienced exceptional surface  
790 melting reaching as far as the summit (Nghiem et al., 2012) and a record mass loss since, at  
791 least 1958, of over 400 Gt (van den Broeke et al., 2016) . The following years, however, show  
792 a reduced loss (not more than 270 Gt in any year). Inclusion of the years since 2012 in the  
793 2005-2016 trend estimate reduces the overall rate of mass loss acceleration and its statistical  
794 significance. There is greater divergence in the GRACE time series for 2016. We associate  
795 this with the degradation of the satellites as they came towards the end of their mission. For  
796 2005-2012, it might be inferred that there is a secular trend towards greater mass loss and  
797 from 2010-2012 the value is relatively constant. Inter-annual variability in mass balance of  
798 the ice sheet is driven, primarily, by the surface mass balance (i.e. atmospheric weather) and it  
799 is apparent that the magnitude of this year to year variability can be large: exceeding 360 Gt  
800 (or 1 mm sea level equivalent) between 2012 and 2013. Caution is required, therefore, in  
801 extrapolating trends from a short record such as this.

802

## 803 **2.6 Antarctica**

804 The annual turn over of mass of Antarctica is about 2,200 Gt/yr (over 6 mm/yr of SLE), 5  
805 times larger than in Greenland (Wessem et al. 2017). In contrast to Greenland, ice and snow  
806 melt have a negligible influence on Antarctica's mass balance which is therefore completely  
807 controlled by the balance between snowfall accumulation in the drainage basins and ice  
808 discharge along the periphery. The continent is also 7 times larger than Greenland, which  
809 makes satellite techniques absolutely essential to survey the continent. Interannual variations  
810 in accumulation are large in Antarctica, showing decadal to multi-decadal variability, so that  
811 many years of data are required to extract trends, and missions limited to only a few years  
812 may produce misleading results (e.g. Rignot et al., 2011).

813 As in Greenland, the estimation of the mass balance has employed a variety of techniques,  
814 including 1) the gravity method with GRACE since April 2002 until the end of the mission in  
815 late 2016; 2) the IOM method using a series of Landsat and Synthetic-Aperture Radar (SAR)  
816 satellites for measuring ice motion along the periphery (Rignot et al., 2011), ice thickness  
817 from airborne depth radar sounders such as Operation IceBridge (Leuschen et al., 2014), and  
818 reconstructions of surface mass balance using regional atmospheric climate models  
819 constrained by re-analysis data (RACMO, MAR and others); and 3) radar/laser altimetry  
820 method which mix various satellite altimeters and correct ice elevation changes with density  
821 changes from firm models. The largest uncertainty in the GRACE estimate in Antarctica is the  
822 GIA which is larger than in Greenland and a large fraction of the observed signal. The IOM  
823 method compares two large numbers with large uncertainties to estimate the mass balance as  
824 the difference. In order to detect an imbalance at the 10% level, surface mass balance and ice  
825 discharge need to be estimated with a precision typically of 5 to 7%. The altimetry method is  
826 limited to areas of shallow slope, hence is difficult to use in the Antarctic Peninsula and in the  
827 deep interior of the Antarctic continent due to unknown variations of the penetration depth of  
828 the signal in snow/firn. The only method that expresses the partitioning of the mass balance  
829 between surface processes and dynamic processes is the IOM method (e.g. Rignot et al.,  
830 2011). The gravity method is an integrand method which does not suffer from the limitations  
831 of SMB models but is limited in spatial resolution (e.g. Velicogna et al., 2014). The altimetry  
832 method provides independent evidence of changes in ice dynamics, e.g. by revealing rapid ice  
833 thinning along the ice streams and glaciers revealed by ice motion maps, as opposed to large  
834 scale variations reflecting a variability in surface mass balance (McMillan et al., 2014).

835 All these techniques have improved in quality over time and have accumulated a decade to  
836 several decades of observations, so that we are now able to assess the mass balance of the  
837 Antarctic continent using methods with reasonably low uncertainties, and multiple lines of

838 evidence as the methods are largely independent, which increases confidence in the results  
 839 (see recent publication by the IMBIE Team, 2018). There is broad agreement in the mass loss  
 840 from the Antarctic Peninsula and West Antarctica; most residual uncertainties are associated  
 841 with East Antarctica as the signal is relatively small compared to the uncertainties, although  
 842 most estimates tend to indicate a low contribution to sea level (e.g. Shepherd et al., 2012).

843

#### 844 2.6.1 Datasets considered for the assessment

845 This assessment considers the following datasets:

846

Reference	Method	2005-2015 SLE Trend (mm/yr)	1993-2015 SLE Trend (mm/yr)
Update from Martín-Español et al. (2016)	Joint inversion GRACE/altimetry /GPS	0.43±0.07	-
Update from Forsberg et al. (2017)	Joint inversion GRACE/CryoSat	0.31±0.02	-
Update from Groh and Horwath (2016)	GRACE	0.32±0.11	-
Update from Luthcke et al. (2013)	GRACE	0.36±0.06	-
Update from Sasgen et al. (2013)	GRACE	0.47±0.07	-
Update from Velicogna et al. (2014)	GRACE	0.33±0.08	-
Update from Wiese et al. (2016)	GRACE	0.39±0.02	-
Update from Wouters et al. (2013)	GRACE	0.41±0.05	-
Update from Rignot et al. 2011	Input/Output method (IOM)	0.46±0.05	0.25±0.1
Update from Schrama et al. (2014); version 1	GRACE ICE6G GIA model	0.47±0.03	
Update from Schrama et al. (2014); version 2	GRACE Updated GIA models	0.33±0.03	



847 *Table 6. Datasets considered in this assessment of the Antarctica mass change, and*  
 848 *associated trends for the 2005-2015 and 1993-2015 expressed in mm/yr SLE. Positive values*  
 849 *mean positive contribution to sea level (i.e. sea level rise)*

850  
 851  
 852 In Table 6, the negative trend estimate by Zwally et al. (2016) is not added. It is worth noting  
 853 that including it would only slightly reduce the ensemble mean trend.

854

855

## 856 **2.6.2 Methods and analyses**

857 The datasets used in this assessment are Antarctica mass balance time series generated using  
 858 different approaches. Two estimates are a joint inversion of GRACE/altimetry/GPS data  
 859 (Martín-Español et al.,2016), and GRACE and CryoSat data (Forsberg et al.,2017). Two  
 860 methods are mascon solutions obtained from the GRACE intersatellite range-rate  
 861 measurements over equal-area spherical caps covering the Earth' surface (Luthcke et al.,  
 862 2013; Wiese et al., 2016), three estimates use the GRACE spherical harmonics solutions  
 863 (Velicogna et al., 2014; Wiese et al., 2016; Wouters et al., 2013) and one gridded GRACE  
 864 products (Sasgen et. al., 2013).

865 All GRACE time series were provided as monthly time series except for the one using the  
 866 Martín-Español et al. (2016) method that were provided as annual estimates. In addition,  
 867 different groups use different GIA corrections, therefore the spread of the trend solutions  
 868 represents also the error associated to the GIA correction which, in Antarctica, is the largest  
 869 source of uncertainty. Sasgen et al. (2013) used their own GIA solution (Sasgen et al., 2017),  
 870 Martín-Español et al. (2016) as well, Luthcke et al., (2013), Velicogna et al. (2014) and Groh  
 871 and Horwath (2016) used IJ05-R2 (Ivins et al., 2013), Wouter et al. (2013) used Whitehouse  
 872 et al. (2012), and Wise et al. (2016) used A et al. (2013). In addition, Groh and Horwath  
 873 (2016) did not include the peripheral glaciers and ice caps, while all other estimates do.

874 Table 6 shows the Antarctic contribution to sea level during 2005-2015 from the different  
 875 GRACE solutions, and for the input and output method (IOM).. There is a single IOM-based  
 876 dataset that provides trends for the period 1993-2015 (update of Rignot et al., 2011). For the  
 877 period 2005-2015, we calculated the annual sea level contribution from Antarctica using  
 878 GRACE and IOM estimates (Table 7).

879 As we are interested in evaluating the long-term trend and inter-annual variability of the  
 880 Antarctic contribution to sea level, for each GRACE datasets available in monthly time series,  
 881 we first removed the annual and sub-annual components of the signal by applying a 13-month  
 882 averaging filter and we then used the smoothed time series to calculate to annual mass

883 change. Figure 10 shows the annual sea level contribution from Antarctica calculated from  
 884 the GRACE-derived estimates and for the Input-Output method. The GRACE mean annual  
 885 estimates are calculated as the mean of the annual contributions from the different groups, and  
 886 the associated error calculated as the sum of the spread of the annual estimates and the mean  
 887 annual error.

888

889

### 890 2.6.3 Results

891

892

893

894

895

896

897

898

899

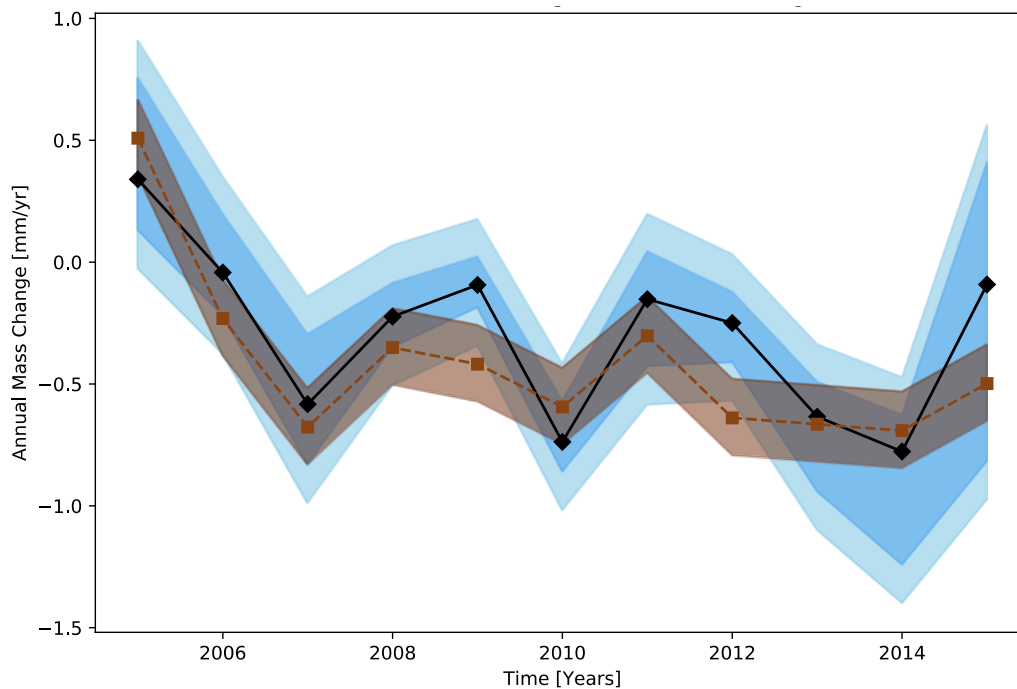
900

901

902

903

904



905 *Figure 10. Antarctic annual sea level contribution during 2005 to 2015. The black squares*  
 906 *are the mean annual sea level calculated using the GRACE datasets listed in Table 6. The*  
 907 *darker blue band shows the range of estimates from the datasets. The light blue band account*  
 908 *for the error in the different GRACE estimates. The brown squares are the annual sea level*  
 909 *contribution calculated using the Input-Output method (updated from Rignot et al., 2011), the*  
 910 *light brown band is the associated error.*

911

912

<b>Year</b>	<b>GRACE mm/yr SLE</b>	<b>IOM mm/yr SLE</b>	<b>Mean mm/yr SLE</b>

2005	-0.34±0.47	-0.51±0.16	-0.42±0.31
2006	0.04±0.36	0.23±0.16	0.14±0.26
2007	0.58±0.42	0.68±0.16	0.63±0.29
2008	0.22±0.29	0.35±0.16	0.29±0.22
2009	0.09±0.26	0.42±0.16	0.26±0.21
2010	0.74±0.30	0.59±0.16	0.67±0.23
2011	0.15±0.39	0.30±0.16	0.23±0.27
2012	0.25±0.30	0.64±0.16	0.44±0.23
2013	0.63±0.38	0.67±0.16	0.65±0.27
2014	0.78±0.46	0.69±0.16	0.73±0.31
2015	0.09±0.77	0.50±0.16	0.29±0.46
Average estimate 2005-2015	0.38±0.06	0.46±0.05	0.42±0.06

913 *Table 7. Annual sea level contribution from Antarctica during 2005-2015 from GRACE and*  
914 *Input-Output method (IOM) calculated as described above and expressed in mm/yr SLE. Also*  
915 *shown is the mean of the estimate from the two methods, associated errors are the mean of the*  
916 *two estimated errors. Positive values mean positive contribution to sea level (i.e. sea level*  
917 *rise)*

918  
919 There is generally broad agreement between the GRACE datasets (Figure 10), as most of the  
920 differences between GRACE estimates are caused by differences in the GIA correction. We  
921 find a reasonable agreement between GRACE and the IOM estimates although the IOM  
922 estimates indicate higher losses. Taken together, these estimates yield an average of 0.42  
923 mm/yr sea level budget contribution from Antarctica for the period 2005 to 2015 (Table 7)  
924 and 0.25 mm/yr sea level for the time period 1993-2005, where the latter value is based on  
925 IOM only.

926 All the datasets illustrate the previously documented accelerating mass loss of Antarctica  
927 (Rignot et al., 2011, Velicogna, 2009). In 2005-2010, the ice sheet experienced ice mass loss  
928 driven by an increase in mass loss in the Amundsen Sea sector of West Antarctica (Mouginot  
929 et al., 2014). The following years showed a reduced increase in mass loss, as colder ocean  
930 conditions prevailed in the Amundsen Sea Embayment sector of West Antarctica in 2012-  
931 2013 which reduced the melting of the ice shelves in front of the glaciers (Dutrieux et al.,

932 2014). Divergence in the GRACE time series is observed after 2015 due to the degradation of  
933 the satellites towards the end of the mission.

934 The large inter-annual variability in mass balance in 2005-2015, characteristic of Antarctica,  
935 nearly masks out the trend in mass loss, which is more apparent in the longer time series than  
936 in short time series. The longer record highlights the pronounced decadal variability in ice  
937 sheet mass balance in Antarctica, demonstrating the need for multi-decadal time series in  
938 Antarctica, which have been obtained only by IOM and altimetry. The inter-annual variability  
939 in mass balance is driven almost entirely by surface mass balance processes. The mass loss of  
940 Antarctica, about 200 Gt/yr in recent years, is only about 10% of its annual turn over of mass  
941 (2,200 Gt/yr), in contrast with Greenland where the mass loss has been growing rapidly to  
942 nearly 100% of the annual turn over of mass. This comparison illustrates the challenge of  
943 detecting mass balance changes in Antarctica, but at the same time, that satellite techniques  
944 and their interpretation have made tremendous progress over the last 10 years, producing  
945 realistic and consistent estimates of the mass using a number of independent methods  
946 (Bamber et al., 2018; the IMBIE Team, 2018).

947

## 948 **2.7 Terrestrial Water Storage**

949 Human transformations of the Earth's surface have impacted the terrestrial water balance,  
950 including continental patterns of river flow and water exchange between land, atmosphere and  
951 ocean, ultimately affecting global sea level. For instance, massive impoundment of water in  
952 man-made reservoirs has reduced the direct outflow of water to the sea through rivers, while  
953 groundwater abstractions, wetland and lake storage losses, deforestation and other land use  
954 changes have caused changes to the terrestrial water balance, including changing  
955 evapotranspiration over land, leading to net changes in land-ocean exchanges (Chao et al.,  
956 2008; Wada et al., 2012a,b; Konikow 2011; Church et al., 2013; Doll et al., 2014a,b). Overall,  
957 the combined effects of direct anthropogenic processes have reduced land water storage,  
958 increasing the rate of sea level rise (SLR) by 0.3-0.5 mm/yr during recent decades (Church et  
959 al., 2013; Gregory et al., 2013; Wada et al., 2016). Additionally, recent work has shown that  
960 climate driven changes in water stores can perturb the rate of sea level change over  
961 interannual to decadal time scales, making global land mass budget closure sensitive to  
962 varying observational periods (Cazenave et al., 2014; Dieng et al., 2015; Reager et al., 2016;  
963 Rietbroek et al., 2016). Here we discuss each of the major component contributions from

964 land, with a summary in Table 8, and estimate the net terrestrial water storage (TWS)  
965 contribution to sea level.

966

### 967 *2.7.1 Direct anthropogenic changes in terrestrial water storage*

968

#### 969 Water impoundment behind dams

970 Wada et al. (2016) built on work by Chao et al. (2008) to combine multiple global reservoir  
971 storage data sets in pursuit of a quality-controlled global reservoir database. The result is a list  
972 of 48064 reservoirs that have a combined total capacity of 7968 km<sup>3</sup>. The time history of  
973 growth of the total global reservoir capacity reflects the history of the human activity in dam  
974 building. Applying assumptions from Chao et al. (2008), Wada et al. (2016) estimated that  
975 humans have impounded a total of 10,416 km<sup>3</sup> of water behind dams, accounting for a  
976 cumulative 29 mm drop in global mean sea level. From 1950 to 2000 when global dam-  
977 building activity was at its highest, impoundment contributed to the average rate of sea level  
978 change at -0.51 mm/year. This was an important process in comparison to other natural and  
979 anthropogenic sources of sea level change over the past century, but has now largely slowed  
980 due to a global decrease in dam building activity.

981

#### 982 Global groundwater depletion

983 Groundwater currently represents the largest secular trend component to the land water  
984 storage budget. The rate of groundwater depletion (GWD) and its contribution to sea level has  
985 been subject to debate (Gregory et al., 2013; Taylor et al., 2013). In the IPCC AR4 (Solomon  
986 et al., 2007), the contribution of non-frozen terrestrial waters (including GWD) to sea-level  
987 variation was not considered due to its perceived uncertainty (Wada, 2016). Observations  
988 from GRACE opened a path to monitor total water storage changes including groundwater in  
989 data scarce regions (Strassberg et al., 2007; Rodell et al. 2009; Tiwari et al. 2009; Jacob et al.,  
990 2012; Shamsudduha et al., 2012; Voss et al., 2013). Some studies have also applied global  
991 hydrological models in combination with the GRACE data (see Wada et al., 2016 for a  
992 review).

993 Earlier estimates of GWD contribution to sea level range from 0.075 mm yr<sup>-1</sup> to 0.30 mm yr<sup>-1</sup>  
994 (Sahagian et al., 1994; Gornitz, 1995, 2001; Foster and Loucks, 2006). More recently, Wada  
995 et al. (2012b), using hydrological modelling, estimated that the contribution of GWD to  
996 global sea level increased from 0.035 (±0.009) to 0.57 (±0.09) mm/yr during the 20<sup>th</sup> century  
997 and projected that it would further increase to 0.82 (±0.13) mm/yr by 2050. Döll et al. (2014)

998 used hydrological modeling, well observations, and GRACE satellite gravity anomalies to  
999 estimate a 2000–2009 global GWD of  $113 \text{ km}^3/\text{yr}$  ( $0.314 \text{ mm}/\text{yr SLE}$ ). This value represents  
1000 the impact of human groundwater withdrawals only and does not consider the effect of  
1001 climate variability on groundwater storage. A study by Konikow (2011) estimated global  
1002 GWD to be  $145 (\pm 39) \text{ km}^3/\text{yr}$  ( $0.41 \pm 0.1 \text{ mm}/\text{yr SLE}$ ) during 1991–2008 based on  
1003 measurements of changes in groundwater storage from in situ observations, calibrated  
1004 groundwater modelling, GRACE satellite data and extrapolation to unobserved aquifers.

1005 An assumption of most existing global estimates of GWD impacts on sea level change is that  
1006 nearly 100% of the GWD ends up in the ocean. However, groundwater pumping can also  
1007 perturb regional climate due to land-atmosphere interactions (Lo and Famiglietti, 2013). A  
1008 recent study by Wada et al. (2016) used a coupled land-atmosphere model simulation to track  
1009 the fate of water pumped from underground and found it more likely that ~80% of the GWD  
1010 ends up in the ocean over the long-term, while 20% re-infiltrates and remains in land storage.  
1011 They estimated an updated contribution of GWD to global sea level rise ranging from  $0.02$   
1012 ( $\pm 0.004$ )  $\text{mm}/\text{yr}$  in 1900 to  $0.27 (\pm 0.04) \text{ mm}/\text{yr}$  in 2000 (Figure 11). This indicates that  
1013 previous studies had likely overestimated the cumulative contribution of GWD to global SLR  
1014 during the 20<sup>th</sup> century and early 21<sup>st</sup> century by 5–10 mm.

1015

#### 1016 Land cover and land-use change

1017 Humans have altered a large part of the land surface, replacing 33% (Vitousek et al., 1997) or  
1018 even 41 % (Sterling et al., 2013) of natural vegetation by anthropogenic land cover such as  
1019 crop fields or pasture. Such land cover change can affect terrestrial hydrology by changing the  
1020 infiltration-to-runoff ratio, and can impact subsurface water dynamics by modifying recharge  
1021 and increasing groundwater storage (Scanlon et al., 2007). The combined effects of  
1022 anthropogenic land cover changes on land water storage can be quite complex. Using a  
1023 combined hydrological and water resource model, Bosmans et al. (2017) estimated that land  
1024 cover change between 1850 and 2000 has contributed to a discharge increase of  $1058 \text{ km}^3/\text{yr}$ ,  
1025 on the same order of magnitude as the effect of human water use. These recent model results  
1026 suggest that land-use change is an important topic for further investigation in the future. So  
1027 far, this contribution remains highly uncertain.

1028

#### 1029 Deforestation/afforestation

1030 At present, large losses in tropical forests and moderate gains in temperate-boreal forests  
1031 result in a net reduction of global forest cover (FAO, 2015; Keenan et al., 2015; MacDicken,

1032 2015; Sloan and Sayer, 2015). Net deforestation releases carbon and water stored in both  
1033 biotic tissues and soil, which leads to sea level rise through three primary processes:  
1034 deforestation-induced runoff increases (Gornitz et al., 1997), carbon loss-related decay and  
1035 plant storage loss, and complex climate feedbacks (Butt et al., 2011; Chagnon and Bras, 2005;  
1036 Nobre et al., 2009; Shukla et al., 1990; Spracklen et al., 2012). Due to these three causes, and  
1037 if uncertainties from the land-atmospheric coupling are excluded, a summary by Wada et al.  
1038 (2016) suggests that the current net global deforestation leads to an upper-bound contribution  
1039 of  $\sim 0.035$  mm/yr SLE.

1040

#### 1041 Wetland degradation

1042 Wetland degradation contributes to sea level primarily through (i) direct water drainage or  
1043 removal from standing inundation, soil moisture, and plant storage, and (ii) water release from  
1044 vegetation decay and peat combustion. Wada et al. (2016) consider a recent wetland loss rate  
1045 of  $0.565\%$   $\text{yr}^{-1}$  since 1990 (Davidson, 2014) and a present global wetland area of 371 mha  
1046 averaged from three databases: Matthews natural wetlands (Matthews and Fung, 1987),  
1047 ISLSCP (Darras, 1999), and DISCover (Belward et al., 1999; Loveland and Belward, 1997).  
1048 They assume a uniform 1-meter depth of water in wetlands (Milly et al., 2010), to estimate a  
1049 contribution of recent global wetland drainage to sea level of 0.067 mm/yr. Wada et al. (2016)  
1050 apply a wetland area and loss rate as used for assessing wetland water drainage, to determine  
1051 the annual reduction of wetland carbon stock since 1990, if completely emitted, releases water  
1052 equivalent to 0.003–0.007 mm/yr SLE. Integrating the impacts of wetland drainage, oxidation  
1053 and peat combustion, Wada et al. (2016) suggest that the recent global wetland degradation  
1054 results in an upper bound of 0.074 mm/yr SLE.

1055

#### 1056 Lake storage changes

1057 Lakes store the greatest mass of liquid water on the terrestrial surface (Oki and Kanae, 2006),  
1058 yet, because of their “dynamic” nature (Sheng et al., 2016; Wang et al., 2012), their overall  
1059 contribution to sea level remains uncertain. In the past century, perhaps the greatest  
1060 contributor in global lake storage was the Caspian Sea (Milly et al., 2010), where the water  
1061 level exhibits substantial oscillations attributed to meteorological, geological, and  
1062 anthropogenic factors (Ozyavas et al., 2010, Chen et al., 2017). Assuming the lake level  
1063 variation kept pace with groundwater changes (Sahagian et al., 1994), the overall contribution  
1064 of the Caspian Sea, including both surface and groundwater storage variations through 2014,  
1065 has been about 0.03 mm/yr SLE since 1900,  $0.075 (\pm 0.002)$  mm/yr since 1995, or 0.109

1066 ( $\pm 0.004$ ) mm/yr since 2002. Additionally, between 1960 and 1990, the water storage in the  
 1067 Aral Sea Basin declined at a striking rate of  $64 \text{ km}^3/\text{yr}$ , equivalent to  $0.18 \text{ mm/yr SLE}$   
 1068 (Sahagian, 2000; Sahagian et al., 1994; Vörösmarty and Sahagian, 2000) due mostly to  
 1069 upstream water diversion for irrigation (Perera, 1993), which was modeled by Pokhrel et al.  
 1070 (2012) to be  $\sim 500 \text{ km}^3$  during 1951–2000, equivalent to  $0.03 \text{ mm/yr SLE}$ . Dramatic decline in  
 1071 the Aral Sea continued in the recent decade, with an annual rate of  $6.043 (\pm 0.082) \text{ km}^3/\text{yr}$   
 1072 measured from 2002 to 2014 (Schwatke et al., 2015). Assuming that groundwater drainage  
 1073 has kept pace with lake level reduction (Sahagian et al., 1994), the Aral Sea has contributed  
 1074  $0.0358 (\pm 0.0003) \text{ mm/yr}$  to the recent sea level rise.

1075

### 1076 Water cycle variability

1077 Natural changes in the interannual to decadal cycling of water can have a large effect on the  
 1078 apparent rate of sea level change over decadal and shorter time periods (Milly et al., 2003;  
 1079 Lettenmaier and Milly, 2009; Llovel et al., 2010). For instance, ENSO-driven modulations of  
 1080 the global water cycle can be important in decadal-scale sea level budgets and can mask  
 1081 underlying secular trends in sea level (Cazenave et al., 2014, Nerem et al., 2018).

1082 Sea level variability due to climate-driven hydrology represents a super-imposed variability  
 1083 on the secular rates of global mean sea level rise. While this term can be large and is  
 1084 important in the interpretation of the sea level record, it is arguably the most difficult term in  
 1085 the land water budget to quantify.

1086

1087

1088

1089

1090

1091

1092

1093

1094

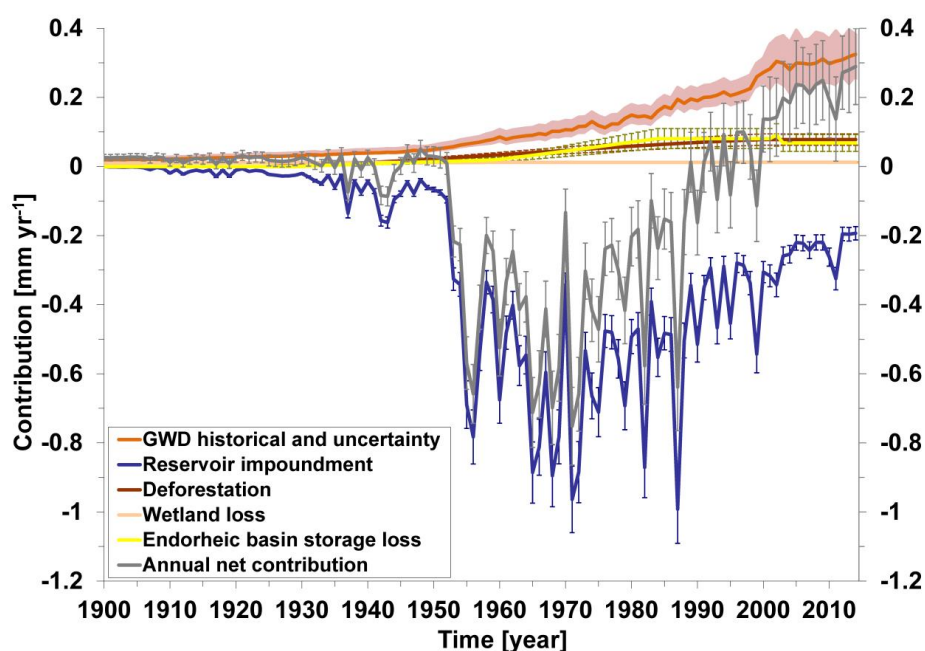
1095

1096

1097

1098

1099





1100  
1101  
1102  
1103  
1104  
1105  
1106  
1107  
1108  
1109  
1110  
1111  
1112  
1113  
1114  
1115  
1116  
1117  
1118  
1119  
1120  
1121  
1122  
1123  
1124  
1125  
1126  
1127  
1128  
1129  
1130  
1131  
1132  
1133  
1134

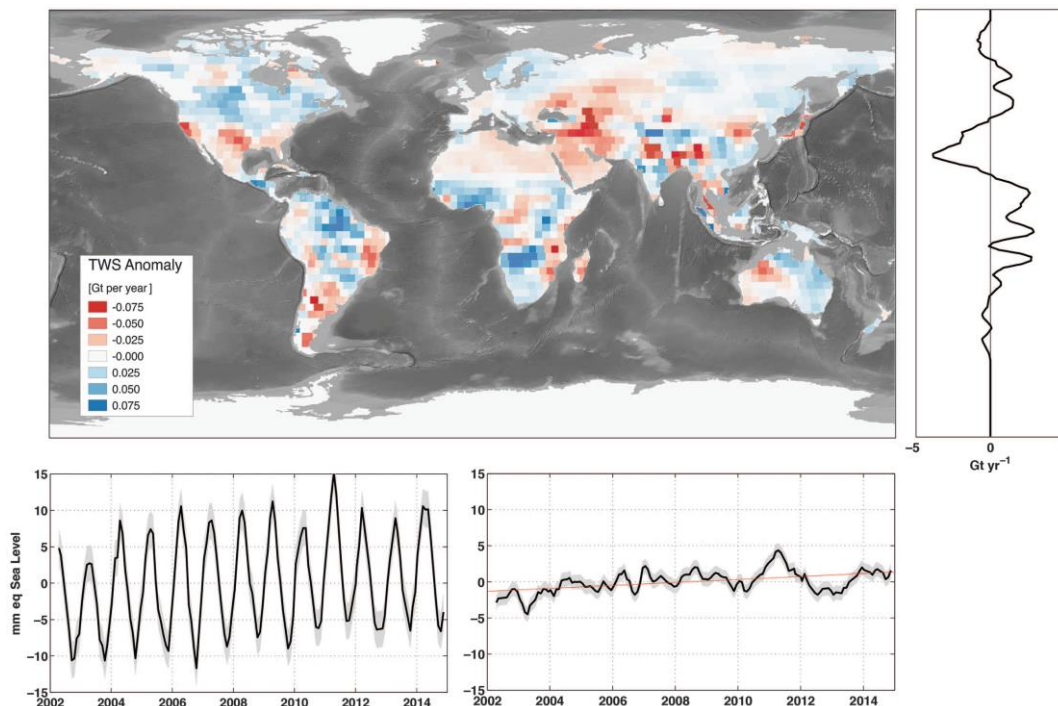
*Figure 11: Time series of the estimated annual contribution of terrestrial water storage change to global sea-level over the period 1900-2014 (rates in  $\text{mm yr}^{-1}$  SLE) (modified from Wada et al., 2016).*

### **2.7.2. Net terrestrial water storage**

#### GRACE-based estimates

Measurements of non-ice-sheet continental land mass from GRACE satellite gravity have been presented in several recent studies (Jensen et al., 2013, Rietbroek et al., 2016; Reager et al., 2016, Scanlon et al., 2018), and can be used to constrain a global land mass budget. Note that these ‘top-down’ estimates contain both climate-driven and direct anthropogenic driven effects, which makes them most useful in assessing the total impact of land water storage changes and closing the budget of all contributing terms. GRACE observations, when averaged over the whole land domain following Reager et al. (2016), indicate a total TWS change (including glaciers) over the 2002-2014 study period of approximately  $+0.32 \pm 0.13$  mm/yr SLE (i.e., ocean gaining mass). Global mountain glaciers have been estimated to lose mass at a rate of  $0.65 \pm 0.09$  mm/yr (e.g. Gardner et al., 2013; Reager et al., 2016) during that period, such that a mass balance indicates that global glacier-free land gained water at a rate of  $-0.33 \pm 0.16$  mm/yr SLE (i.e., ocean losing mass; Figure 12). A roughly similar estimate was found from GRACE using glacier free river basins globally ( $-0.21 \pm 0.09$  mm/yr) (Scanlon et al., 2018). Thus, the GRACE-based net TWS estimates suggest a negative sea level contribution from land over the GRACE period (Table 8). However, mass change estimate from GRACE incorporates uncertainty from all potential error sources that arise in processing and post-processing of the data, including from the GIA model, and from the geocenter and mean pole corrections.

1135  
 1136  
 1137  
 1138  
 1139  
 1140  
 1141  
 1142  
 1143  
 1144  
 1145  
 1146  
 1147  
 1148  
 1149  
 1150



1151 *Figure 12: An example of trends in land water storage from GRACE observations, April*  
 1152 *2002 to November 2014. Glaciers and ice sheets are excluded. Shown are the global map*  
 1153 *(gigatons per year), zonal trends, and full time series of land water storage (in mm/yr SLE).*  
 1154 *Following methods details in Reager et al., (2016), GRACE shows a total gain in land water*  
 1155 *storage during the 2002-2014 period, corresponding to a sea level trend of  $-0.33 \pm 0.16$*   
 1156 *mm/yr<sup>1</sup> SLE (modified from Reager et al., 2016). These trends include all human-driven and*  
 1157 *climate-driven processes in Table 1, and can be used to close the land water budget over the*  
 1158 *study period.*

1159

### 1160 Estimates based on global hydrological models

1161 Global land water storage can also be estimated from global hydrological models (GHMs)  
 1162 and global land surface models. These compute water, or water and energy balances, at the  
 1163 Earth surface, yielding time variations of water storage in response to prescribed  
 1164 atmospheric data (temperature, humidity and wind) and the incident water and energy  
 1165 fluxes from the atmosphere (precipitation and radiation). Meteorological forcing is usually  
 1166 based on atmospheric model reanalysis. Model uncertainties result from several factors.  
 1167 Recent work has underlined the large differences among different state-of-the-art  
 1168 precipitation datasets (Beck et al., 2017) with large impacts on model results at seasonal  
 1169 (Schellekens et al., 2017) and longer time scales (Felfelani et al., 2017). Another source of  
 1170 uncertainty is the treatment of subsurface storage in soils and aquifers, as well as dynamic

1171 changes in storage capacity due to representation of frozen soils and permafrost, the  
 1172 complex effects of dynamic vegetation, atmospheric vapor pressure deficit estimation and  
 1173 an insufficiently deep soil column. A recent study by Scanlon et al. (2018) compared water  
 1174 storage trends from five global land surface models and two global hydrological models to  
 1175 GRACE storage trends, and found that models estimated the opposite trend in net land  
 1176 water storage to GRACE over the 2002 – 2014 period. These authors attributed this  
 1177 discrepancy to model deficiencies, in particular soil depth limitations. These combined error  
 1178 sources are responsible for a range of storage trends across models of approximately  $0.5 \pm$   
 1179  $0.2$  mm/yr SLE. In terms of global land average, model differences can cause up to  $\sim 0.4$   
 1180 mm/yr SLE uncertainty.

1181

1182

<b>Estimate Terrestrial Water Storage contribution to sea level</b>		<b>2002-2014/15 (mm/yr) SLE (Positive values mean sea level rise)</b>
<b>Human contributions by component</b>		
Ground water depletion	<i>Wada et al. (2016)</i>	0.30 ( $\pm$ 0.1)
Reservoir impoundment	<i>Wada et al. (2017)</i>	-0.24 ( $\pm$ 0.02)
Deforestation (after 2010)	<i>Wada et al. (2017)</i>	0.035
Wetland loss (after 1990)	<i>Wada et al. (2017)</i>	0.074
Endorheic basin storage loss		
Caspian Sea	<i>Wada et al. (2017)</i>	0.109 ( $\pm$ 0.004)
Aral Sea	<i>Wada et al. (2017)</i>	0.036 ( $\pm$ 0.0003)
Aggregated human intervention (sum of above)	<i>Scanlon et al. (2018)</i>	0.15 to 0.24
<b>Hydrological model-based estimates</b>		
WGHM model ( <i>natural variability plus human intervention; P. Döll, personal communication</i> )		0.15 +/- 0.14
ISBA-TRIP model ( <i>natural variability only ; Decharme et al., 2016</i> ) + human intervention from <i>Wada et al. (2016)</i> (from <i>Dieng et al., 2017</i> )		0.23 +/- 0.10
<b>GRACE-based estimates of total land water storage (not including glaciers)</b> ( <i>Reager et al., 2016; Rietbroek et al., 2016; Scanlon et al., 2018</i> )		-0.20 to -0.33 ( $\pm$ 0.09 - 0.16)

1183

1184 *Table 8. Estimates of TWS components due to human intervention and net TWS based on*  
 1185 *hydrological models and GRACE*

1186

1187

1188 **2.7.3 Synthesis**

1189 Based on the different approaches to estimate the net land water storage contribution, we  
1190 estimate that corresponding sea level rate ranges from -0.33 to 0.23 mm/yr during the period  
1191 of 2002-2014/15 due to water storage changes (Table 8). According to GRACE, the net TWS  
1192 change (i.e. not including glaciers) over the period 2002-2014 shows a negative contribution  
1193 to sea level of -0.33 mm/yr and -0.21 mm/yr by Reager et al. (2016) and Scanlon et al. (2018)  
1194 respectively. Such a negative signal is not currently reproduced by hydrological models which  
1195 estimate slightly positive trends over the same period (see Table 8). It is to be noted however  
1196 that looking at trends only over periods of the order of a decade may not be appropriate due  
1197 the strong interannual variability of TWS at basin and global scales. For example, Figure 5  
1198 from Scanlon et al. (2018) (see also Figure S9 from their Supplementary Material), that  
1199 compares GRACE TWS and model estimates over large river basins over 2002-2014, clearly  
1200 show that the discrepancies between GRACE and models occur at the end of the record for  
1201 the majority of basins. This is particularly striking for the Amazon basin (the largest  
1202 contributor to TWS), for which GRACE and models agree reasonably well until 2011, and  
1203 then depart significantly, with GRACE TWS showing strongly positive trend since then,  
1204 unlike models. Such a divergence at the end of the record is also noticed for several other  
1205 large basins (see Scanlon et al., Figure S9 SM). No clear explanation can be provided yet,  
1206 even though one may question the quality of the meteorological forcing used by hydrological  
1207 models for the recent years. But this calls for some caution when comparing GRACE and  
1208 models on the basis of trends only because of the dominant interannual variability of the TWS  
1209 component. Much more work is needed to understand differences among models, and  
1210 between models and GRACE. Of all components entering in the sea level budget, the TWS  
1211 contribution currently appears as the most uncertain one.

1212

1213 **2.8 Glacial Isostatic Adjustment**

1214 The Earth's dynamic response to the waxing and waning of the late-Pleistocene ice sheets is  
1215 still causing isostatic disequilibrium in various regions of the world. The accompanying slow  
1216 process of GIA is responsible for regional and global fluctuations in relative and absolute sea  
1217 level, 3D crustal deformations and changes of the Earth's gravity field (for a review, see  
1218 Spada, 2017). To isolate the contribution of current climate change, geodetic observations  
1219 must be corrected for the effects of GIA (King et al., 2010). These are obtained by solving the

1220 “Sea Level Equation” (Farrell and Clark 1976, Mitrovica and Milne 2003). The sea level can  
 1221 be expressed as  $S=N-U$ , where  $S$  is the rate of change of sea-level relative to the solid Earth,  $N$   
 1222 is the geocentric rate of sea-level change, and  $U$  is the vertical rate of displacement of the  
 1223 solid Earth. The sea level equation accounts for solid Earth deformational, gravitational and  
 1224 rotational effects on sea level, which are sensitive to the Earth’s mechanical properties and to  
 1225 the melting chronology of continental ice. Forward GIA modeling, based on the solution of  
 1226 the sea level equation, provides predictions of unique spatial patterns (or *fingerprints*, see Plag  
 1227 and Juetner, 2001) of relative and geocentric sea-level change (e.g., Milne et al. 2009, Kopp  
 1228 et al. 2015). During the last decades, the two fundamental components of GIA modeling have  
 1229 been progressively constrained from the observed history of relative sea level during the  
 1230 Holocene (see e.g., Lambeck and Chappell 2001, Peltier 2004). In the context of climate  
 1231 change, the importance of GIA has been recognized in the mid 1980s, when the awareness of  
 1232 global sea-level rise stimulated the evaluation of the isostatic contribution to tide gauge  
 1233 observations (see Table 1 in Spada and Galassi 2012). Subsequently, GIA models have been  
 1234 applied to the study of the pattern of sea level change from satellite altimetry (Tamisiea  
 1235 2011), and since 2002 to the study of the gravity field variations from GRACE. Our primary  
 1236 goal here is to analyse GIA model outputs that have been used to infer global mean sea level  
 1237 change and ice sheet volume change from geodetic datasets during the altimetry era. These  
 1238 outputs are the sea-level variations detected by satellite altimetry across oceanic regions ( $n$ ),  
 1239 the ocean mass change ( $w$ ) and the modern ice sheets mass balance from GRACE. We also  
 1240 discuss the GIA correction that needs to be applied to GRACE-based land water storage  
 1241 changes. The GIA correction applied to tide gauge-based sea level observations at the  
 1242 coastlines is not discussed here. Since GIA evolves on time scales of millennia (e.g., Turcotte  
 1243 and Schubert, 2014), the rate of change of all the isostatic signals can be considered constant  
 1244 on the time scale of interest.

1245

### 1246 **2.8.1 GIA correction to altimetry-based sea level**

1247 Unlike tide gauges, altimeters directly sample the sea surface in a geocentric reference frame.  
 1248 Nevertheless, GIA contributes significantly to the rates of absolute sea-level change observed  
 1249 over the “altimetry era”, which require a correction  $N_{gia}$  that is obtained by solving the SLE  
 1250 (e.g., Spada 2017). As discussed in detail by Tamisiea (2011),  $N_{gia}$  is sensitive to the assumed  
 1251 rheological profile of the Earth and to the history of continental glacial ice sheets. The  
 1252 variance of  $N_{gia}$  over the surface of the oceans is much reduced, being primarily determined  
 1253 by the change of the Earth’s gravity potential, apart from a spatially uniform shift. As

1254 discussed by Spada and Galassi (2016), the GIA contribution  $N_{gia}$  is strongly affected by  
 1255 variations in the centrifugal potential associated with Earth rotation, whose fingerprint is  
 1256 dominated by a spherical harmonic contribution of degree  $l=2$  and order  $m=\pm 1$ . Since  $N_{gia}$  has  
 1257 a smooth spatial pattern, the global the GIA correction to altimetry data can be obtained by  
 1258 simply subtracting its average  $n = \langle N_{gia} \rangle$  over the ocean sampled by the altimetry missions.  
 1259 The computation of the GIA contribution  $N_{gia}$  has been the subject of various investigations,  
 1260 based on different GIA models. The estimate by Peltier (2001) of  $n$  equals  $-0.30$  mm/yr,  
 1261 based on the ICE-4G (VM2) GIA model. Such a value has been adopted in the majority of  
 1262 studies estimating the GMSL rise from altimetry. Since  $n$  appears to be small compared to the  
 1263 global mean sea-level rise from altimetry ( $\sim 3$  mm/yr), a more precise evaluation has not been  
 1264 of concern until recently. However, it is important to notice that  $n$  is of comparable magnitude  
 1265 as the GMSL trend uncertainty, currently estimated to  $\sim 0.3$  mm/yr (see sub section 2.2). In  
 1266 Table 9a, we summarize the values of  $n$  according to works in the literature where various  
 1267 GIA model models and averaging methods have been employed. Based on values in Table 9a  
 1268 for which a standard deviation is available, the average of  $n$  (weighted by the inverse of  
 1269 associated errors), assumed to represent the best estimate, is  $n = (-0.29 \pm 0.02)$  mm/yr where  
 1270 the uncertainty corresponds to  $2\sigma$ .

1271

### 1272 **2.8.2 GIA correction to GRACE-based ocean mass**

1273 GRACE observations of present-day gravity variations are sensitive to GIA, due to the sheer  
 1274 amount of rock material that is transported by GIA throughout the mantle and the resulting  
 1275 changes in surface topography, especially over the formerly glaciated areas. The continuous  
 1276 change in the gravity field results in a nearly linear signal in GRACE observations. Since the  
 1277 gravity field is determined by global mass redistribution, GIA models used to correct GRACE  
 1278 data need to be global as well, especially when the region of interest is represented by all  
 1279 ocean areas. To date, the only global ice reconstruction publicly available is provided by the  
 1280 University of Toronto. Their latest product, named ICE-6G, has been published and  
 1281 distributed in 2015 (Peltier et al., 2015); note that the ice history has been simultaneously  
 1282 constrained with a specific Earth model, named VM5a. During the early period of the  
 1283 GRACE mission, the available Toronto model was ICE-5G (VM2) (Peltier, 2004). However,  
 1284 different groups have independently computed GIA model solutions based on the Toronto ice  
 1285 history reconstruction, by using different implementations of GIA codes and somehow  
 1286 different Earth models. The most widely used model is the one by Paulson et al. (2007), later  
 1287 updated by A et al. (2013). Both studies use a deglaciation history based on ICE-5G, but

1288 differ for the viscosity profile of the mantle: A et al. use a 3D compressible Earth with VM2  
1289 viscosity profile and a PREM-based elastic structure used by Peltier (2004), whereas Paulson  
1290 et al. (2007) use an incompressible Earth with self-gravitation, and a Maxwell 1-D multi-layer  
1291 mantle. Over most of the oceans, the GIA signature is much smaller than over the continents.  
1292 However, once integrated over the global ocean, the signal  $w$  due to GIA is about -1 mm/yr of  
1293 equivalent sea level change (Chambers et al., 2010), which is of the same order of magnitude  
1294 as the total ocean mass change induced by increased ice melt (Leuliette and Willis, 2011). The  
1295 main uncertainty in the GIA contribution to ocean mass change estimates, apart from the  
1296 general uncertainty in ice history and Earth mechanical properties, originates from the  
1297 importance of changes in the orientation of the Earth's rotation axis (Chambers et al., 2010,  
1298 Tamisiea, 2011). Different choices in implementing the so-called "rotational feedback" lead  
1299 to significant changes in the resulting GIA contribution to GRACE estimates. The issue of  
1300 properly accounting from rotational effects has not been settled yet (Mitrovica et al., 2005,  
1301 Peltier and Luthcke, 2009, Mitrovica and Wahr, 2011, Martinec and Hagedoorn, 2014). Table  
1302 9b summarizes the values of the mass-rate GIA contribution  $w$  according to the literature,  
1303 where various models and averaging methods are employed. The weighed average of the  
1304 values in Table 9b for which an assessment of the standard deviation is available, is  $w = (-$   
1305  $1.44 \pm 0.36)$  mm/yr (the uncertainty is  $2\sigma$ ), which we assume to represent the preferred  
1306 estimate.

1307

### 1308 ***2.8.3 GIA correction to GRACE-based terrestrial water storage***

1309 As discussed in the previous section, the GIA correction to apply to GRACE over land is  
1310 significant, especially in regions formerly covered by the ice sheets (Canada and  
1311 Scandinavia). Over Canada, GIA models significantly differ. This is illustrated in Figure 13  
1312 that shows difference between two models of GIA correction to GRACE over land, the A et  
1313 al. (2013) and Peltier et al. (2009) models. We see that over the majority of the land areas,  
1314 differences are small, except over north Canada, in particular around the Hudson Bay, where  
1315 differences larger than +/- 20 mm/yr SLE are noticed. This may affect GRACE-based TWS  
1316 estimates over Canadian river basins.

1317

1318

1319

1320

1321

1322  
 1323  
 1324  
 1325  
 1326  
 1327  
 1328  
 1329  
 1330  
 1331  
 1332  
 1333  
 1334  
 1335  
 1336  
 1337  
 1338  
 1339  
 1340  
 1341  
 1342  
 1343  
 1344  
 1345  
 1346  
 1347  
 1348  
 1349  
 1350  
 1351  
 1352  
 1353  
 1354  
 1355

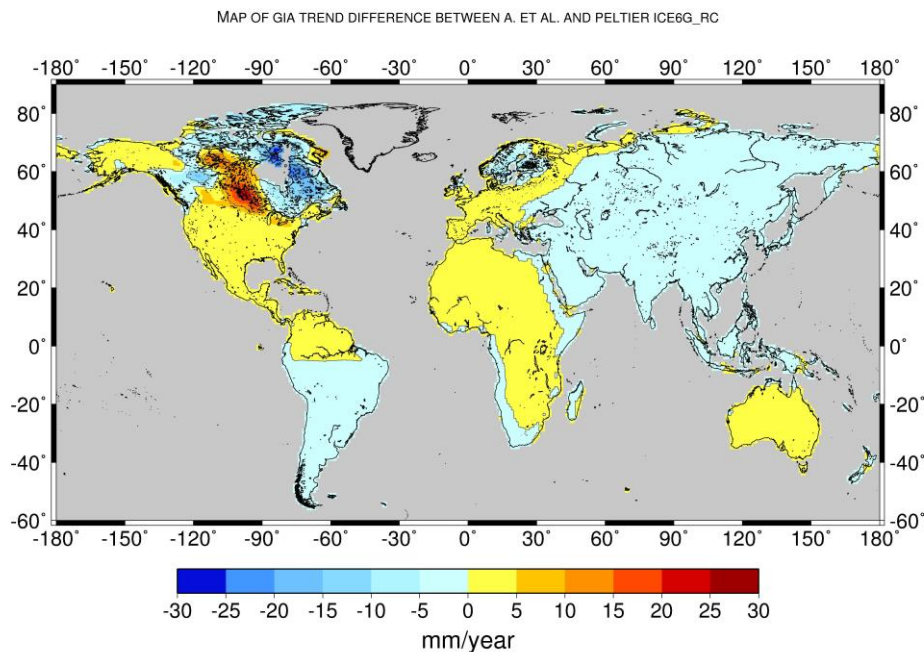


Figure 13: Difference map between two models of GIA correction to GRACE over land: A et al. (2013) versus Peltier et al. (2015), the units in mm/yr SLE.

When averaged over the whole land surface as done in some studies to estimate the combined effect of land water storage and glacier melting from GRACE (e.g., Reager et al., 2015; see section 2.7), the GIA correction ranges from  $\sim 0.5$  to  $0.7$  mm/yr (in mm/yr SLE). Values for different GIA models are given in Table 9c.

#### 2.8.4 GIA correction to GRACE-based ice sheet mass balance

The GRACE gravity field observations allow the determination of mass balances of ice sheets and large glacier systems with inaccuracy similar or superior to the input-output method or satellite laser and radar altimetry (Shepherd et al., 2012). However, GRACE ice-mass balances rely on successfully separating and removing the apparent mass change related to GIA. While the GIA correction is small compared to the mass balance for Greenland ice sheet (ca.  $< 10\%$ ), its magnitude and uncertainty in Antarctica is of the order of the ice-mass balance itself (e.g. Martín-Español et al., 2016). Particularly for today's glaciated areas, GIA remains poorly resolved due to the sparse data constraining the models, leading to large uncertainties in the climate history, the geometry and retreat chronology of the ice sheet, as well as the Earth structure. The consequences are ambiguous GIA predictions, despite fitting



1356 the same observational data. There are two principal approaches towards resolving GIA  
 1357 underneath the ice sheets. Empirical estimates can be derived making use of the different  
 1358 sensitivities of satellite observations to ice-mass changes and GIA (e.g. Riva et al., 2009, Wu  
 1359 et al., 2010). Alternatively, GIA can be modeled numerically by forcing an Earth model with  
 1360 a fixed ice retreat scenario (e.g., Peltier 2009, Whitehouse et al., 2012) or with output from a  
 1361 thermodynamic ice sheet model (Gomez et al., 2013, Konrad et al., 2015). Values of GIA-  
 1362 induced apparent mass change for Greenland and Antarctica as listed in the literature should  
 1363 be applied with caution (Table 9d) when applying them to GRACE mass balances. Each of  
 1364 these estimates may rely on a different GRACE post-processing strategy and may differ in the  
 1365 approach used for solving the gravimetric inverse problem (mascon analysis, forward-  
 1366 modeling, averaging kernels). Of particular concern is the modeling and filtering of the pole  
 1367 tide correction caused by the rotational variations related to GIA, affecting coefficients of  
 1368 harmonic degree  $l=2$  and order  $m=\pm 1$ . As mentioned above, agreement on the modeling of  
 1369 the rotational feedback has not been reached within the GIA community. Furthermore, the  
 1370 pole tide correction applied during the determination gravity-field solutions differs between  
 1371 the GRACE processing centres and may not be consistent with the GIA correction listed. This  
 1372 inconsistency may introduce a significant bias in the ice-mass balance estimates (e.g. Sasgen  
 1373 et al., 2013, Supplementary Material). Wahr et al. (2015) presented recommendations on how  
 1374 to treat the pole tides in GRACE analysis. However, a systematic inter-comparison of the GIA  
 1375 predictions in terms of their low-degree coefficients and their consistency with the GRACE  
 1376 processing standards still need to be done.

1377

1378 *Table 9. Estimated contributions of GIA to the rate of absolute sea level change observed by*  
 1379 *altimetry (a), to the rate of mass change observed by GRACE over the global oceans (b), to*  
 1380 *the rate of mass change observed by GRACE over land (c), and to Greenland and Antarctic*  
 1381 *ice sheets (c), during the altimetry era. The GIA corrections are expressed in mm/yr SLE*  
 1382 *except over Greenland and Antarctica where values are given in Gt/yr (ice mass equivalent).*  
 1383 *Most of the GIA contributions are expressed as a value  $\pm$  one standard deviation; a few*  
 1384 *others are given in terms of a plausible range, for some the uncertainties are not specified.*

1385

(a) GIA correction to absolute sea level measured by altimetry

<i>Reference</i>	<i>GIA</i> ( <i>mm/yr</i> )	<i>Notes</i>
Peltier (2009) (Table 3)	-0.30 ± 0.02 -0.29 ± 0.03 -0.28 ± 0.02	Average of 3 groups of 4 values obtained by variants of the analysis procedure, using ICE-5G(VM2), over a global ocean, in the range of latitudes 66°S to 66°N and 60°S to 60°N, respectively.
Tamisiea (2011) (Figure 2)	-0.15 to -0.45 -0.20 to -0.50	Simple average over the oceans for a range of estimates obtained varying the Earth model parameters, over a global ocean and between latitudes 66°S and 66°N.
Huang (2013) (Table 3.6)	-0.26 ± 0.07 -0.27 ± 0.08	Average from an ensemble of 14 GIA models over a global ocean and between latitude from 66°S to 66°N.
Spada (2017) (Table 1)	-0.32 ± 0.08	Based on four runs of the Sea Level Equation solver SELEN (Spada and Stocchi, 2007) using model ICE-5G(VM2), with different assumptions in solving the SLE.

(b) GIA contribution to GRACE mass-rate of change over the oceans

<i>Reference</i>	<i>GIA</i> ( <i>mm/yr SLE</i> )	<i>Notes</i>
Peltier (2009) (Table 3)	-1.60 ± 0.30	Average of values from 12 corrections for variants of the analysis procedure, using ICE-5G (VM2).
Chambers (2010) (Table 1)	-1.45 ± 0.35	Average over the oceans for a range of estimates produced by varying the Earth models.
Tamisiea (2011) (Figures 3 and 4)	-0.5 to -1.9 -0.9 to -1.5	Ocean average of a range of estimates varying the Earth model, and based on a restricted set, respectively.
Huang (2013) (Table 3.7)	-1.31 ± 0.40 -1.26 ± 0.43	Average from an ensemble of 14 GIA models over a global ocean and between latitude from 66°S to 66°N, respectively.

(c) GIA contribution to GRACE-based terrestrial water storage change

*Reference*                      *GIA correction (mm/yr SLE)*  
*(without Greenland, Antarctica, Iceland,*  
*Svalbard, Hudson Bay and Black Sea*

A et al. (2013)	0.63
Peltier ICE5G	0.68
Peltier ICE6G_rc	0.71
ANU_ICE6G	0.53

(d) GIA contribution to GRACE mass-rate of the ice sheets

<i>Reference</i>	<b><i>Greenland</i></b>	
	<i>GIA</i> <i>(Gt/yr)</i>	<i>Notes</i>
Simpson et al. (2009) <sup>r</sup>	$-3 \pm 12^m$	Thermodynamic sheet / solid Earth model, 1D (uncoupled); constrained by geomorphology; inversion results in Sutterley <i>et al.</i> (2014).
Peltier (2009) (ICE-5G) <sup>g</sup>	$-4^f$	Ice load reconstruction / solid Earth model, 1D (ICE-5G / similar to VM2); Greenland component of ICE-5G (13 Gt/yr) + Laurentide component of ICE-5G (-17 Gt/yr); inversion results in Khan <i>et al.</i> 2016, Discussion.
Khan <i>et al.</i> (2016) (GGG-1D) <sup>r</sup>	$15 \pm 10^f$	Ice load reconstruction / solid Earth model, 1D (uncoupled); constrained with geomorphology & GPS; Greenland component (+32 Gt/yr) + Laurentide component of ICE-5G (-17 Gt/yr); inversion results in Khan <i>et al.</i> (2016), Discussion.
Fleming <i>et al.</i> (2004) <sup>r</sup> (Green1)	$3^f$	Ice load reconstruction / solid Earth model, 1D (uncoupled); constrained with geomorphology; Greenland component (+ 20 Gt/yr) + Laurentide component of ICE-5G (-17 Gt/yr); inversion in Sasgen <i>et al.</i> (2012, supplement).

Wu *et al.* (2010)<sup>g</sup>  $-69 \pm 19^m$  Joint inversion estimate based on GPS, satellite laser ranging, and very long baseline interferometry, and bottom pressure from ocean model output; inversion results in Sutterley *et al.* (2014).

### ***Antarctica***

<i>Reference</i>	<i>GIA</i> ( <i>Gt/yr</i> )	<i>Notes</i>
Whitehouse <i>et al.</i> (2012) (W12a) <sup>r</sup>	60 <sup>n</sup>	Thermodynamic sheet / solid Earth model, 1D (uncoupled); constrained by geomorphology; inversion results in Shepherd <i>et al.</i> 2012, supplement (Fig. S8).
Ivins <i>et al.</i> (2013) (IJ05_R2) <sup>r</sup>	40-65 <sup>n</sup>	Ice load reconstruction / solid Earth model, 1D; constrained by geomorphology and GPS uplift rates; Ivins <i>et al.</i> 2013; inversion results in Shepherd <i>et al.</i> 2012, supplement (Fig. S8).
Peltier (2009) (ICE-5G) <sup>g</sup>	140-180 <sup>n</sup>	Ice load reconstruction / solid Earth model ICE-5G(VM2); constrained by geomorphology; inversion results in Shepherd <i>et al.</i> 2012, supplement (Fig. S8).
Argus <i>et al.</i> (2014) (ICE-6G) <sup>g</sup>	107 <sup>n</sup>	Ice load reconstruction / solid Earth model ICE-6G(VM5a); constrained by geomorphology and GPS; theory recently corrected by Purcell <i>et al.</i> 2016; inversion results in Argus <i>et al.</i> (2014), conclusion 7.8.
Sasgen <i>et al.</i> (2017) (REGINA) <sup>r</sup>	$55 \pm 22^f$	Joint inversion estimate based on GRACE, altimetry, GPS and viscoelastic response functions; lateral heterogeneous Earth model parameters; inversion results in Sasgen <i>et al.</i> (2017), Table 1.
Gunter <i>et al.</i> (2014) (G14) <sup>r</sup>	ca. $64 \pm 40^a$ (multimodel uncert.)	Joint inversion estimate based on GRACE, altimetry, GPS and regional climate model output; conversion of uplift to mass using average rock density; inversion results in, Gunter <i>et al.</i> (2014) Table 1.

Martin-Español *et al.*  $55 \pm 8$  Joint inversion estimate based on GRACE, altimetry,  
 (2016) (RATES)<sup>r</sup>  $45 \pm 7^*$  GPS and regional climate model output; inversion results  
 in Sasgen *et al.* (2017), \* is improved for GIA of smaller  
 spatial scales; inversion results in Martin-Español *et al.*  
 (2016), Fig. 6.

---

1386  
 1387 <sup>r</sup> regional model; <sup>g</sup> global model; <sup>m</sup> mascon inversion; <sup>f</sup> forward modeling inversion; <sup>a</sup>  
 1388 averaging kernel inversion; <sup>n</sup> inversion method not specified.  
 1389

1390 The GRACE-based ocean mass, Antarctica mass and terrestrial water storage changes are  
 1391 much model dependent. As these GIA corrections cannot be assessed from independent  
 1392 information, they represent a large source of uncertainties to the sea level budget components  
 1393 based on GRACE.

1394

## 1395 **2.9 Ocean mass change from GRACE**

1396

1397 Since 2002, GRACE satellite gravimetry has provided a revolutionary means for  
 1398 measuring global mass change and redistribution at monthly intervals with unprecedented  
 1399 accuracy, and offered the opportunity to directly estimate ocean mass change due to water  
 1400 exchange between the ocean and other components of the Earth (e.g., ice sheets, mountain  
 1401 glaciers, terrestrial water). GRACE time-variable gravity data have been successfully applied  
 1402 in a series of studies of ice mass balance of polar ice sheets (e.g., Velicogna and Wahr, 2006;  
 1403 Luthcke *et al.*, 2006) and mountain glaciers (e.g., Tamisiea *et al.*, 2005; Chen *et al.*, 2007) and  
 1404 their contributions to global sea level change. GRACE data can also be used to directly study  
 1405 long-term oceanic mass change or non-steric sea level change (e.g., Willis *et al.*, 2008;  
 1406 Leuliette *et al.*, 2009; Cazenave *et al.*, 2009), and provide a unique opportunity to study  
 1407 interannual or long-term TWS change and its potential impacts on sea level change (Richey *et al.*  
 1408 *et al.*, 2015; Reager *et al.*, 2016).

1409 GRACE time-variable gravity data can be used to quantify ocean mass change from three  
 1410 different main approaches. One is through measuring ice mass balance of polar ice sheets and  
 1411 mountain glaciers and variations of TWS, and their contributions to the GMSL (e.g.,  
 1412 Velicogna and Wahr, 2005; Schrama *et al.*, 2014). The second approach is to directly quantify  
 1413 ocean mass change using ocean basin mask (kernel) (e.g., Chambers *et al.*, 2004; Llovel *et al.*,  
 1414 2010; Johnson and Chambers, 2013). In the ocean basin kernel approach, coastal ocean areas

1415 within certain distance (e.g., 300 or 500 km) from the coast are excluded, in order to minimize  
 1416 contaminations from mass change signal over the land (e.g., glacial mass loss and TWS  
 1417 change). The third approach solves mass changes on land and over ocean at the same time via  
 1418 forward modeling (e.g., Chen et al., 2013; Yi et al., 2015). The forward modeling is a global  
 1419 inversion to reconstruct the “true” mass change magnitudes over land and ocean with  
 1420 geographical constraint of locations of the mass change signals, and can help effectively  
 1421 reduce leakage between land and ocean (Chen et al., 2015).

1422

1423 Estimates of ocean mass changes from GRACE are subject to a number of major error  
 1424 sources. These include : (1) leakage errors from the larger signals over ice sheets and land  
 1425 hydrology due to GRACE’s low spatial resolution (of at least a few to several hundred km)  
 1426 and the need of coastal masking, (2) spatial filtering of GRACE data to reduce spatial noise,  
 1427 (3) errors and biases in geophysical model corrections (e.g., GIA, atmospheric mass) that need  
 1428 to be removed from GRACE observations to isolate oceanic mass change and/or polar ice  
 1429 sheets and mountain glaciers mass balance, and (4) residual measurement errors in GRACE  
 1430 gravity measurements, especially those associated with GRACE low-degree gravity changes.  
 1431 In addition, how to deal with the absent degree-1 terms, i.e., geocenter motion in GRACE  
 1432 gravity fields, is expected to affect estimates of GRACE-based oceanic mass rates and ice  
 1433 mass balances.

1434

<b>Data sources</b>	<b>Time Period</b>	<b>Ocean mass trends (mm/yr)</b>
Chen et al. (2013) (A13 GIA)	2005.01- 2011.12	$1.80 \pm 0.47$
Johnson and Chambers (2013) (A13 GIA)	2003.01- 2012.12	$1.80 \pm 0.15$
Purkey et al. (2014) (A13 GIA)	2003.01- 2013.01	$1.53 \pm 0.36$
Dieng et al. (2015a) (Paulson07 GIA)	2005.01- 2012.12	$1.87 \pm 0.11$
Dieng et al. (2015b) (Paulson07 GIA)	2005.01- 2013.12	$2.04 \pm 0.08$

Yi et al. (2015) (A13 GIA)	2005.01- 2014.07	$2.03 \pm 0.25$
Rietbroek et al. (2016)	2002.04- 2014.06	$1.08 \pm 0.30$
Chambers et al. (2017)	2005.0 – 2015.0	$2.11 \pm 0.36$

1435 *Table 10. Recently published (since 2013) estimates of GRACE-based ocean mass rates*  
 1436 *(GIA corrected). Most of the listed studies use either the A13 (A et al., 2013) or*  
 1437 *Paulson07 (Paulson et al., 2007) GIA model.*

1438

1439

1440 With a different treatment of the GRACE land-ocean signal leakage effect through global  
 1441 forward modeling, Chen et al. (2013) estimated ocean mass rates using GRACE RL05 time-  
 1442 variable gravity solutions over the period 2005-2011. They demonstrated that the ocean mass  
 1443 change contributes to  $1.80 \pm 0.47$  mm/yr (over the same period), which is significantly larger  
 1444 than previous estimates over about the same period. Yi et al. (2015) further confirmed that  
 1445 correct calibration of GRACE data and appropriate treatment of GRACE leakage bias are  
 1446 critical to improve the accuracy of GRACE estimated ocean mass rates. Table 10 summarizes  
 1447 different estimates of GRACE ocean mass rates. The uncertainty estimates of the listed  
 1448 studies (Table 10) are computed from different methods, with different considerations of error  
 1449 sources into the error budget, and represent different confidence levels.

1450

1451 As demonstrated in Chen et al. (2013), different treatments of just the degree-2 spherical  
 1452 harmonics of GRACE gravity solution alone can lead to substantial differences in GRACE  
 1453 estimated ocean mass rates (ranging from 1.71 to 2.17 mm/yr). Similar estimates from  
 1454 GRACE gravity solutions from different data processing centers can also be different. In the  
 1455 meantime, long-term degree-1 spherical harmonics variation, representing long-term  
 1456 geocenter motion and neglected in some of the previous studies (due to the lack of accurate  
 1457 observations) are also expected to have non-negligible effect on GRACE derived ocean mass  
 1458 rates (Chen et al., 2013). Different methods for computing ocean mass change using GRACE  
 1459 data may also lead to different estimates (Chen et al., 2013; Johnson and Chambers, 2013,  
 1460 Jensen et al., 2013).

1461 To help better understand the potential and uncertainty of GRACE satellite gravimetry in  
 1462 quantification of the ocean mass rate, Table 11 provides a comparison of GRACE-estimated

1463 ocean mass rates over the period January 2005 to December 2016 based on different GRACE  
1464 data products and different data processing methods, including the CSR, GFZ and JPL  
1465 GRACE RL05 spherical harmonic solutions (i.e., the so-called GSM solutions), and CSR,  
1466 JPL, and GSFC mascon solutions (the available GSFC mascons only cover the period up to  
1467 July 2016). The three GRACE GSM results (CSR, GFZ, and JPL) are updates from Johnson  
1468 and Chambers (2013), with degree-2 zonal term replaced by satellite laser ranging results  
1469 (Cheng and Ries, 2012), geocenter motion from Swenson et al. (2008), GIA model from A et  
1470 al. (2013), an averaging kernel with a land mask that extends out 300 km, and no destriping or  
1471 smoothing, as described in Johnson and Chambers (2013). An update of GRACE ocean mass  
1472 rate from Chen et al. (2013) is also included for comparisons, which is based on the CSR  
1473 GSM solutions using forward modeling (a global inversion approach), with similar treatments  
1474 of the degree-2 zonal term, geocenter motion, and GIA effects.

1475 The JPL mascon ocean mass rate is computed from all mascon grids over the ocean, and  
1476 the GSFC mascon ocean mass rate is computed from all ocean mascons, with the  
1477 Mediterranean, Black and Red Seas excluded. A coastline resolution improvement (CRI)  
1478 filter is already applied in the JPL mascons to reduce leakage (Wiese et al., 2016), and in both  
1479 the GSFC and JPL mascon solutions, the ocean and land are separately defined (Luthcke et  
1480 al., 2013; Watkins et al., 2015). For the CSR mascon results, an averaging kernel with a land  
1481 mask that extends out 200 km is applied to reduced leakage (Chen et al., 2017). Similar  
1482 treatments or corrections of degree-2 zonal term, geocenter motion, and GIA effects are also  
1483 applied in the three mascon solutions. When solving GRACE mascon solutions, the GRACE  
1484 GAD fields (representing ocean bottom pressure changes, or combined atmospheric and  
1485 oceanic mass changes) have been added back to the mascon solutions. To correctly quantify  
1486 ocean mass change using GRACE mascon solutions, the means of the GAD fields over the  
1487 oceans, which represents mean atmospheric mass changes over the ocean (as ocean mass is  
1488 conserved in the GAD fields) need to be removed from GRACE mascon solutions. The  
1489 removal of GAD average over the ocean in GRACE mascon solutions has very minor or  
1490 negligible effect (of  $\sim 0.02$  mm/yr) on ocean mass rate estimates, but is important for studying  
1491 GMSL change at seasonal time scales.

1492 Over the 12-year period (2005-2016), the three GRACE GSM solutions show pretty  
1493 consistent estimates of ocean mass rate, in the range of 2.3 to 2.5 mm/yr. Greater differences  
1494 are noticed for the mascon solutions. The GSFC mascons show the largest rate of 2.61mm/yr.  
1495 The CSR and JPL mascon solutions show relatively smaller ocean mass rates of 1.76 and 2.02  
1496 mm/yr, respectively, over the studied period. Based on the same CSR GSM solutions, the



1497 forward modeling and basin kernel estimates agree reasonably well (2.52 vs. 2.44 mm/yr). In  
 1498 addition to the degree-2 zonal term, geocenter motion, and GIA correction, the degree-2,  
 1499 order-1 spherical harmonics of the current GRACE RL05 solutions are affected by the  
 1500 definition of the reference mean pole in GRACE pole tide correction (Wahr et al., 2015). This  
 1501 mean pole correction, excluded in all estimates listed in Table 11 (for fair comparison), is  
 1502 estimated to contribute  $\sim -0.11$  mm/yr to GMSL. How to reduce errors from the different  
 1503 sources play a critical role in estimating ocean mass change from GRACE time-variable  
 1504 gravity data.

1505

1506

<b>Data sources</b>	<b>Ocean mass trend (mm/yr)</b>
GSM CSR Forward Modeling (update from Chen et al., 2013)	2.52±0.17
GSM CSR (update from Johnson and Chambers, 2013)	2.44±0.15
GSM GFZ (update from Johnson and Chambers, 2013)	2.30±0.15
GSM JPL (update from Johnson and Chambers, 2013)	2.48±0.16
Mascon CSR (200 km)	1.76±0.16
Mascon JPL	2.02±0.16
Mascon GSFC (update from Luthcke et al., 2013)	2.61±0.16
Ensemble mean	2.3 ± 0.19

1507 *Table 11. Ocean mass trends (in mm/yr) estimated from GRACE for the period January 2005*  
 1508 *– December 2016 (the GSFC mascon solutions cover up to July 2016). The uncertainty is*  
 1509 *based on 2 times the sigma of least-squares fitting.*

1510

1511 GRACE satellite gravimetry has brought a completely new era for studying global ocean  
 1512 mass change. Owing to the extended record of GRACE gravity measurements (now over 15  
 1513 years), improved understanding of GRACE gravity data and methods for addressing GRACE  
 1514 limitations (e.g., leakage and low-degree spherical harmonics), and improved knowledge of  
 1515 background geophysical signals (e.g., GIA), GRACE-derived ocean mass rates from different  
 1516 studies in recent years show clearly increased consistency (Table 11). Most of the results  
 1517 agree well with independent observations from satellite altimeter and Argo floats, although  
 1518 the uncertainty ranges are still large. The GRACE Follow-On (FO) mission has been launched  
 1519 in May 2018. The GRACE and GRACE-FO together are expected to provide at least over two  
 1520 (or even three) decades of time-variable gravity measurements. Continuous improvements of

1521 GRACE data quality (in future releases) and background geophysical models are also  
 1522 expected, which will help improve the accuracy GRACE observed ocean mass change.

1523 For the sea level budget assessment over the GRACE period, we will use the ensemble mean.

1524

### 1525 **3. Sea Level Budget results**

1526 In section 2, we have presented the different terms of the sea level budget equation, mostly  
 1527 based on published estimates (and in some cases, from their updates). We now use them to  
 1528 examine the closure of the sea level budget. For all terms, we only consider ensemble mean  
 1529 values.

1530

#### 1531 **3.1 Entire altimetry era (1993-Present)**

1532

##### 1533 *3.1.1 Trend estimates over 1993-Present*

1534 Because it is now clear that the GMSL and some components are accelerating (e.g., Nerem et  
 1535 al., 2018), we propose to characterize the long term variations of the time series by both a  
 1536 trend and an acceleration. We start looking at trends. Table 12 gathers the trends estimated in  
 1537 section 2. The end year is not always the same for all components (see section 2). Thus the  
 1538 word ‘present’ means either 2015 or 2016 depending on the component. As no trend estimate  
 1539 is available for the entire altimetry era for the terrestrial water storage contribution, we do not  
 1540 consider this component. The residual trend (GMSL minus sum of components trend) may  
 1541 then provide some constraint on the TWS contribution.

1542

1543

<b>Component</b>	<b>Trends (mm/yr) 1993-Present</b>
1. GMSL (TOPEX-A drift corrected)	3.07 +/- 0.37
2. Thermosteric sea level (full depth)	1.3 +/- 0.4
3. Glaciers	0.65 +/- 0.15
4. Greenland	0.48 +/- 0.10
5. Antarctica	0.25 +/- 0.10
6. TWS	/
7. Sum of components (without TWS → 2.+3.+4.+5.)	2.7 +/- 0.23

8. GMSL minus sum of components (without TWS)	0.37 +/- 0.3
--	--------------

1544

1545 *Table 12: Trend estimates for individual components of the sea level budget, sum of*  
 1546 *components and GMSL minus sum of components over 1993-present. Uncertainties of the*  
 1547 *sum of components and residuals represent rooted mean squares of components errors,*  
 1548 *assuming that errors are independent.*  
 1549

1550 Results presented in Table 12 are discussed in detail in section 4.

1551

### 1552 **3.1.2 Acceleration**

1553 The GMSL acceleration estimated in section 2.2 using Ablain et al. (2017b)'s TOPEX-A drift  
 1554 correction amounts to 0.10 mm/yr<sup>2</sup> for the 1993-2017 time span. This value is in good  
 1555 agreement with Nerem et al. (2018) estimate (of 0.084 +/- 0.025 mm/yr<sup>2</sup>) over nearly the  
 1556 same period, after removal of the interannual variability of the GMSL. In Nerem et al.  
 1557 (2018), acceleration of individual components are also estimated as well as acceleration of the  
 1558 sum of components. The latter agrees well with the GMSL acceleration. Here we do not  
 1559 estimate the acceleration of the component ensemble means because time series are not  
 1560 always available. We leave this for a future assessment.

1561

## 1562 **3.2 GRACE and Argo period (2005- Present)**

1563

### 1564 **3.2.1 Sea level budget using GRACE-based ocean mass**

1565 If we consider the ensemble mean trends for the GMSL, thermosteric and ocean mass  
 1566 components given in sections 2.2, 2.3 and 2.9 over 2005-present, we find agreement (within  
 1567 error bars) between the observed GMSL (3.5 +/- 0.2 mm/yr) and the sum of Argo-based  
 1568 thermosteric plus GRACE-based ocean mass (3.6 +/- 0.4 mm/yr) (see Table 13). The residual  
 1569 (GMSL minus sum of components) trend amounts to -0.1 mm/yr. Thus in terms of trends, the  
 1570 sea level budget appears closed over this time span within quoted uncertainties.

1571

### 1572 **3.2.2 Trend estimates over 2005-Present from estimates of individual contributions**

1573

1574 Table 13 gathers trends of individual components of the sea level budget over 2005-present,  
 1575 as well sum of components and residuals (GMSL minus sum of components) trend. As for the  
 1576 longer period, ensemble mean values are considered for each component.

1577

<b>Component</b>	<b>Trend (mm/yr) 2005-Present</b>
1. GMSL	3.5 +/- 0.2
2. Thermosteric sea level (full depth)	1.3 +/- 0.4
3. Glaciers	0.74 +/- 0.1
4. Greenland	0.76 +/- 0.1
5. Antarctica	0.42 +/- 0.1
6. TWS from GRACE (mean of Reager et al. and Scanlon et al.)	-0.27 +/- 0.15
7. Sum of components (2.+3.+4.+5.+6.)	2.95 +/- 0.21
8. Sum of components (thermosteric full depth + GRACE-based ocean mass)	3.6 +/- 0.4
9. GMSL minus sum of components (including GRACE-based TWS→2.+3.+4.+5.+6.)	0.55 +/- 0.3
10. GMSL minus sum of components (without GRACE-based TWS→ 2.+3.+4.+5.)	0.28 +/- 0.2
11. GMSL minus sum of components (thermosteric full depth + GRACE-based ocean mass)	-0.1 +/- 0.3

1578

1579 *Table 13: Trend estimates for individual components of the sea level budget, sum of*  
1580 *components and GMSL minus sum of components over 2005-present.*

1581

1582 As for Table 12, the results presented in Table 13 are discussed in detail in section 4.

1583

1584

1585

1586

1587

### 1588 **3.2.3 Year-to-year budget over 2005-Present using GRACE-based ocean mass**

1589

1590 We now examine the year-to-year sea level and mass budgets. Table 14 provides annual mean  
1591 values for the ensemble mean GMSL, GRACE-based ocean mass and Argo-based  
1592 thermosteric component. The components are expressed as anomalies and their reference is  
1593 arbitrary. So to compare with the GMSL, a constant offset for all years was applied to the

1594 thermosteric and ocean mass annual means. The reference year (where all values are set to  
 1595 zero) is 2003.

1596

1597

1598

<b>Year</b>	<b>Ensemble mean GMSL mm</b>	<b>Sum of components mm</b>	<b>GMSL minus sum of components mm</b>
2005	7.00	8.78	-0.78
2006	10.25	10.78	-0.53
2007	10.51	11.35	-0.85
2008	15.33	15.07	0.25
2009	18.78	18.88	-0.10
2010	20.64	20.53	0.11
2011	20.91	21.38	-0.48
2012	31.10	29.33	1.77
2013	33.40	33.87	-0.47
2014	36.65	36.22	0.43
2015	46.34	45.69	0.65

1599

1600 *Table 14. Annual mean values for the ensemble means GMSL and sum of components*  
 1601 *(GRACE-based ocean mass and Argo-based thermosteric, full depth). Constant offset applied*  
 1602 *to the sum of components. The reference year (where all values are set to zero) is 2003.*

1603

1604 Figure 14 shows the sea level budget over 2005-2015 in terms of annual bar chart using  
 1605 values given in Table 14. It compares for years 2005 to 2016 the annual mean GMSL (blue  
 1606 bars) and annual mean sum of thermosteric and GRACE-based ocean mass (red bars). Annual  
 1607 residuals are also shown (green bars). These are either positive or negative depending on  
 1608 years. The trend of these annual residuals is estimated to 0.135 mm/yr.

1609 In Figure 15 is also shown the annual sea level budget over 2005-2015 but now using the  
 1610 individual components for the mass terms. As we have no annual estimates for TWS, we

1611 ignore it, so that the total mass includes only glaciers, Greenland and Antarctica. The annual  
 1612 residuals thus include the TWS component in addition to the missing contributions (e.g., deep  
 1613 ocean warming). For years 2006 to 2011, the residuals are negative, an indication of a  
 1614 negative TWS to sea level as suggested by GRACE results (Reager et al., 2016, Scanlon et al.,  
 1615 2018). But as of 2012, the residuals become positive and on average over 2005-2015, the  
 1616 residual trend amounts +0.28 mm/yr, a value larger than when using GRACE ocean mass.  
 1617 Finally, Figure 16 presents the mass budget. It compares annual GRACE-based ocean mass to  
 1618 the sum of the mass components, without TWS as in Figure 15. The residual trends over  
 1619 2005-2015 time span is 0.14 mm/yr. It may dominantly represent the TWS contribution. From  
 1620 one year to another residuals can be either positive or negative, suggesting important  
 1621 interannual variability in the TWS or even in the deep ocean.

1622

1623

1624

1625

1626

1627

1628

1629

1630

1631

1632

1633

1634

1635

1636

1637

1638

1639

1640

1641

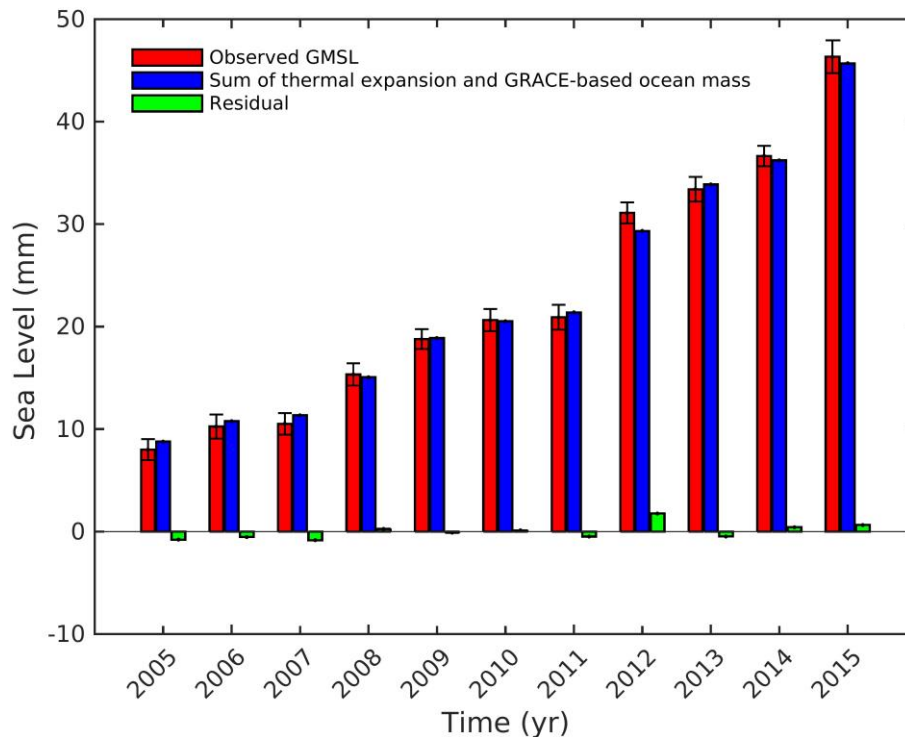
1642

1643

1644

1645

1646



1640 *Figure 14: Annual sea level (blue bars) and sum of thermal expansion (full depth) and*  
 1641 *GRACE ocean mass component (red bars). Black vertical bars are associated uncertainties.*  
 1642 *Annual residuals (green bars) are also shown.*

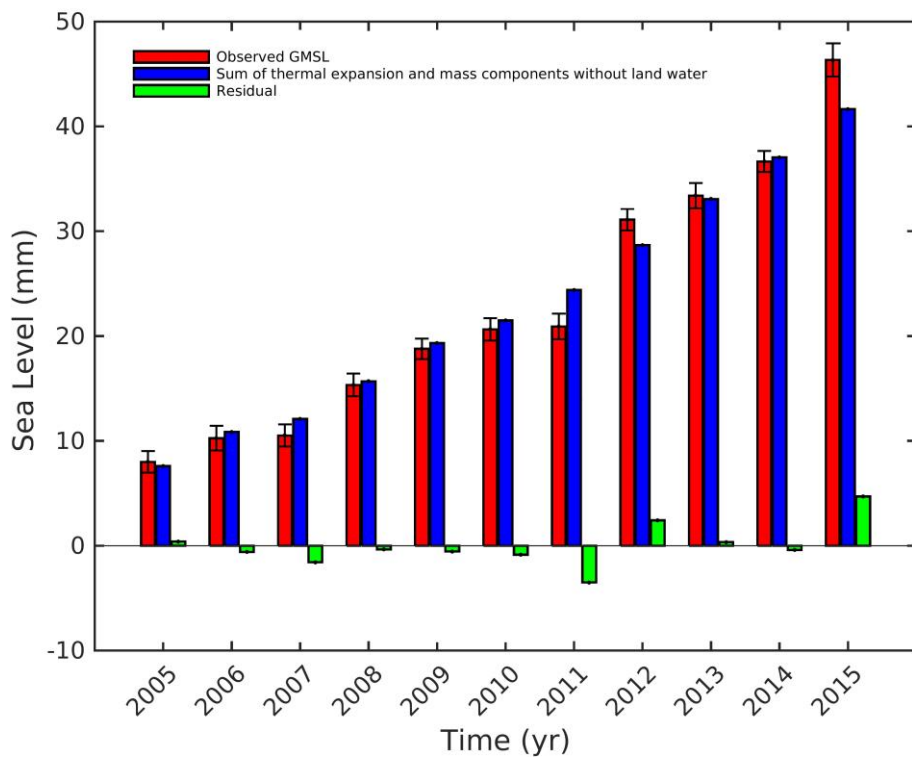


Figure 15: Annual global mean sea level (blue bars) and sum components without TWS (full depth thermal expansion+ glaciers + Greenland + Antarctica) (red bars). Black vertical bars are associated uncertainties. Annual residuals (green bars) are also shown.

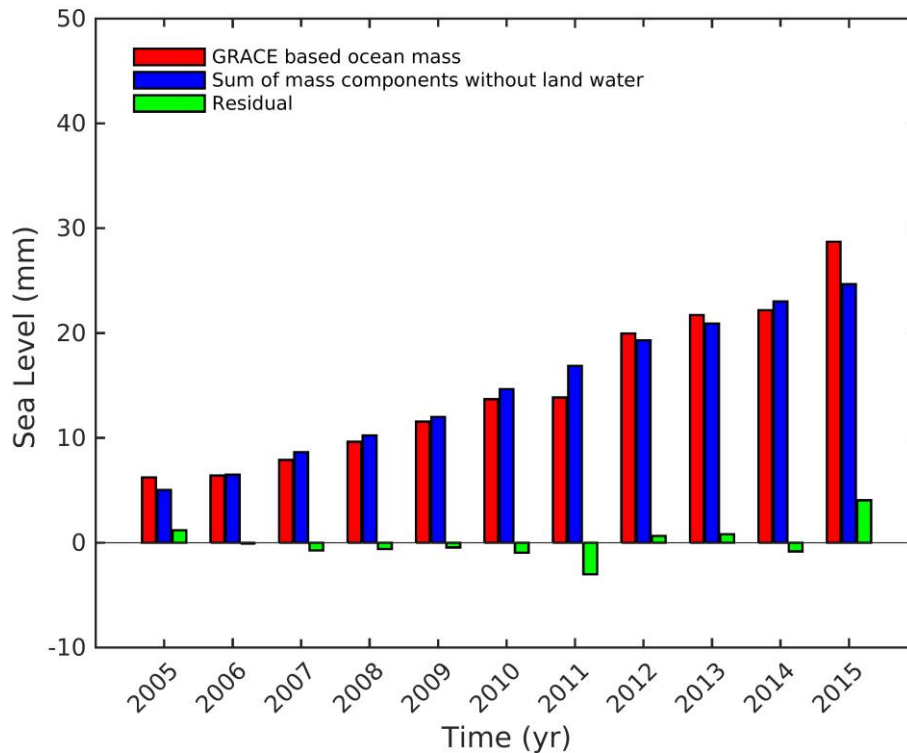


Figure 16: Annual GRACE-based ocean mass (red bars) and sum components without TWS (full depth thermal expansion+ glaciers + Greenland + Antarctica) (blue bars). Annual residuals (green bars) are also shown.

## 4. Discussion

The results presented in section 2 for the components of the sea level budget are based on syntheses of the recently published literature. When needed, the time series have been updated. In section 3, we considered ensemble means for each component to average out random errors of individual estimates. We examined the closure/non closure of the sea level budget using these ensemble mean values, for 2 periods: 1993-present and 2005-present (Argo and GRACE period). Because of the lack of observation-based TWS estimate for the 1993-present time span, we compared the observed GMSL trend to the sum of components excluding TWS. We found a positive residual trend of  $0.37 \pm 0.3$  mm/yr, supposed to



1734 include the TWS contribution, plus other imperfectly known contributions (deep ocean  
1735 warming) and data errors.

1736 For the 2005-present time span, we considered both GRACE-based ocean mass and sum of  
1737 individual mass components, allowing us to also look at the mass budget. For TWS, as  
1738 discussed in section 2.7, GRACE provides a negative trend contribution to sea level over the  
1739 last decade (i.e., increase on water storage on land) attributed to internal natural variability  
1740 (Reager et al., 2016), unlike hydrological models that lead to a small (possible not  
1741 significantly different from zero) positive contribution to sea level over the same period .  
1742 Assuming that GRACE observations are perfect, such discrepancies could be attributed to the  
1743 inability of models to correctly account for uncertainties in meteorological forcing and  
1744 inadequate modeling of soil storage capacity (see discussion in section 2.7). However, when  
1745 looking at the sea level budget over the GRACE time span and using the GRACE-based  
1746 TWS, we find a rather large positive residual trend ( $> 0.5$  mm/yr) that needs to be explained.  
1747 Since GRACE-based ocean mass is supposed to represent all mass terms, one may want to  
1748 attribute this residual trend to an additional contribution of the deep ocean to the abyssal  
1749 contribution already taken into account here, but possibly underestimated because of  
1750 incomplete monitoring by current observing systems. If such a large positive contribution  
1751 from the deep ocean (meaning ocean warming) is real (which is unlikely, given the high  
1752 implied heat storage), this has to be confirmed by independent approaches e.g., using ocean  
1753 reanalysis, and eventually model-based and top-of-the-atmosphere estimates of the Earth  
1754 Energy Imbalance.

1755 In addition to mean trends over the period, we also looked at the annual budget for all years  
1756 starting in 2005. For most components, annual mean values are provided during the Argo-  
1757 GRACE era, except for the terrestrial water storage component. However, the sea level  
1758 budget based on GRACE ocean mass (plus ocean thermal expansion; Figure 14) includes the  
1759 TWS contribution. As shown in Figure 14, yearly residuals are small, suggesting near closure  
1760 of the sea level budget. The residual trend amounts to 0.13 mm/yr. It could be interpreted as  
1761 an additional deep ocean contribution not accounted by the SIO estimate (see section 2.3).  
1762 However, when looking at Figure 14, we note that yearly residuals are either positive or  
1763 negative, an indication of interannual variability that can hardly be explained by a deep ocean  
1764 contribution. The residual trend derived from the difference (GMSL minus sum of  
1765 components) (Table 13) amounts  $-0.1 \pm 0.3$  mm/yr, suggesting a sea level budget closed  
1766 within 0.3 mm/yr over 2005-present, with no substantial deep ocean contribution.

1767 Figure 16 compares GRACE ocean mass to the sum of mass components (excluding TWS,  
1768 for the reasons mentioned above). In principle, this mass budget may provide a constraint on  
1769 the TWS contribution. The corresponding residual trend amounts to 0.14 mm/yr over the  
1770 GRACE period, a value that disagrees with the above quote GRACE-based TWS estimates.  
1771 However, it is worth noting that the GRACE-based TWS trend is much dependent on the  
1772 considered time span because of the strong interannual variability; a recent study by  
1773 Palanisamy et al. (in preparation), based on 347 land river basins, found zero GRACE-based  
1774 TWS trend over 2005-2015. Given the remaining data uncertainties, any robust conclusion  
1775 can hardly be reached so far. That being said, more work is needed to clarify the sign  
1776 discrepancy between GRACE-based and model-based TWS estimates.

1777

## 1778 **5. Concluding Remarks**

1779 As mentioned in the introduction, the global mean sea level budget has been the object of  
1780 numerous previous studies, including successive IPCC assessments of the published literature.  
1781 What is new in the effort presented here, is that it involves the international community  
1782 currently studying present-day sea level and its components. Moreover, it relies on a large  
1783 variety of datasets derived from different space-based and in situ observing systems. Near  
1784 closure of the sea level budget as reported here over the GRACE and Argo era suggests that  
1785 no large systematic errors affect these independent observing systems, including the satellite  
1786 altimetry system. Study of the sea level budget allows improved understanding of the  
1787 different processes causing sea level rise, such as ocean warming and land ice melt. When  
1788 accuracy increases, it will offer an integrative view of the response of the Earth system to  
1789 natural & anthropogenic forcing and internal variability, and provide an independent  
1790 constraint on the current Earth Energy Imbalance. Validation of climate models against  
1791 observations is another important application of this kind of assessment (e.g., Slangen et al.,  
1792 2017).

1793 However, important uncertainties still remain, that affect several terms of the budget; for  
1794 example the GIA correction applied to GRACE data over Antarctica or the net land water  
1795 storage contribution to sea level. The latter results from a variety of factors but is dominated  
1796 by ground water pumping and natural climate variability. Both terms are still uncertain and  
1797 accurately quantifying them remains a challenge.

1798 Several ongoing international projects related to sea level should provide in the near future  
1799 improved estimates of the components of the sea level budget. This is the case, for example,

1800 of the ice sheet mass balance inter-comparison exercise (IMBIE, 2<sup>nd</sup> assessment), a  
1801 community effort supported by NASA (National Aeronautics and Space Administration) and  
1802 ESA, dedicated to reconcile satellite measurements of ice sheet mass balance (The IMBIE  
1803 Team, 2018). This is also the case for the ongoing ESA Sea level Budget Closure project  
1804 (Horwath et al., 2018) that uses a number of space-based Essential Climate Variables (ECVs)  
1805 reprocessed during the last few years in the context of the ESA Climate Change Initiative  
1806 project. The recently launched GRACE follow-on mission will lengthen the current mass  
1807 component time series, with hopefully increased precision and resolution. Finally, the deep  
1808 Argo project, still in an experimental phase, will provide important information on the deep  
1809 ocean heat content in the coming years. Availability of this new data set will be open new  
1810 insight on the total thermosteric component of the sea level budget, allowing constraining  
1811 other missing or poorly known contributions, from the evaluation of the budget.

1812 The sea level budget assessment discussed here essentially relies on trend estimates. But  
1813 annual budget estimates have been proposed for the first time over the GRACE-Argo era. It is  
1814 planned to provide updates of the global sea level budget every year, as done for more than a  
1815 decade for the global carbon budget (Le Quéré et al., 2018). In the next assessments, updates  
1816 of all components will be considered, accounting for improved evaluation of the raw data,  
1817 improved processing and corrections, use of ocean reanalysis, etc. Need for additional  
1818 information where gaps exist should also be considered. As a closing remark, study of the sea  
1819 level budget in terms of time series, not just trends as done here, will be required.

1820 **List of authors and affiliations:**

1821 Anny Cazenave (LEGOS, France & ISSI, Switzerland), Benoit Meyssignac (LEGOS,  
1822 France);

1823 Michael Ablain (CLS, France), Jonathan Bamber (U. Bristol, UK), Valentina Barletta (DTU-  
1824 SPACE, Denmark), Brian Beckley (SGT Inc./NASA GSFC, USA), Jérôme Benveniste  
1825 (ESA/ESRIN, Italy), Etienne Berthier (LEGOS, France), Alejandro Blazquez (LEGOS,  
1826 France), Tim Boyer (NOAA, USA), Denise Caceres (Goethe U., Germany), Don Chambers  
1827 (U. South Florida, USA), Nicolas Champollion (U. Bremen, Germany), Ben Chao (IES-AS,  
1828 Taiwan), Jianli Chen (U. Texas, USA), Lijing Cheng (IAP-CAS, China), John A. Church (U.  
1829 New South Wales, Australia), Stephen Chuter (U. Bristol, UK), J. Graham Cogley (Trent U.,  
1830 Canada), Soenke Dangendorf (U. Siegen, Germany), Damien Desbruyères (IFREMER,  
1831 France), Petra Döll (Goethe U., Germany), Catia Domingues (CSIRO, Australia), Ulrike Falk  
1832 (U. Bremen, Germany), James Famiglietti (JPL/Caltech, USA), Luciana Fenoglio-Marc (U.  
1833 Bonn, Germany), Rene Forsberg (DTU-SPACE, Denmark), Gaia Galassi (U. Urbino, Italy),  
1834 Alex Gardner (JPL/Caltech, USA), Andreas Groh (TU-Dresden, Germany), Benjamin  
1835 Hamlington (Old Dominion U., USA), Anna Hogg (U. Leeds, UK), Martin Horwath (TU-  
1836 Dresden, Germany), Vincent Humphrey (ETHZ, Switzerland), Laurent Husson (U. Grenoble,  
1837 France), Masayoshi Ishii (MRI-JMA, Japan), Adrian Jaeggi (U. Bern, Switzerland), Svetlana  
1838 Jevrejeva (NOC, UK), Gregory Johnson (NOAA/PMEL, USA), Jürgen Kusche (U. Bonn,  
1839 Germany), Kurt Lambeck (ANU, Australia & ISSI, Switzerland), Felix Landerer  
1840 (JPL/Caltech, USA), Paul Leclercq (UIO, Norway), Benoit Legresy (CSIRO, Australia), Eric  
1841 Leuliette (NOAA, USA), William Llovel (LEGOS, France), Laurent Longuevergne (U.  
1842 Rennes, France), Bryant D. Loomis (NASA GSFC, USA), Scott B. Luthcke (NASA GSFC,  
1843 USA), Marta Marcos (UIB, Spain), Ben Marzeion (U. Bremen, Germany), Chris Merchant  
1844 (U. Reading, UK), Mark Merrifield (UCSD, USA), Glenn Milne (U. Ottawa, Canada), Gary  
1845 Mitchum (U. South Florida, USA), Yara Mohajerani (UCI, USA), Maeva Monier (Mercator-  
1846 Ocean, France), Steve Nerem (U. Colorado, USA), Hindumathi Palanisamy (LEGOS,  
1847 France), Frank Paul (UZH, Switzerland), Begoña Perez (Puertos del Estados, Spain),  
1848 Christopher G. Piecuch (WHOI, USA), Rui M. Ponte (AER inc., USA), Sarah G. Purkey  
1849 (SIO/UCSD, USA), John T. Reager (JPL/Caltech, USA), Roelof Rietbroek (U. Bonn,  
1850 Germany), Eric Rignot (UCI and JPL, USA), Riccardo Riva (TU Delft, The Netherlands),  
1851 Dean H. Roemmich (SIO/UCSD USA), Louise Sandberg Sørensen (DTU-SPACE,  
1852 Denmark), Ingo Sasgen (AWI, Germany), E.J.O. Schrama (TU Delft, The Netherlands), Sonia  
1853 I. Seneviratne (ETHZ, Switzerland), C.K. Shum (Ohio State U., USA), Giorgio Spada (U.

1854 Urbino, Italy), Detlef Stammer (U. Hamburg, Germany), Roderic van de Wal (U. Utrecht,  
1855 The Netherlands), Isabella Velicogna (UCI and JPL, USA), Karina von Schuckmann  
1856 (Mercator-Océan, France), Yoshihide Wada (U. Utrecht, The Netherlands), Yiguo Wang  
1857 (NERSC/BCCR, Norway), Christopher Watson (U. Tasmania, Australia), David Wiese  
1858 (JPL/Caltech, USA), Susan Wijffels (CSIRO, Australia), Richard Westaway (U. Bristol, UK),  
1859 Guy Woppelmann (U. La Rochelle, France), Bert Wouters (U. Utrecht, The Netherlands)

1860

1861 **Acknowledgements and author contributions:**

1862 This community assessment was initiated by A. Cazenave and B. Meyssignac as a  
1863 contribution to the Grand Challenge ‘Regional Sea Level and Coastal Impacts’ of the World  
1864 Climate Research Programme (WCRP). The results presented in this paper were prepared by  
1865 9 different teams dedicated to the various terms of the sea level budget (i.e., altimetry-based  
1866 sea level, tide gauges, thermal expansion, glaciers, Greenland, Antarctica, terrestrial water  
1867 storage, glacial isostatic adjustment, ocean mass from GRACE). Thanks to the team leaders  
1868 (in alphabetic order), M. Ablain, J. Bamber, N. Champollion, J. Chen, C. Domingues, S.  
1869 Jevrejeva, J.T. Reager, K. von Schuckmann, G. Spada, I. Velicogna and R. van de Wal, who  
1870 interacted with their team members, collected all needed information, provided a synthesized  
1871 assessment of the literature and when needed, updated the published results. The coordinators  
1872 A.C. and B.M. collected those materials and prepared a first draft of the manuscript, but all  
1873 authors contributed to its refinement and to the discussion of the results. Special thanks are  
1874 addressed to J. Benveniste, E. Berthier, G. Cogley, J. Church, G. Johnson (PMEL  
1875 Contribution Number 4776), B. Marzeion, F. Paul, R. Ponte, and E. Schrama for improving  
1876 the successive versions of the manuscript, and to H. Palanisamy for providing all figures  
1877 presented in section 3.

1878 The views, opinions, and findings contained in this paper are those of the authors and should  
1879 not be construed as an official NOAA, U.S. Government or other institutions position, policy,  
1880 or decision.

1881 We are grateful to the anonymous reviewer for his/her thorough comments that helped to  
1882 improve the manuscript.

1883

1884 **References**

- 1885 1. A G., Chambers, D. P., Calculating trends from GRACE in the presence of large  
1886 changes in continental ice storage and ocean mass. *Geophys. J. Int.*, pp. 272,  
1887 doi:10.1111/j.1365-246X.2008.04012.x, 2008.
- 1888 2. A G., Wahr J. and Zhong S., Computations of the viscoelastic response of a 3-D  
1889 compressible Earth to surface loading: an application to Glacial Isostatic Adjustment  
1890 in Antarctica and Canada, *Geophysical Journal International*, 192.2, 557-572, 2013.
- 1891 3. Ablain M., A. Cazenave, G. Valladeau, and S. Guinehut, "A New Assessment of the  
1892 Error Budget of Global Mean Sea Level Rate Estimated by Satellite Altimetry over  
1893 1993–2008." *Ocean Science*, doi:10.5194/os-5-193-2009, 2009.
- 1894 4. Ablain, M., S. Philipps, M. Urvoy, N. Tran, and N. Picot, "Detection of Long-Term  
1895 Instabilities on Altimeter Backscatter Coefficient Thanks to Wind Speed Data  
1896 Comparisons from Altimeters and Models." *Marine Geodesy* 35 (sup1):258–75,  
1897 doi:10.1080/01490419.2012.718675, 2012.
- 1898 5. Ablain M., A. Cazenave, G. Larnicol, M. Balmaseda, P. Cipollini, Y. Faugère, M. J.  
1899 Fernandes, et al., "Improved Sea Level Record over the Satellite Altimetry Era (1993–  
1900 2010) from the Climate Change Initiative Project." *Ocean Science*, doi:10.5194/os-11-  
1901 67-2015, 2015.
- 1902 6. Ablain M., J. F. Legeais, P. Prandi, M. Marcos, L. Fenoglio-Marc, H. B. Dieng, J.  
1903 Benveniste, and A. Cazenave, "Satellite Altimetry-Based Sea Level at Global and  
1904 Regional Scales." *Surveys in Geophysics*, doi:10.1007/s10712-016-9389-8, 2017a.
- 1905 7. Ablain M., R. Jugier, L. Zawadki, and N. Taburet, "The TOPEX-A Drift and Impacts  
1906 on GMSL Time Series." AVISO Website. October 2017.  
1907 [https://meetings.aviso.altimetry.fr/fileadmin/user\\_upload/tx\\_ausycslseminar/files/Post  
1908 er\\_OSTST17\\_GMSL\\_Drift\\_TOPEX-A.pdf](https://meetings.aviso.altimetry.fr/fileadmin/user_upload/tx_ausycslseminar/files/Poster_OSTST17_GMSL_Drift_TOPEX-A.pdf), 2017b.
- 1909 8. Abraham J. P., et al., A review of global ocean temperature observations: Implications  
1910 for ocean heat content estimates and climate change, *Rev. Geophys.*, 51, 3, 450-483,  
1911 doi:10.1002/rog.20022, 2013.
- 1912 9. Adrian R et al., Lakes as sentinels of climate change *Limnology and Oceanography*  
1913 54:2283-2297 doi:10.4319/lo.2009.54.6\_part\_2.2283, 2009.
- 1914 10. Ahmed M, Sultan M, Wahr J, Yan E, The use of GRACE data to monitor natural and  
1915 anthropogenic induced variations in water availability across Africa *Earth-Science*  
1916 *Reviews* 136:289-300, 2014.
- 1917 11. Argus D.F. Peltier, W. R., Drummond, R., The Antarctica component of postglacial  
1918 rebound model ICE-6G\_C (VM5a) based on GPS positioning, exposure age dating of  
1919 ice thicknesses, and relative sea level histories. *Geophysical Journal International*  
1920 198, 1, 537-563, 2014.
- 1921 12. Armentano TV, Menges ES, Patterns of Change in the Carbon Balance of Organic  
1922 Soil-Wetlands of the Temperate Zone *J Ecol*, 74:755-774, doi:10.2307/2260396,  
1923 1986.
- 1924 13. Awange J.L., Sharifi M.A., Ogonda G., Wickert J., Grafarend E.W., Omulo M., The  
1925 falling Lake Victoria water level: GRACE, TRIMM and CHAMP satellite analysis of  
1926 the lake basin, *Water Resources Management* 22:775-796, 2008.
- 1927 14. Bahr, D. and Radic, V., Significant contribution to total mass from very small glaciers,  
1928 *The Cryosphere*, 6, 763-770, 2012.
- 1929 15. Bahr, D., Pfeffer, W., Sassolas, C. and Meier, M., Response time of glaciers as a  
1930 function of size and mass balance: 1. Theory, *Journal of Geophysical Research: Solid*  
1931 *Earth*, 103, 9777-9782, 1998.
- 1932 16. Balmaseda M.A., K. Mogensen, A. Weaver (2013b). Evaluation of the ECMWF  
1933 Ocean Reanalysis ORAS4. *Q. J. R. Meteorol. Soc.*, doi:10.1002/qj.2063, 2013.

- 1934  
1935  
1936  
1937  
1938  
1939  
1940  
1941  
1942  
1943  
1944  
1945  
1946  
1947  
1948  
1949  
1950  
1951  
1952  
1953  
1954  
1955  
1956  
1957  
1958  
1959  
1960  
1961  
1962  
1963  
1964  
1965  
1966  
1967  
1968  
1969  
1970  
1971  
1972  
1973  
1974  
1975  
1976  
1977  
1978  
1979  
1980  
1981  
1982  
1983
17. Bamber J.L., R.M. Westaway, B. Marzeion and B. Wouters, The land ice contribution to sea level during the satellite era, *Environ. Res. Lett.*, 13, 063008, [doi:10.1088/1748-9326/aac2f0](https://doi.org/10.1088/1748-9326/aac2f0), 2018.
  18. Barletta, V. R., Sørensen, L. S. & Forsberg, R. Scatter of mass changes estimates at basin scale for Greenland and Antarctica, *The Cryosphere*, 7, 1411-1432, 2013.
  19. Barnett, T.P.. The estimation of “global” sea level change: A problem of uniqueness. *J. Geophys. Res.*, 89 (C5), 7980-7988, 1984.
  20. Beck, H. E., van Dijk, A. I., de Roo, A., Dutra, E., Fink, G., Orth, R., & Schellekens, J., Global evaluation of runoff from 10 state-of-the-art hydrological models. *Hydrology and Earth System Sciences*, 21, 6, 2881, 2017.
  21. Becker M, L Lovel W, Cazenave A, Güntner A, Crétaux J-F, Recent hydrological behavior of the East African great lakes region inferred from GRACE, satellite altimetry and rainfall observations, *C. R. Geosci* 342:223-233, 2010.
  22. Beckley, B. D., P. S. Callahan, D. W. Hancock, G. T. Mitchum, and R. D. Ray. “On the ‘Cal-Mode’ Correction to TOPEX Satellite Altimetry and Its Effect on the Global Mean Sea Level Time Series.” *Journal of Geophysical Research, C: Oceans* 122 (11):8371–84. <https://doi.org/10.1002/2017jc013090>, 2017.
  23. Belward AS, Estes JE, Kline KD, The IGBP-DIS global 1-km land-cover data set DISCover: A project overview *Photogrammetric Engineering and Remote Sensing* 65:1013-1020, 1999.
  24. Bindoff, N., J. Willebrand, V. Artale, et al., Observations: Oceanic climate and sea level. In *Climate Change 2007: The Physical Science Basis; Contribution of Working Group I to the Fourth Assessment Report of the Intergovernmental Panel on Climate Change*. Edited by S. Solomon, D. Qin, M. Manning, et al., 386–432. Cambridge, UK, and New York: Cambridge Univ. Press, 2007.
  25. Boening, C., J. K. Willis, F. W. Landerer, R. S. Nerem, and J. Fasullo, The 2011 La Niña: So strong, the oceans fell, *Geophys. Res. Lett.*, 39(19), n/a-n/a, [doi:10.1029/2012GL053055](https://doi.org/10.1029/2012GL053055), 2012.
  26. Bosmans, J. H. C., van Beek, L. P. H., Sutanudjaja, E. H., and Bierkens, M. F. P.: Hydrological impacts of global land cover change and human water use, *Hydrol. Earth Syst. Sci.* 21, 5603–5626, [doi.org/10.5194/hess-21-5603-2017](https://doi.org/10.5194/hess-21-5603-2017), 2017.
  27. Boyer, T., C. Domingues, S. Good, G. C. Johnson, J. M. Lyman, M. Ishii, V. Gouretski, J., Antonov, N. Bindoff, J. Church, R. Cowley, J. Willis, and S. Wijffels. 2015. Sensitivity of global ocean heat content estimates to mapping methods, XBT bias corrections, and baseline climatology, *Journal of Climate*, 29, 4817–4842, [doi:10.1175/JCLI-D-15-0801.1](https://doi.org/10.1175/JCLI-D-15-0801.1), 2016.
  28. Bredehoeft, J. D., The water budget myth revisited: why hydrogeologists model?, *Ground Water*, 40, 340–345, [doi:10.1111/j.1745-6584.2002.tb02511.x](https://doi.org/10.1111/j.1745-6584.2002.tb02511.x), 2002.
  29. Butt N, de Oliveira PA, Costa MH, Evidence that deforestation affects the onset of the rainy season in Rondonia, Brazil *Journal of Geophysical Research-Atmospheres* 116: D11120 [doi:10.1029/2010jd015174](https://doi.org/10.1029/2010jd015174), 2011.
  30. Bolch, T., Sandberg Sørensen, L., Simonsen, S. B., Mölg, N., Machguth, H., Rastner, P. & Paul, F. Mass loss of Greenland's glaciers and ice caps 2003–2008 revealed from ICESat laser altimetry data. *Geophysical Research Letters*, 40, 875-881, 2013.
  31. Box, J. E. & Colgan, W. T., Sea level rise contribution from Arctic land ice: 1850-2100. Snow, Water, Ice and Permafrost in the Arctic (SWIPA) 2017. Oslo, Norway: Arctic Monitoring and Assessment Programme (AMAP), 2017.
  32. Brun, F., Berthier, E., Wagnon, P., Käab, A. and Treichler, D., A spatially resolved estimate of High Mountain Asia mass balances from 2000 to 2016, *Nature Geoscience*, 2017.

- 1984  
1985  
1986  
1987  
1988  
1989  
1990  
1991  
1992  
1993  
1994  
1995  
1996  
1997  
1998  
1999  
2000  
2001  
2002  
2003  
2004  
2005  
2006  
2007  
2008  
2009  
2010  
2011  
2012  
2013  
2014  
2015  
2016  
2017  
2018  
2019  
2020  
2021  
2022  
2023  
2024  
2025  
2026  
2027  
2028  
2029  
2030  
2031  
2032  
2033
33. Cao, G., C. Zheng, B. R. Scanlon, J. Liu, and W. Li, Use of flow modeling to assess sustainability of groundwater resources in the North China Plain, *Water Resour. Res.*, 49, doi:10.1029/2012WR011899, 2013.
  34. Calafat, F.M., Chambers, D.P., and M.N. Tsimplis. On the ability of global sea level reconstructions to determine trends and variability. *J. Geophys. Res.*, 119, 1572-1592, 2014.
  35. Cazenave, A., Dominh, K., Guinehut, S., Berthier, E., Llovel, W., Ramillien, G., Ablain, M., and Larnicol, G., 2009. Sea level budget over 2003–2008: A reevaluation from GRACE space gravimetry, satellite altimetry and Argo, *Glob. Planet. Change* **65**:83–88, doi:10.1016/j.gloplacha.2008.10.004, 2009.
  36. Cazenave, A., Llovel, W., Contemporary Sea Level Rise, *Annu. Rev. Mar. Sci.* 2:145–73, 10.1146/annurev-marine-120308-081105, 2010.
  37. Cazenave, A., Champollion, N., Paul, F. and Benveniste, J. Integrative Study of the Mean Sea Level and Its Components, *Space Science Series of ISSI - Spinger*, 416 pp, vol 58., 2017.
  38. Cazenave, A, H.B. Dieng, B. Meyssignac, K. von Schuckmann, B. Decharme, and E. Berthier. “The Rate of Sea-Level Rise.” *Nature Climate Change* 4 (5):358–61. <https://doi.org/10.1038/nclimate2159>, 2014.
  39. Chagnon FJF, Bras RL (2005) Contemporary climate change in the Amazon *Geophysical Research Letters* 32:L13703 doi:10.1029/2005gl022722, 2005.
  40. Chao, B. F., Y. H. Wu, and Y. S. Li, Impact of artificial reservoir water impoundment on global sea level, *Science*, 320, 212-214, doi:10.1126/science.1154580, 2008.
  41. Cheema, M. J., W. W. Immerzeel, and W. G. Bastiaanssen, Spatial quantification of groundwater abstraction in the irrigated Indus basin, *Ground Water*, 52, 25-36, doi:10.1111/gwat.12027, 2014.
  42. Chambers, D. P., J. Wahr, M. E. Tamisiea, and R. Steven Nerem, Reply to Comments by Peltier et al., 2012 (“Concerning the Interpretation of GRACE Time Dependent Gravity Observations and the Influence Upon them of Rotational Feedback in Glacial Isostatic Adjustment.”) *J. Geophys. Res.*, 117, doi: 10.1029/2012JB009441, 2012.
  43. Chambers, D. P., Wahr, J., Tamisiea, M. E., and Nerem, R. S., Ocean mass from GRACE and glacial isostatic adjustment. *Journal of Geophysical Research (Solid Earth)*, 115(B14): L11415, doi:10.1029/2010JB007530, 2010.
  44. Chambers, D. P., A. Cazenave, N. Champollion, H. Dieng, W. Llovel, R. Forsberg, K. von Schuckmann, and Y. Wada, Evaluation of the Global Mean Sea Level Budget between 1993 and 2014, *Surv. Geophys.* 38, 309-327, doi: 10.1007/s10712-016-9381-3, 2017.
  45. Chen, Xianyao, Xuebin Zhang, John A. Church, Christopher S. Watson, Matt A. King, Didier Monselesan, Benoit Legresy, and Christopher Harig. “The Increasing Rate of Global Mean Sea-Level Rise during 1993–2014.” *Nature Climate Change* [7, 492–95. https://doi.org/10.1038/nclimate3325](https://doi.org/10.1038/nclimate3325), 2017.
  46. Chen, J. L., Wilson, C. R., and Tapley, B. D., Contribution of ice sheet and mountain glacier melt to recent sea level rise, *Nature Geoscience*, doi: 10.1038/NGEO1829, 2013.
  47. Chen, J. L., Wilson, C. R., Tapley, B. D., Blankenship, D. D., and Ivins, E. R., Patagonia Icefield Melting Observed by GRACE, *Geophys. Res. Lett.*, Vol. 34, No. 22, L22501, 10.1029/2007GL031871, 2007.
  48. Chen, J. L., Wilson, C. R., Tapley, B. D., Save, H., and Cretaux, J.-F., Long-term and seasonal Caspian Sea level change from satellite gravity and altimeter measurements. *Journal of Geophysical Research (Solid Earth)*, 122:2274–2290, doi:10.1002/2016JB013595, 2017.



- 2034 49. Chen, J. L., C. R. Wilson, and B. D. Tapley (2010), The 2009 exceptional Amazon  
 2035 flood and interannual terrestrial water storage change observed by GRACE, *Water*  
 2036 *Resour. Res.*, 46, W12526, doi:10.1029/2010WR009383.
- 2037 50. Chen, J., J. S. Famiglietti, B. R. Scanlon, and M. Rodell, Groundwater Storage  
 2038 Changes: Present Status from GRACE Observations, *Surveys in Geophysics*, 37, 397–  
 2039 417, doi:10.1007/s10712-015-9332-4, 2017.
- 2040 51. Cheng, M.K., and Ries, J.R., Monthly estimates of C20 from 5 SLR satellites based on  
 2041 GRACE RL05 models, GRACE Technical Note 07, The GRACE Project, Center for  
 2042 Space Research, University of Texas at Austin, 2012.
- 2043 52. Cheng L., Trenberth K., Fasullo J., Boyer T., Abraham J. and Zhu J., Improved  
 2044 estimates of ocean heat content from 1960-2015, *Science Advances*, 3, e1601545,  
 2045 2017.
- 2046 53. Choblet, G., Husson, L., Bodin, T., Probabilistic surface re- construction of coastal sea  
 2047 level rise during the twentieth century *J. Geophys. Res.*, 119, 9206-9236, 2014.
- 2048 54. Church, J. et al., Sea level change, in Stocker, T. et al. (eds.) *Climate Change 2013:*  
 2049 *The Physical Science Basis. Contribution of Working Group I to the Fifth Assessment*  
 2050 *Report of the Intergovernmental Panel on Climate Change* (Cambridge University  
 2051 Press, Cambridge, United Kingdom and New York, NY, USA), 2013.
- 2052 55. Church, John, Jonathan Gregory, Neil White, Skye Platten, and Jerry Mitrovica.  
 2053 “Understanding and Projecting Sea Level Change.” *Oceanography* 24 (2):130–43.  
 2054 <https://doi.org/10.5670/oceanog.2011.33>, 2011.
- 2055 56. Church, J. A., and N. J. White. A 20th century acceleration in global sea-level rise,  
 2056 *Geophys. Res. Lett.*, 33, L01602, doi:10.1029/2005GL024826, 2006.
- 2057 57. Church, J. A., and N. J. White, Sea-Level Rise from the Late 19th to the Early 21st  
 2058 Century, *Surveys in Geophysics*, 32(4-5), 585-602, doi:10.1007/s10712-011-9119-1.,  
 2059 2011.
- 2060 58. Ciais P et al., Carbon and other biogeochemical cycles. In: Stocker TF et al. (eds)  
 2061 *Climate change 2013: the physical science basis. Contribution of working group I to*  
 2062 *the fifth assessment report of the Intergovernmental Panel on Climate Change.*  
 2063 Cambridge University Press, Cambridge, United Kingdom and New York, NY, USA,  
 2064 pp 465-570, 2013.
- 2065 59. Cretaux JF et al., SOLS: A lake database to monitor in the Near Real Time water level  
 2066 and storage variations from remote sensing data *Adv Space Res* 47:1497-1507  
 2067 doi:10.1016/j.asr.2011.01.004, 2011.
- 2068 60. Cogley, J., Geodetic and direct mass-balance measurements: comparison and joint  
 2069 analysis, *Annals of Glaciology*, 50, 96-100, 2009.
- 2070 61. Couhert, Alexandre, Luca Cerri, Jean-François Legeais, Michael Ablain, Nikita P.  
 2071 Zelensky, Bruce J. Haines, Frank G. Lemoine, William I. Bertiger, Shailen D. Desai,  
 2072 and Michiel Otten. “Towards the 1mm/y Stability of the Radial Orbit Error at  
 2073 Regional Scales.” *Advances in Space Research: The Official Journal of the Committee*  
 2074 *on Space Research* 55 (1):2–23. <https://doi.org/10.1016/j.asr.2014.06.041>, 2015.
- 2075 62. Dangendorf, S., M. Marcos, A. Müller, E. Zorita, R. Riva, K. Berk, and J. Jensen,  
 2076 Detecting anthropogenic footprints in sea level rise. *Nature Communications*, 6, 7849,  
 2077 2015.
- 2078 63. Dangendorf, Sönke, Marta Marcos, Guy Wöppelmann, Clinton P. Conrad, Thomas  
 2079 Frederikse, and Riccardo Riva. “Reassessment of 20th Century Global Mean Sea  
 2080 Level Rise.” *Proceedings of the National Academy of Sciences* 114 (23):5946–51.  
 2081 <https://doi.org/10.1073/pnas.1616007114>, 2017.

- 2082 64. Davaze, L., Rabatel, A., Arnaud, Y., Sirguey, P., Six, D., Letreguilly, A. and Dumont,  
 2083 M., Monitoring glacier albedo as a proxy to derive summer and annual mass balances  
 2084 from optical remote-sensing data, *The Cryosphere*, 12, 271-286, 2018.
- 2085 65. Darras S, IGBP-DIS wetlands data initiative, a first step towards identifying a global  
 2086 delineation of wetlands. IGBP-DIS Office, Toulouse, France, 1999.
- 2087 66. Davidson NC, How much wetland has the world lost? Long-term and recent trends in  
 2088 global wetland area *Marine and Freshwater Research* 65:934-941  
 2089 doi:10.1071/Mf14173, 2014.
- 2090 67. DeAngelis, A., F. Dominguez, Y. Fan, A. Robock, M. D. Kustu, and D. Robinson,  
 2091 Evidence of enhanced precipitation due to irrigation over the Great Plains of the  
 2092 United States, *J. Geophys. Res.*, 115, D15115, doi:10.1029/2010JD013892, 2010.
- 2093 68. Decharme B., R. Alkama, F. Papa, S. Faroux, H. Douville and C. Prigent, Global  
 2094 off-line evaluation of the ISBA-TRIP flood model, *Climate Dynamics*, 38, 1389-  
 2095 1412, doi:10.1007/s00382-011-1054-9, 2012.
- 2096 69. Decharme, B., Brun, E., Boone, A., Delire, C., Le Moigne, P., and Morin, S. (2016),  
 2097 Impacts of snow and organic soils parameterization on northern Eurasian soil  
 2098 temperature profiles simulated by the ISBA land surface model, *The Cryosphere*, 10,  
 2099 853-877, doi:10.5194/tc-10-853-2016.
- 2100 70. Dieng, H. B., N. Champollion, A. Cazenave, Y. Wada, E. Schrama, and B.  
 2101 Meyssignac, Total land water storage change over 2003-2013 estimated from a global  
 2102 mass budget approach, *Environ. Res. Lett.*, 10, 124010, doi:10.1088/1748-  
 2103 9326/10/12/124010, 2015a.
- 2104 71. Dieng, H. B., Cazenave, A., von Schuckmann, K., Ablain, M., and Meyssignac, B.,  
 2105 2015b. Sea level budget over 2005-2013: missing contributions and data errors. *Ocean*  
 2106 *Science*, 11:789-802, doi:10.5194/os-11-789-2015, 2015b.
- 2107 72. Dieng, H. B., Palanisamy, H., Cazenave, A., Meyssignac, B., and von Schuckmann,  
 2108 K., The Sea Level Budget Since 2003: Inference on the Deep Ocean Heat Content.  
 2109 *Surveys in Geophysics*, 36:209-229, doi:10.1007/s10712-015-9314-6, 2015c.
- 2110 73. Dieng, H.B, A.Cazenave, B.Meyssignac, M.Ablain, New estimate of the current rate  
 2111 of sea level rise from a sea level budget approach, *Geophysical Research Letters*, 44,  
 2112 doi:10.1002/2017GL073308, 2017.
- 2113 74. Döll, P., H. Hoffmann-Dobrev, F. T. Portmann, S. Siebert, A. Eicker, M. Rodell, and  
 2114 G. Strassberg, Impact of water withdrawals from groundwater and surface water on  
 2115 continental water storage variations, *J. Geodyn.*, 59-60, 143-156,  
 2116 doi:10.1016/j.jog.2011.05.001, 2012.
- 2117 75. Döll, P., M. Fritsche, A. Eicker, and S. H. Mueller, Seasonal water storage variations  
 2118 as impacted by water abstractions: Comparing the output of a global hydrological  
 2119 model with GRACE and GPS observations, *Surv. Geophys.*, doi:10.1093/gji/ggt485,  
 2120 2014a.
- 2121 76. Döll, P., H. Müller Schmied, C. Schuh, F. T. Portmann, and A. Eicker, Global-scale  
 2122 assessment of groundwater depletion and related groundwater abstractions:  
 2123 Combining hydrological modeling with information from well observations and  
 2124 GRACE satellites, *Water Resour. Res.*, 50, 5698-5720, doi:10.1002/2014WR015595,  
 2125 2014b.
- 2126 77. Döll, P., H. Douville, A. Güntner, H. Müller Schmied, and Y. Wada, Modelling  
 2127 freshwater resources at the global scale: Challenges and prospects, *Surv. Geophys.*, 37,  
 2128 195-221, Special Issue: ISSI Workshop on Remote Sensing and Water Resources,  
 2129 2017.

- 2130 78. Domingues C, Church J, White N, Gleckler PJ, Wijffels SE, et al. 2008. Improved  
 2131 estimates of upper ocean warming and multidecadal sea level rise. *Nature* 453:1090–  
 2132 93, doi:10.1038/nature07080, 2008.
- 2133 79. Douglas B., Global sea level rise, *Journal of Geophysical Research: Oceans*  
 2134 96(C4):6981-6992, 1991.
- 2135 80. Douglas B., Global sea rise: a redetermination, *Surveys in Geophysics* 18(2-3):279-  
 2136 292, 1997.
- 2137 81. Douglas, B.C., Sea level change in the era of recording tide gauges, in *Sea Level Rise,*  
 2138 *History and Consequences*, pp. 37–64, eds Douglas, B.C., Kearney, M.S. &  
 2139 Leatherman, S.P., Academic Press, San Diego, CA, 2001.
- 2140 82. Durack P., Gleckler, P., Landerer, F., and Taylor, K., Quantifying underestimates of  
 2141 long-term upper-ocean warming, *Nature Climate Change* 4, 999–1005, doi:10.1038/  
 2142 nclimate2389, 2014.
- 2143 83. Dutrioux P et al., Strong sensitivity of Pine Island ice shelf melting to climatic  
 2144 variability, *Science* 343(6167), 2014.
- 2145 84. Escudier et al., Satellite radar altimetry: principle, accuracy and precision, in ‘Satellite  
 2146 altimetry over oceans and land surfaces, D.L Stammer and A. Cazenave eds., 617  
 2147 pages, CRC Press, Taylor and Francis Group, Boca Raton, New York, London, ISBN:  
 2148 13: 978-1-4987-4345-7, 2018.
- 2149 85. Famiglietti, J. S., The global groundwater crisis, *Nature Clim. Change*, 4, 945-948,  
 2150 doi:10.1038/nclimate2425, 2014.
- 2151 86. FAO, Global forest resources assessment 2015: how have the world's forests changed?  
 2152 Rome, 2015.
- 2153 87. Farinotti, D. et al. (2017). How accurate are estimates of glacier ice thickness ?, *The*  
 2154 *Cryosphere*, 11, 949-970, 2004.
- 2155 88. Farrell W., Clark J., On postglacial sea level, *Geophysical Journal International*  
 2156 46.3:647-667, 1976.
- 2157 89. Fasullo, J. T., C. Boening, F. W. Landerer, and R. S. Nerem, Australia's unique  
 2158 influence on global sea level in 2010–2011, *Geophys. Res. Lett.*, 40, 4368–4373,  
 2159 doi:10.1002/grl.50834, 2013.
- 2160 90. Felfelani, F., Wada, Y., Longuevergne, L., & Pokhrel, Y. N., Natural and human-  
 2161 induced terrestrial water storage change: A global analysis using hydrological models  
 2162 and GRACE. *Journal of Hydrology*, 553, 105-118, 2017.
- 2163 91. Feng, W., M. Zhong, J.-M. Lemoine, R. Biancale, H.-T. Hsu, and J. Xia, Evaluation of  
 2164 groundwater depletion in North China using the Gravity Recovery and Climate  
 2165 Experiment (GRACE) data and ground-based measurements, *Water Resour. Res.*, 49,  
 2166 2110–2118, doi:10.1002/wrcr.20192, 2013.
- 2167 92. Fleming K., Lambeck K., Constraints on the Greenland Ice Sheet since the Last  
 2168 Glacial Maximum from sea-level observations and glacial-rebound models,  
 2169 *Quaternary Science Reviews*23(9), 1053-1077, 2004.
- 2170 93. Forsberg, R., Sørensen, L. & Simonsen, S: Greenland and Antarctica Ice Sheet Mass  
 2171 Changes and Effects on Global Sea Level. *Surveys in Geophysics*, 38, 89.  
 2172 doi:10.1007/s10712-016-9398-7, 2017.
- 2173 94. Foster, S. and D. P. Loucks (eds.), *Non-Renewable Groundwater Resources: A*  
 2174 *guidebook on socially-sustainable management for water-policy makers*, IHP-VI,  
 2175 Series on Groundwater No. 10, UNESCO, Paris, France, 2006.
- 2176 95. Frederikse et al, A consistent sea-level reconstruction and its budget on basin and  
 2177 global scales over 1958-2014, *Journal of Climate*, [https://doi.org/10.1175/JCLI-D-17-](https://doi.org/10.1175/JCLI-D-17-0502.1)  
 2178 [0502.1](https://doi.org/10.1175/JCLI-D-17-0502.1), 2017.

- 2179 96. Frey, H., Machguth, H., Huss, M., Huggel, C., Bajracharaya, S., Bolch, T., Kulkarni,  
2180 A., Linsbauer, A., Salzmann, N. and Stoffel, M., Estimating the volume of glaciers in  
2181 the Himalayan-Karakoram region using different methods, *The Cryosphere*, 2014.
- 2182 97. Gardner, A.S., G. Moholdt, J.G. Cogley, B. Wouters, A.A. Arendt, J. Wahr, E.  
2183 Berthier, R. Hock, W.T. Pfeffer, G. Kaser, S.R.M. Ligtenberg, T. Bolch, M.J. Sharp,  
2184 J.O. Hagen, M.R. van den Broeke, and F. Paul, A reconciled estimate of glacier  
2185 contributions to sea level rise: 2003 to 2009. *Science*, 340, 852-857,  
2186 doi:10.1126/science.1234532, 2013.
- 2187 98. Gleick, P. H., Global Freshwater Resources: Soft-Path Solutions for the 21st Century,  
2188 *Science*, 302, 1524-1528, doi:10.1126/science.1089967, 2003.
- 2189 99. Golytsyn GS, Panin GN, Once more on the water level changes of the Caspian Sea  
2190 Vestnik Akademii Nauk SSSR 9:59-63 (in Russian), 1989.
- 2191 100. Gomez N., Pollard D., Mitrovica J.X., A 3-D coupled ice sheet–sea level  
2192 model applied to Antarctica through the last 40 ky, *Earth and Planetary Science  
2193 Letters* 384, 88-99, 2013.
- 2194 101. Gornitz V, Rosenzweig C, Hillel D, Effects of anthropogenic intervention in  
2195 the land hydrologic cycle on global sea level rise *Global and Planetary Change  
2196 14:147-161* doi:10.1016/s0921-8181(96)00008-2, 1997.
- 2197 102. Gornitz, V., Sea-level rise: A review of recent past and near-future trends.  
2198 *Earth Surf. Process. Landforms*, 20, 7–20. doi: 10.1002/esp.3290200103, 1995.
- 2199 103. Gornitz, V., In *Sea Level Rise: History and Consequences*, Douglas, B. C., M.  
2200 S. Kearney, and S. P. Leatherman (eds.), 97-119, Academic Press, San Diego, CA,  
2201 USA, 2001.
- 2202 104. Gornitz, V., Lebedeff, S. and Hansen, J., Global sea level trend in the past  
2203 century, *Science*, 215, 1611–1614, 1982.
- 2204 105. Gouretski, V. and K. Peter Koltermann. How much is the ocean really  
2205 warming? *Geophysical Research Letters*, 34, L01610, doi:10.1029/2006GL027834,  
2206 2007.
- 2207 106. Gregory, J. M., and J. A. Lowe. Predictions of global and regional sea-level  
2208 rise using AOGCMs with and without flux adjustment. *Geophys. Res. Lett.*, **27**, 3069–  
2209 3072, 2000..
- 2210 107. Gregory, J. M., N. J. White, J. A. Church, M. F. P. Bierkens, J. E. Box, M. R.  
2211 van den Broeke, J. G. Cogley, X. Fettweis, E. Hanna, P. Huybrechts, L. F. Konikow,  
2212 P. W. Leclercq, B. Marzeion, J. Oerlemans, M. E. Tamisiea, Y. Wada, L. M. Wake, R.  
2213 S. W. van de Wal, Twentieth-Century Global-Mean Sea Level Rise: Is the Whole  
2214 Greater than the Sum of the Parts? *J. Climate*, 26, 4476–4499, doi:10.1175/JCLI-D-  
2215 12-00319.1, 2013.
- 2216 108. Grinsted, A., An estimate of global glacier volume, *The Cryosphere*, 7, 141–  
2217 151, 2013.
- 2218 109. Groh, A., & Horwath, M., The method of tailored sensitivity kernels for  
2219 GRACE mass change estimates. *Geophysical Research Abstracts*, 18, EGU2016-  
2220 12065, 2016.
- 2221 110. Gunter B.C., Didova O., Riva R.E.M., Ligtenberg S.R.M., Lenaerts J.T.M.,  
2222 King M.A., Van den Broeke M.R., Urban T., and others, Empirical estimation of  
2223 present-day Antarctic glacial isostatic adjustment and ice mass change, *The  
2224 Cryosphere* 8(2), 743-760, 2014.
- 2225 111. Haeberli, W. and Linsbauer, A., Brief communication: global glacier volumes  
2226 and sea level; small but systematic effects of ice below the surface of the ocean and of  
2227 new local lakes on land, *The Cryosphere*, 7, 817-821, 2013.

- 2228 112. Hamlington, B. D., R. R. Leben, R. S. Nerem, W. Han, and K.-Y. Kim,  
 2229 Reconstructing sea level using cyclostationary empirical orthogonal functions, *J.*  
 2230 *Geophys. Res.*, 116, C12015, doi:10.1029/2011JC007529, 2011.
- 2231 113. Hamlington, B.D., Thompson, P., Hammond, W.C., Blewitt, G., and R.D.  
 2232 Ray, Assessing the impact of vertical land motion on twentieth century global mean  
 2233 sea level estimates, *Journal of Geophysical Research: Oceans*, 121(7), 4980-4993. doi:  
 2234 10.1002/2016JC011747, 2016.
- 2235 114. Hay, Carling C., Eric Morrow, Robert E. Kopp, and Jerry X. Mitrovica.  
 2236 “Probabilistic Reanalysis of Twentieth-Century Sea-Level Rise.” *Nature* 517, 7535,  
 2237 481–84, doi:10.1038/nature14093, 2015.
- 2238 115. Henry, O., M.Ablain, B. Meyssignac, A. Cazenave, D. Masters, S. Nerem, and  
 2239 G. Garric. “Effect of the Processing Methodology on Satellite Altimetry-Based  
 2240 Global Mean Sea Level Rise over the Jason-1 Operating Period.” *Journal of Geodesy*  
 2241 88, 4, 351-361, doi: 10.1007/s00190-013-0687-3, 2014.
- 2242 116. Horwath, M., Novotny K, Cazenave, A., Palanisamy, H., Marzeion, B., Paul,  
 2243 F., Döll, P., Cáceres, D., Hogg, A., Shepherd, A., Forsberg, R., Sørensen, L.,  
 2244 Barletta, V.R., Andersen, O.B., Ramndal, H., Johannessen, J., Nilsen, J.E.,  
 2245 Gutknecht, B.D., Merchant, Ch.J., MacIntosh, C.R., von Schuckmann, K., *ESA*  
 2246 *Climate Change Initiative (CCI) Sea Level Budget Closure (SLBC\_cci) Sea Level*  
 2247 *Budget Closure Assessment Report D3.1. Version 1.0*, 2018.
- 2248 117. Hosoda, S., T. Ohira and T. Nakamura. A monthly mean dataset of global  
 2249 oceanic temperature and salinity derived from Argo float observations. *JAMSTEC*  
 2250 *Rep. Res. Dev.*, Volume 8, November 2008, 47–59, 2008.
- 2251 118. Khan, S. A., Sasgen, I., Bevis, M., Van Dam, T., Bamber, J. L., Wahr, J.,  
 2252 Willis, M., Kjær, K. H., Wouters, B., Helm, V., Csatho, B., Fleming, K., Bjørk, A. A.,  
 2253 Aschwanden, A., Knudsen, P. & Munneke, P. K., Geodetic measurements reveal  
 2254 similarities between post–Last Glacial Maximum and present-day mass loss from the  
 2255 Greenland ice sheet. *Science Advances*, 2, 2016.
- 2256 119. Huang, Z., Y. Pan, H. Gong, P. J. Yeh, X. Li, D. Zhou, and W. Zhao,  
 2257 Subregional-scale groundwater depletion detected by GRACE for both shallow and  
 2258 deep aquifers in North China Plain, *Geophys. Res. Lett.*, 42, 1791–1799. doi:  
 2259 10.1002/2014GL062498, 2015.
- 2260 120. Huang Z., The Role of glacial isostatic adjustment (GIA) process on the  
 2261 determination of present-day sea level rise, Report n° 505, Geodetic Science, The  
 2262 Ohio State University, 2013.
- 2263 121. Huntington TG, Can we dismiss the effect of changes in land-based water  
 2264 storage on sea-level rise? *Hydrological Processes* 22:717-723 doi:10.1002/hyp.7001,  
 2265 2008.
- 2266 122. Hurkmans, R. T. W. L., Bamber, J. L., Davis, C. H., Joughin, I. R.,  
 2267 Khvorostovsky, K. S., Smith, B. S. & Schoen, N., Time-evolving mass loss of the  
 2268 Greenland Ice Sheet from satellite altimetry. *The Cryosphere*, 8, 1725-1740, 2014.
- 2269 123. Huss, M. and Hock, R., A new model for global glacier change and sea-level  
 2270 rise, *Front Earth Science*, 2015.
- 2271 124. IMBIE Team (the), Mass balance of the Antarctic ice sheet from 1992 to 2017,  
 2272 *Nature*, 558, 219-222, doi:10.1038/s41586-018-0179-y, 2018.
- 2273 125. Ishii, M., and M. Kimoto, Reevaluation of Historical Ocean Heat Content  
 2274 Variations with Time-varying XBT and MBT Depth Bias Corrections. *Journal of*  
 2275 *Oceanography* 65 (3) (June 1): 287–299. doi:10.1007/s10872-009-0027-7., 2009.
- 2276 126. Ivins, E. R., T. S. James, J. Wahr, E. J. O Schrama, F. W. Landerer, and K. M.  
 2277 Simon, Antarctic contribution to sea level rise observed by GRACE with improved

- 2278 GIA correction, *J. Geophys. Res. Solid Earth*, 118, 3126–3141,  
 2279 doi:10.1002/jgrb.50208, 2013.
- 2280 127. Jacob, T., J. Wahr, W. T. Pfeffer, and S. Swenson, Recent contributions of  
 2281 glaciers and ice caps to sea level rise, *Nature* 482, 514–518, doi:10.1038/nature10847,  
 2282 2012.
- 2283 128. Jensen, L., R. Rietbroek, and J. Kusche, Land water contribution to sea level  
 2284 from GRACE and Jason-1 measurements, *J. Geophys. Res. Oceans*, 118, 212–226,  
 2285 doi:10.1002/jgrc.20058, 2013.
- 2286 129. Jevrejeva S et al.. Nonlinear trends and multi-year cycle in sea level records,  
 2287 *Journal of Geophysical Research*, 111, 2005JC003229, 2006.
- 2288 130. Jevrejeva, S., J. C. Moore, A. Grinsted, A. P. Matthews, and G. Spada,  
 2289 “Trends and Acceleration in Global and Regional Sea Levels since 1807.” *Global and*  
 2290 *Planetary Change* 113:11–22. <https://doi.org/10.1016/j.gloplacha.2013.12.004>, 2014.
- 2291 131. Johannesson, T., Raymond, C. and Waddington, E., Time-Scale for  
 2292 Adjustment of Glaciers to Changes in Mass Balance, *Journal of Glaciology*, 35, 355-  
 2293 369, 1989.
- 2294 132. Johnson, G. C. and Chambers, D. P., Ocean bottom pressure seasonal cycles  
 2295 and decadal trends from GRACERelease-05: Ocean circulation implications, *J.*  
 2296 *Geophys. Res. Oceans*, 118, 4228–4240, doi:10.1002/jgrc.20307, 2013.
- 2297 133. Johnson, G. C., and A. N. Birnbaum. 2017. As El Niño builds, Pacific Warm  
 2298 Pool expands, ocean gains more heat. *Geophysical Research Letters*, 44, 438-445,  
 2299 doi:10.1002/2016GL071767, 2017.
- 2300 134. Khan, S. A., Sasgen, I., Bevis, M., Van Dam, T., Bamber, J. L., Wahr, J.,  
 2301 Willis, M., Kjær, K. H., Wouters, B., Helm, V., Csatho, B., Fleming, K., Bjørk, A. A.,  
 2302 Aschwanden, A., Knudsen, P. and Munneke, P. K., Geodetic measurements reveal  
 2303 similarities between post–Last Glacial Maximum and present-day mass loss from the  
 2304 Greenland ice sheet. *Science Advances*, 2., 2016.
- 2305 135. Kääh, A., Treichler, D., Nuth, C. and Berthier, E., Brief communication:  
 2306 contending estimates of 2003–2008 glacier mass balance over the Pamir–Karakoram–  
 2307 Himalaya, *The Cryosphere*, 9, 557–564, 2015.
- 2308 136. Kaser, G., Cogley, J., Dyurgerov, M., Meier, M. and Ohmura, A., Mass  
 2309 balance of glaciers and ice caps: Consensus estimates for 1961–2004, *Geophysical*  
 2310 *Research Letters*, 33, L19501, 2006.
- 2311 137. Keenan RJ, Reams GA, Achard F, de Freitas JV, Grainger A, Lindquist E.,  
 2312 Dynamics of global forest area: Results from the FAO Global Forest Resources  
 2313 Assessment 2015 *Forest Ecol Manag* 352:9-20 doi:10.1016/j.foreco.2015.06.014,  
 2314 2015.
- 2315 138. Kemp, A. C., B. Horton, J. P. Donnelly, M. E. Mann, M. Vermeer, and S.  
 2316 Rahmstorf, Climate related sea level variations over the past two millennia. *PNAS*  
 2317 108.27: 11017–11022, 2011.
- 2318 139. Khatiwala S, Primeau F, Hall T., Reconstruction of the history of  
 2319 anthropogenic CO<sub>2</sub> concentrations in the ocean *Nature* 462:346-U110  
 2320 doi:10.1038/nature08526, 2009.
- 2321 140. King M.A., Altamimi Z., Boehm J., Bos M., Dach R., Elosegui P., and others,  
 2322 Improved constraints on models of glacial isostatic adjustment: a review of the  
 2323 contribution of ground-based geodetic observations, *Surveys in geophysics*  
 2324 31(5):465, 2010.
- 2325 141. Klige RK, Myagkov MS, Changes in the water regime of the Caspian Sea,  
 2326 *Geol. Journal* 27:299-307, 1992.

- 2327 142. Konikow, L. F., Contribution of global groundwater depletion since 1900 to  
 2328 sea-level rise, *Geophys. Res. Lett.*, 38, L17401, doi:10.1029/2011GL048604, 2011.
- 2329 143. Konrad H., Sasgen I., Pollard D., Klemann V., Potential of the solid-Earth  
 2330 response for limiting long-term West Antarctic Ice Sheet retreat in a warming climate,  
 2331 *Earth and Planetary Science Letters* 432, 254-264, 2015.
- 2332 144. Kopp R.E., Hay C.C., Little C.M., Mitrovica J.X., Geographic variability of  
 2333 sea-level change, *Current Climate Change Reports* 1(3):192, 2015.
- 2334 145. Kustu, M., Y. Fan, and A. Robock, Large-scale water cycle perturbation due to  
 2335 irrigation pumping in the US High Plains: A synthesis of observed streamflow  
 2336 changes, *J. Hydrol.*, 390, 222–244, doi:10.1016/j.jhydrol.2010.06.045, 2010.
- 2337 146. Kustu, M. D., Y. Fan, and M. Rodell, Possible link between irrigation in the  
 2338 U.S. High Plains and increased summer streamflow in the Midwest, *Water Resour.*  
 2339 *Res.*, 47, W03522, doi:10.1029/2010WR010046, 2011.
- 2340 147. Lambeck K, Chappell J., *Science* 292(5517):679, 2001.
- 2341 148. Lambeck K., Sea-level change from mid-Holocene to recent time: An  
 2342 Australian example with global implications, In: Ice Sheets, Sea Level and the  
 2343 Dynamic Earth, JX Mitrovica and LLA Vermeersen, Eds., Geodynamics Series,  
 2344 29:33-50, 2002.
- 2345 149. Lambeck K. et al., Paleoenvironmental records, geophysical modelling and  
 2346 reconstruction of sea level trends and variability on centennial and longer time scales,  
 2347 *In Understanding sea level rise and variability*, JA Church et al ed., Wiley-Blackwell,  
 2348 2010.
- 2349 150. Leclercq, P., Oerlemans, J. and Cogley, J., Estimating the glacier contribution  
 2350 to sea-level rise for the period 1800–2005, *Surveys in Geophysics*, 32, 519–535, 2011.
- 2351 151. Legeais, J-F, Michaël Ablain, Lionel Zawadzki, Hao Zuo, Johnny A.  
 2352 Johannessen, Martin G. Scharffenberg, Luciana Fenoglio-Marc, et al., “An Accurate  
 2353 and Homogeneous Altimeter Sea Level Record from the ESA Climate Change  
 2354 Initiative.” *Earth System Science Data Discussions*, 1–35, doi:10.5194/essd-2017-116,  
 2355 2018.
- 2356 152. Lehner, B., C. Reidy Liermann, C. Revenga, C. Vörösmarty, B. Fekete, P.  
 2357 Crouzet, P. Döll, M. Endejan, K. Frenken, J. Magome, C. Nilsson, J. C. Robertson, R.  
 2358 Rödel, N. Sindorf, and D. Wisser, High-resolution mapping of the world's reservoirs  
 2359 and dams for sustainable river-flow management, *Fron. Ecol. Environ.*, 9, 494-502,  
 2360 doi:10.1890/100125, 2011.
- 2361 153. Le Queré et al., Global Carbon Budget 2017, *Earth Syst. Sci. Data*, 10, 405-  
 2362 448, 2018, doi.org/10.5194/essd-10-405-2018, 2018.
- 2363 154. Lettenmaier, D. P., and P. C. D. Milly, Land waters and sea level, *Nat. Geosci.*,  
 2364 2, 452-454, doi:10.1038/ngeo567, 2009.
- 2365 155. Leuliette, E. W., and Miller, L., Closing the sea level rise budget with altimetry,  
 2366 Argo, and GRACE, *Geophys. Res. Lett.*, 36, L04608, doi:10.1029/2008GL036010,  
 2367 2009.
- 2368 156. Leuliette, E.W., and Willis, J.K., Balancing the sea level budget,  
 2369 *Oceanography* 24 (2): 122–129, doi:10.5670/oceanog.2011.32, 2011.
- 2370 157. Leuschen, C.: IceBridge Geolocated Radar Echo Strength Profiles, Boulder,  
 2371 Colorado, NASA DAAC at the National Snow and Ice Data Center,  
 2372 http://dx.doi.org/10.5067/FAZTWP500V70, last access: 15 June 2014
- 2373 158. Levitus S., J.I. Antonov, T.P. Boyer, O.K. Baranova, H.E. Garcia, R.A.  
 2374 Locarnini, A.V. Mishonov, J.R. Reagan, D. Seidov, E.S. Yarosh and M.M. Zweng,  
 2375 World ocean heat content and thermosteric sea level change (0-2000 m), 1955-2010,  
 2376 *Geophys. Res. Lett.*, 39, L10603, doi:10.1019/2012GL051106, 2012.

- 2377 159. Llovel, W., J. K. Willis, F. W. Landerer, and I. Fukumori, Deep-ocean  
 2378 contribution to sea level and energy budget not detectable over the past decade, *Nature*  
 2379 *Clim. Change* 4, 1031–1035, doi:10.1038/nclimate2387, 2014.
- 2380 160. Llovel, W., M. Becker, A. Cazenave, J.-F. Crétaux, and G. Ramillien, *C. R.*  
 2381 *Geosci.* 342, 179–188, doi :10.1016/j.crte.2009.12.004, 2010.
- 2382 161. Lo, M.-H., and J. S. Famiglietti, Irrigation in California’s Central Valley  
 2383 strengthens the southwestern U.S. water cycle, *Geophys. Res. Lett.*, 40,  
 2384 doi:10.1002/grl.50108, 2013.
- 2385 162. Loriaux, T. and Casassa, G., Evolution of glacial lakes from the Northern  
 2386 Patagonia Icefield and terrestrial water storage in a sea-level rise context, *Global and*  
 2387 *Planetary Change*, 102, 33-40, 2013.
- 2388 163. Lovel TR, Belward AS, The IGBP-DIS global 1 km land cover data set,  
 2389 DISCover: first results *International Journal of Remote Sensing* 18:3291-3295, 1997.
- 2390 164. Luthcke, S. B., Sabaka, T. J., Loomis, B. D., Arendt, A. A., McCarthy, J. J.,  
 2391 and Camp, J., Antarctica, Greenland and Gulf of Alaska land-ice evolution from an  
 2392 iterated GRACE global mascon solution. *Journal of Glaciology*, 59:613–631,  
 2393 doi:10.3189/2013JoG12J147, 2013.
- 2394 165. Luthcke, S. B., Zwally, H. J., Abdalati, W., Rowlands, D. D., Ray, R. D.,  
 2395 Nerem, R. S., Lemoine, F. G., McCarthy, J. J., and Chinn, D. S., Recent Greenland Ice  
 2396 Mass Loss by Drainage System from Satellite Gravity Observations. *Science*,  
 2397 314:1286–1289, doi:10.1126/science.1130776, 2006.
- 2398 166. Luthcke, S. B., Sabaka, T., Loomis, B., Arendt, A., Mccarthy, J. & Camp, J.,  
 2399 Antarctica, Greenland and Gulf of Alaska land-ice evolution from an iterated GRACE  
 2400 global mascon solution. *Journal of Glaciology*, 59, 613-631, 2013.
- 2401 167. Lyman, J. M., S. A. Godd, V. V. Gouretski, et al., Robust warming of the  
 2402 global upper ocean. *Nature* 465:334–337, 2010.
- 2403 168. MacDicken KG, Global Forest Resources Assessment, What, why and how?  
 2404 *Forest Ecol Manag* 352:3-8 doi:10.1016/j.foreco.2015.02.006, 2015.
- 2405 169. Martín-Español, A., Zammit-Mangion, A., Clarke, P. J., Flament, T., Helm, V.,  
 2406 King, M. A., and Wouters, B., Spatial and temporal Antarctic Ice Sheet mass trends,  
 2407 glacio-isostatic adjustment, and surface processes from a joint inversion of satellite  
 2408 altimeter, gravity, and GPS data. *Journal of Geophysical Research: Earth*  
 2409 *Surface*, 121(2), 182-200, 2016.
- 2410 170. Martinec Z., Hagedoorn J., The rotational feedback on linear-momentum  
 2411 balance in glacial isostatic adjustment, *Geophysical Journal International* 199, 3,  
 2412 1823-1846, 2014.
- 2413 171. Merrifield MA et al., An anomalous recent acceleration of global sea level rise.  
 2414 *J. Clim.* 22: 5772–5781. doi:10.1175/2009JCLI2985.1., 2009.
- 2415 172. Meyssignac B., M. Becker, W. Llovel, and A. Cazenave, An Assessment of  
 2416 Two-Dimensional Past Sea Level Reconstructions Over 1950–2009 Based on Tide-  
 2417 Gauge Data and Different Input Sea Level Grids, *Surveys in Geophysics*,  
 2418 doi:10.1007/s10712-011-9171-x, 2011.
- 2419 173. Milne G.A., Gehrels W.R., Hughes C.W., Tamisiea M.E., Identifying the  
 2420 causes of sea-level change, *Nature Geoscience* 2.7:471, 2009.
- 2421 174. Mitrovica J.X., Milne G.A., On the origin of late Holocene sea-level  
 2422 highstands within equatorial ocean basins, *Quaternary Science Reviews* 21, 20-22,  
 2423 2179-2190, 2002.
- 2424 175. Mitrovica J.X., Milne G.A., On post-glacial sea level: I. General theory,  
 2425 *Geophysical Journal International* 154, 2, 253, 2003.



- 2426 176. Mitrovica J.X., Wahr J., Matsuyama I., Paulson A., The rotational stability of  
2427 an ice-age earth, *Geophysical Journal International*, 161.2, 491-506, 2005.
- 2428 177. Mitrovica J.X., Wahr J., Matsuyama I., Paulson A., and Tamisiea M.E.,  
2429 Reanalysis of ancient eclipse, astronomic and geodetic data: A possible route to  
2430 resolving the enigma of global sea-level rise. *Earth and Planetary Science*  
2431 *Letters*, 243, 3-4, 390-399, doi: 10.1016/j.epsl.2005.12.029, 2006.
- 2432 178. Mitrovica J.X., Wahr J., Ice age Earth rotation, *Annual Review of Earth and*  
2433 *Planetary Sciences* 39, 577-616, 2011.
- 2434 179. Marzeion, B., Jarosch, A., Hofer, M., Past and future sea-level change from  
2435 the surface mass balance of glaciers, *The Cryosphere*, 6, 1295–1322, 2012.
- 2436 180. Marzeion, B., Cogley, J., Richter, K. and Parkes, D., Attribution of global  
2437 glacier mass loss to anthropogenic and natural causes, *Science*, 345, 919–92, 2014.
- 2438 181. Marzeion, B., Champollion, N., Haeberli, W., Langley, K., Leclercq, P. and  
2439 Paul, F., Observation-Based Estimates of Global Glacier Mass Change and Its  
2440 Contribution to Sea-Level Change, *Surveys in Geophysics*, 28, 105-130, 2017.
- 2441 182. Marzeion, B., Kaser, G., Maussion, F. and Champollion, N., Limited influence  
2442 of climate change mitigation on short-term glacier mass loss, *Nature Climate Change*,  
2443 doi:[10.1038/s41558-018-0093-1](https://doi.org/10.1038/s41558-018-0093-1), 2018.
- 2444 183. Masters, D., R. S. Nerem, C. Choe, E. Leuliette, B. Beckley, N. White, and M.  
2445 Ablain., “Comparison of Global Mean Sea Level Time Series from TOPEX/Poseidon,  
2446 Jason-1, and Jason-2.” *Marine Geodesy* 35 (sup1):20–41.  
2447 <https://doi.org/10.1080/01490419.2012.717862>, 2012.
- 2448 184. Matthews E, Fung I, Methane emission from natural wetlands: Global  
2449 distribution, area, and environmental characteristics of sources *Global Biogeochemical*  
2450 *Cycles* 1:61-86, 1987.
- 2451 185. Matthews GVT, *The Ramsar Convention on wetlands: its history and*  
2452 *development*. Ramsar Convention Bureau, Gland, Switzerland, 1993.
- 2453 186. Maussion, F, Butenko, A., Eis, J., Fourteau, K., Jarosch, A., Landmann, J.,  
2454 Oesterle, J., Recinos, B., Rothenpieler, T., Vlug, A., Wild, C. and Marzeion; B., *The*  
2455 *Open Global Glacier Model (OGGM) v1.0, subm. to The Cryosphere*, 2018.
- 2456 187. McMillan M. et al. Increased ice losses from Antarctica detected by Cryosat-2,  
2457 *Geophys. Res. Lett.*, 41(11), 3899-3905, 2014.
- 2458 188. Meherhomji VM, Probable Impact of Deforestation on Hydrological Processes  
2459 *Climatic Change* 19:163-173 doi:10.1007/Bf00142223, 1991.
- 2460 189. Micklin PP, *The Aral Crisis - Introduction to the Special Issue Post-Sov Geogr*  
2461 *33:269-282*, 1992.
- 2462 190. Milly P. C. D. et al., Terrestrial water-storage contributions to sea-level rise  
2463 and variability , in *Understanding Sea-Level Rise and Variability:226-255*, 2010.
- 2464 191. Milly, P. C. D., A. Cazenave, and M. C. Gennero, Contribution of climate-  
2465 driven change in continental water storage to recent sea-level rise. *Proc. Natl. Acad.*  
2466 *Sci.*, 100, 13158–13161, 2003.
- 2467 192. Mitra S, Wassmann R, Vlek PLG, An appraisal of global wetland area and its  
2468 organic carbon stock *Curr Sci India* 88:25-35, 2005.
- 2469 193. Mitsch WJ, Gosselink JG, *Wetlands*, 2nd ed. Van Nostrand Reinhold, New  
2470 York, 1993.
- 2471 194. Mouginot J., E. Rignot, B. Scheuchl, Sustained increase in ice discharge from  
2472 the Amundsen Sea Embayment, West Antarctica, from 1973 to 2013, *Geophys. Res.*  
2473 *Lett.* 41, 1576-1584, 2014.
- 2474 195. Munk W., Twentieth century sea level: An enigma, *PNAS*, 99, 10, 6550-6555,  
2475 doi/10.1073/pnas092704599, 2002.

- 2476 196. Natarov, S. I., M. A. Merrifield, J. M. Becker, and P. R. Thompson, Regional  
 2477 influences on reconstructed global mean sea level, *Geophys. Res. Lett.*, 44, 3274-  
 2478 3282, 2017.
- 2479 197. Nerem, R. S., D. P. Chambers, C. Choe, and G. T. Mitchum. “Estimating Mean  
 2480 Sea Level Change from the TOPEX and Jason Altimeter Missions.” *Marine Geodesy*  
 2481 33 (sup1):435–46. <https://doi.org/10.1080/01490419.2010.491031>, 2010.
- 2482 198. Nerem R.S., Beckley B.D., Fasullo J., Hamlington B.D., Masters D. and  
 2483 Mitchum G.T., Climate Change Driven Accelerated Sea Level Rise Detected In The  
 2484 Altimeter Era, *PNAS*, 2018.
- 2485 199. Nghiem, S., Hall, D., Mote, T., Tedesco, M., Albert, M., Keegan, K., Shuman,  
 2486 C., Digirolamo, N. & Neumann, G., The extreme melt across the Greenland ice sheet  
 2487 in 2012. *Geophysical Research Letters*, 39, 2012.
- 2488 200. Nobre P, Malagutti M, Urbano DF, de Almeida RAF, Giarolla E, Amazon  
 2489 Deforestation and Climate Change in a Coupled Model Simulation *J Climate* 22:5686-  
 2490 5697 doi:10.1175/2009jcli2757.1, 2009.
- 2491 201. Oki, T. and S. Kanae, Global hydrological cycles and world water resources,  
 2492 *Science*, 313, 1068-1072, doi:10.1126/science.1128845, 2006.
- 2493 202. Ozyavas A, Khan SD, Casey JF, A possible connection of Caspian Sea level  
 2494 fluctuations with meteorological factors and seismicity *Earth Planet Sc Lett* 299:150-  
 2495 158 doi:10.1016/j.epsl.2010.08.030, 2010.
- 2496 203. Pala, C., Once a Terminal Case, the North Aral Sea Shows New Signs of Life,  
 2497 *Science*, 312, 183, doi:10.1126/science.312.5771.183, 2006.
- 2498 204. Pala, C., In Northern Aral Sea, Rebound Comes With a Big Catch, *Science*,  
 2499 334, 303, doi:10.1126/science.334.6054.303, 2011.
- 2500 205. Palmer M. et al., 2016.
- 2501 206. Paul, F., Huggel, C. and Kääh, Combining satellite multispectral image data  
 2502 and a digital elevation model for mapping of debris-covered glaciers, *Remote Sensing*  
 2503 *of Environment*, 89, 510–518, 2004.
- 2504 207. Paulson, A., Zhong, S., and Wahr, J., Inference of mantle viscosity from  
 2505 GRACE and relative sea level data. *Geophysical Journal International*, 171:497–508,  
 2506 doi:10.1111/j.1365-246X.2007.03556.x, 2007.
- 2507 208. Peltier W.R., Global glacial isostatic adjustment and modern instrumental  
 2508 records of relative sea level history, in: B.C. Douglas, M.S. Kearney, S.P. Leatherman  
 2509 (Eds.), *Sea-Level Rise: History and Consequences*, vol. 75, Academic Press, San  
 2510 Diego, 2001, pp. 65–95.
- 2511 209. Peltier W.R., Luthcke S.B., On the origins of Earth rotation anomalies: New  
 2512 insights on the basis of both “paleogeodetic” data and Gravity Recovery and Climate  
 2513 Experiment (GRACE) data, *Journal of Geophysical Research: Solid Earth* 114,  
 2514 B11405, 2009.
- 2515 210. Peltier W.R., Global glacial isostasy and the surface of the ice-age Earth: the  
 2516 ICE-5G (VM2) model and GRACE, *Annual Review of Earth and Planetary Sciences*  
 2517 32, 111, 2004.
- 2518 211. Peltier W.R., Argus D.F., Drummond R., Space geodesy constrains ice age  
 2519 terminal deglaciation: The global ICE-6G\_C (VM5a) model, *Journal of Geophysical*  
 2520 *Research: Solid Earth* 120, 1, 450-487, 2015.
- 2521 212. Peltier W.R., Closure of the budget of global sea level rise over the GRACE  
 2522 era: the importance and magnitudes of the required corrections for global glacial  
 2523 isostatic adjustment. *Quaternary Science Reviews*, 28, 1658-1674, 2009.

- 2524 213. Peltier, W. R., R. Drummond, and K. Roy, Comment on "Ocean mass from  
2525 GRACE and glacial isostatic adjustment" by D. P. Chambers et al. *Journal of*  
2526 *Geophysical Research-Solid Earth*, **117**, B11403, 2012.
- 2527 214. Perera J, A Sea Turns to Dust *New Sci* 140:24-27, 1993.
- 2528 215. Pfeffer, W., Arendt, A., Bliss, A., Bolch, T., Cogley, J., Gardner, A., Hagen, J.-  
2529 O., Hock, R., Kaser, G., Kienholz, C., Miles, E., Moholdt, G., Mölg, N., Paul, F.,  
2530 Radić, V., Rastner, P., Raup, B., Rich, J. and Sharp, M., The Randolph Glacier  
2531 Inventory: a globally complete inventory of glaciers., *Journal of Glaciology*, 60, 537–  
2532 552, 2014.
- 2533 216. Plag H.P., Juettner H.U., Inversion of global tide gauge data for present-day ice  
2534 load changes, *Memoirs of National Institute of Polar Research* 54:301, 2001.
- 2535 217. Pokhrel, Y. N., N. Hanasaki, P. J.-F. Yeh, T. Yamada, S. Kanae, and T. Oki,  
2536 Model estimates of sea level change due to anthropogenic impacts on terrestrial water  
2537 storage, *Nat. Geosci.*, 5, 389–392, doi:10.1038/ngeo1476, 2012.
- 2538 218. Pokhrel, Y. N., S. Koirala, P. J.-F. Yeh, N. Hanasaki, L. Longuevergne, S.  
2539 Kanae, and T. Oki, Incorporation of groundwater pumping in a global Land Surface  
2540 Model with the representation of human impacts, *Water Resour. Res.*, 51, 78–96,  
2541 doi:10.1002/2014WR015602, 2015.
- 2542 219. Postel, S. L., Pillar of Sand: Can the Irrigation Miracle Last? W.W. Norton,  
2543 New York USA, ISBN 0-393-31937-7, 1999.
- 2544 220. Purcell A.P., Tregoning P., Dehecq A., An assessment of the ICE6G\_C  
2545 (VM5a) glacial isostatic adjustment model, *Journal of Geophysical Research: Solid*  
2546 *Earth* 121, 5, 3939-3950, 2016.
- 2547 221. Purkey, S. G., Johnson, G. C., and Chambers, D. P., Relative contributions of  
2548 ocean mass and deep steric changes to sea level rise between 1993 and 2013, *J.*  
2549 *Geophys. Res. Oceans*, 119, 7509–7522, doi:10.1002/2014JC010180, 2014.
- 2550 222. Purkey, S., and G. C. Johnson, Warming of global abyssal and deep southern  
2551 ocean waters between the 1990s and 2000s: Contributions to global heat and sea level  
2552 rise budget, *J. Clim.*, 23, 6336–6351, doi:10.1175/2010JCLI3682.1, 2010.
- 2553 223. Radic, V. and Hock, R., Regional and global volumes of glaciers derived from  
2554 statistical upscaling of glacier inventory data, *Journal of Geophysical Research Earth*  
2555 *Surface*, 115, F01010, 2010.
- 2556 224. Radic, V. and Hock, R., Regionally differentiated contribution of mountain  
2557 glaciers and ice caps to future sea-level rise, *Nature Geoscience*, 4, 91-94, 2011.
- 2558 225. Ramillien G, Frappart F, Seoane L, Application of the regional water mass  
2559 variations from GRACE Satellite Gravimetry to large-scale water management in  
2560 Africa *Remote Sensing* 6:7379-7405, 2014.
- 2561 226. Ray, R.D. and B.C. Douglas, Experiments in reconstructing twentieth-century  
2562 sea levels, *Prog. Oceanogr.* 91, 495–515, 2011.
- 2563 227. Reager, J. T., Gardner, A. S., Famiglietti, J. S., Wiese, D. N., Eicker, A., & Lo,  
2564 M. H., A decade of sea level rise slowed by climate-driven hydrology. *Science*,  
2565 351(6274), 699-703, doi:10.1126/science.aad8386, 2016.
- 2566 228. Reager, J. T., Thomas, B. F., and Famiglietti, J. S., River basin flood potential  
2567 inferred using GRACE gravity observations at several months lead time. *Nature*  
2568 *Geoscience*, 7:588–592, doi:10.1038/ngeo2203, 2014.
- 2569 229. Rhein, M., S.R. Rintoul, S. Aoki, E. Campos, D. Chambers, R.A. Feely, S.  
2570 Gulev, G.C. Johnson, S.A. Josey, A. Kostianoy, C. Mauritzen, D. Roemmich, L.D.  
2571 Talley and F. Wang: Observations: Ocean. In: Climate Change 2013: The Physical  
2572 Science Basis. Contribution of Working Group I to the Fifth Assessment Report of the  
2573 Intergovernmental Panel on Climate Change [Stocker, T.F., D. Qin, G.-K. Plattner, M.

- 2574 Tignor, S.K. Allen, J. Boschung, A. Nauels, Y. Xia, V. Bex and P.M. Midgley (eds.)].  
 2575 Cambridge University Press, Cambridge, United Kingdom and New York, NY, USA.,  
 2576 2013.
- 2577 230. Richey, A. S., B. F. Thomas, M.-H. Lo, J. T. Reager, J. S. Famiglietti, K. Voss,  
 2578 S. Swenson, and M. Rodell, Quantifying renewable groundwater stress with GRACE,  
 2579 *Water Resour. Res.*, 51, 5217–5238, doi:10.1002/2015WR017349, 2015.
- 2580 231. Rietbroek, R., Brunnabend, S.-E., Kusche, J. and Schröter, J., Resolving sea  
 2581 level contributions by identifying fingerprints in time-variable gravity and altimetry, *J.*  
 2582 *Geodyn.*, 59-60, 72-81, 2012.
- 2583 232. Rietbroek, R., Brunnabend, S.-E., Kusche, J., Schröter, J., and Dahle, C.,  
 2584 Revisiting the contemporary sea-level budget on global and regional scales.  
 2585 *Proceedings of the National Academy of Sciences*, 113(6):1504–1509,  
 2586 doi:10.1073/pnas.1519132113, 2016.
- 2587 233. Rignot, E. J., I. Velicogna, M. R. van den Broeke, A. J. Monaghan, and J. T.  
 2588 M. Lenaerts, Acceleration of the contribution of the Greenland and Antarctic ice  
 2589 sheets to sea level rise, *Geophys. Res. Lett.*, 38, L05503, doi:10.1029/2011GL046583,  
 2590 2011.
- 2591 234. Rignot, E., J. Mouginot, and B. Scheuchl, Ice flow of the Antarctic Ice  
 2592 Sheet, *Science*, 333(6048), 1427–1430, doi:10.1126/science.1208336, 2011.
- 2593 235. Riva R.E., Gunter B.C., Urban T.J., Vermeersen B.L., Lindenbergh R.C.,  
 2594 Helsen M.M., and others, Glacial isostatic adjustment over Antarctica from combined  
 2595 ICESat and GRACE satellite data, *Earth and Planetary Science Letters* 288(3), 516-  
 2596 523, 2009.
- 2597 236. Riva, R. E. M., J. L. Bamber, D. A. Lavallée, and B. Wouters, Sea-level  
 2598 fingerprint of continental water and ice mass change from GRACE, *Geophys. Res.*  
 2599 *Lett.*, 37, L19605, doi:10.1029/2010GL044770, 2010.
- 2600 237. Rodell, M., I. Velicogna, and J. S. Famiglietti, Satellite-based estimates of  
 2601 groundwater depletion in India, *Nature*, 460, 999-1002, doi:10.1038/nature08238,  
 2602 2009.
- 2603 238. Roemmich, D., Owens, W.B., The ARGO project: global ocean observations  
 2604 for understanding for understanding and prediction of climate variability.  
 2605 *Oceanography* 13 (2), 45–50, 2000.
- 2606 239. Roemmich, D., W. J. Gould, and J. Gilson, 135 years of global ocean warming  
 2607 between the Challenger expedition and the Argo Programme, *Nature Climate Change*,  
 2608 2(6), 425-428, doi:10.1038/nclimate1461, 2012.
- 2609 240. Roemmich, D, Gilson J, Sutton P, Zilberman N. 2016. Multidecadal change  
 2610 of the South Pacific gyre circulation. *Journal of Physical Oceanography*. 46:1871-  
 2611 1883. 10.1175/jpo-d-15-0237.1 , 2016.
- 2612 241. Roemmich, D. and J. Gilson. The 2004–2008 mean and annual cycle of  
 2613 temperature, salinity, and steric height in the global ocean from the Argo Program,  
 2614 *Progress in Oceanography*, Volume 82, Issue 2, August 2009, Pages 81-100, 2009.
- 2615 242. Rohrig E, Biomass and productivity. In: Rohrig E (edt.) *Ecosystems of the*  
 2616 *world*. Elsevier, New York, pp 165-174, 1991.
- 2617 243. Sabine C.L. et al., The oceanic sink for anthropogenic CO<sub>2</sub> *Science* 305:367-  
 2618 371 doi:10.1126/science.1097403, 2004.
- 2619 244. Sahagian D., Global physical effects of anthropogenic hydrological alterations:  
 2620 sea level and water redistribution *Global and Planetary Change* 25:39-48  
 2621 doi:10.1016/S0921-8181(00)00020-5, 2000.

- 2622 245. Sahagian, D. L., F. W. Schwartz, and D. K. Jacobs, Direct anthropogenic  
 2623 contributions to sea level rise in the twentieth century, *Nature*, 367, 54-57,  
 2624 doi:10.1038/367054a0, 1994.
- 2625 246. Sasgen I., Konrad H., Ivins E.R., Van den Broeke M.R., Bamber J.L., Martinec  
 2626 Z., Klemann V., Antarctic ice-mass balance 2003 to 2012: regional reanalysis of  
 2627 GRACE satellite gravimetry measurements with improved estimate of glacial-isostatic  
 2628 adjustment based on GPS uplift rates, *The Cryosphere*, 7, 1499-1512, 2013.
- 2629 247. Sasgen I., Martín-Español A., Horvath A., Klemann V., Petrie E.J., Wouters  
 2630 B., and others Joint inversion estimate of regional glacial isostatic adjustment in  
 2631 Antarctica considering a lateral varying Earth structure (ESA STSE Project REGINA),  
 2632 *Geophysical Journal International* 211, 3, , 1534-1553, 2017.
- 2633 248. Sasgen, I., Van Den Broeke, M., Bamber, J. L., Rignot, E., Sørensen, L. S.,  
 2634 Wouters, B., Martinec, Z., Velicogna, I. & Simonsen, S. B., Timing and origin of  
 2635 recent regional ice-mass loss in Greenland. *Earth and Planetary Science Letters*, 333,  
 2636 293-303, 2012.
- 2637 249. Sasgen, I., Konrad, H., Ivins, E. R., Van den Broeke, M. R., Bamber, J. L.,  
 2638 Martinec, Z., & Klemann, V., Antarctic ice-mass balance 2003 to 2012: regional  
 2639 reanalysis of GRACE satellite gravimetry measurements with improved estimate of  
 2640 glacial-isostatic adjustment based on GPS uplift rates. *The Cryosphere*, 7, 1499- 1512,  
 2641 2013.
- 2642 250. Sasgen, I., Martín-Español, A., Horvath, A., Klemann, V., Petrie, E. J.,  
 2643 Wouters, B., & Konrad, Joint inversion estimate of regional glacial isostatic  
 2644 adjustment in Antarctica considering a lateral varying Earth structure (ESA STSE  
 2645 Project REGINA). *Geophysical Journal International*, 211, 3, 1534-1553, 2017.
- 2646 251. Scanlon, B. R., I. Jolly, M. Sophocleous, and L. Zhang, Global impacts of  
 2647 conversions from natural to agricultural ecosystems on water resources: Quantity  
 2648 versus quality, *Water Resources Res.*, 43, 3, W03437, 2007.
- 2649 252. Scanlon, B. R., C. C. Faunt, L. Longuevergne, R. C. Reedy, W. M. Alley, V. L.  
 2650 McGuire, and P. B. McMahon, Groundwater depletion and sustainability of irrigation  
 2651 in the U.S. High Plains and Central Valley, *PNAS*, 109, 9320-9325,  
 2652 doi:10.1073/pnas.1200311109, 2012a.
- 2653 253. Scanlon, B. R., L. Longuevergne, and D. Long, Ground referencing GRACE  
 2654 satellite estimates of groundwater storage changes in the California Central Valley,  
 2655 USA, *Water Resour. Res.*, 48, W04520, doi:10.1029/2011WR011312, 2012b.
- 2656 254. Scanlon, B. R., Zhang, Z., Save, H., Sun, A. Y., Schmied, H. M., van Beek, L.  
 2657 P., & Longuevergne, L., Global models underestimate large decadal declining and  
 2658 rising water storage trends relative to GRACE satellite data. *PNAS*, 201704665, 2018.
- 2659 255. Schrama, E. J., Wouters, B. & Rietbroek, R., A mascon approach to assess ice  
 2660 sheet and glacier mass balances and their uncertainties from GRACE data. *Journal of*  
 2661 *Geophysical Research: Solid Earth*, 119, 6048-6066, 2014.
- 2662 256. Schellekens, J., Dutra, E., Martínez-de la Torre, A., Balsamo, G., van Dijk, A.,  
 2663 Weiland, F. S., & Fink, G., A global water resources ensemble of hydrological  
 2664 models: the earthH2Observe Tier-1 dataset. *Earth System Science Data*, 9(2), 389,  
 2665 2017.
- 2666 257. Schwatke C, Dettmering D, Bosch W, Seitz F, DAHITI – an innovative  
 2667 approach for estimating water level time series over inland waters using multi-mission  
 2668 satellite altimetry, *Hydrol. Earth Syst. Sci.*, 19, 4345-4364, 2015.
- 2669 258. Shamsudduha, M., R. G. Taylor, and L. Longuevergne, Monitoring  
 2670 groundwater storage changes in the highly seasonal humid tropics: Validation of

- 2671 GRACE measurements in the Bengal Basin, *Water Resour. Res.*, 48, W02508,  
 2672 doi:10.1029/2011WR010993, 2012.
- 2673 259. Sheng Y, Song C, Wang J, Lyons EA, Knox BR, Cox JS, Gao F.,  
 2674 Representative lake water extent mapping at continental scales using multi-temporal  
 2675 Landsat-8 imagery *Remote Sensing of Environment* in  
 2676 press:doi:10.1016/j.rse.2015.1012.1041, 2016.
- 2677 260. Shepherd, A., Ivins E.R., Geruo A., Barletta V.R., Bentley M.J., Bettadpur S.,  
 2678 and others, A reconciled estimate of ice-sheet mass balance. *Science*, 338(6111),  
 2679 1183-1189, doi:10.1126/science.1228102, 2012.
- 2680 261. Shukla J, Nobre C, Sellers P., Amazon Deforestation and Climate Change  
 2681 *Science* 247:1322-1325 doi:10.1126/science.247.4948.1322, 1990.
- 2682 262. Singh A, Seitz F, Schwatke C., Inter-annual water storage changes in the Aral  
 2683 Sea from multi-mission satellite altimetry, optical remote sensing, and GRACE  
 2684 satellite gravimetry *Remote Sens Environ* 123:187-195, 2012.
- 2685 263. Slangen, A.B.A., Meyssignac, B., Agosta, C., Champollion, N., Church, J.A.,  
 2686 Fettweis, X., Ligtenberg, S.R.M., Marzeion, B., Melet, A., Palmer, M.D., Richter, K.,  
 2687 Roberts, C.D., Spada, G., Evaluating model simulations of 20th century sea-level rise.  
 2688 Part 1: global mean sea-level change. *J. Clim.* 30, 21, 8539–  
 2689 8563. <https://dx.doi.org/10.1175/jcli-d-17-0110.1>, 2017.
- 2690 264. Sloan S, Sayer JA., Forest Resources Assessment of 2015 shows positive  
 2691 global trends but forest loss and degradation persist in poor tropical countries, *Forest*  
 2692 *Ecol Manag*, 352:134-145 doi:10.1016/j.foreco.2015.06.013, 2015.
- 2693 265. Smith LC, Sheng Y, MacDonald GM, Hinzman LD, Disappearing Arctic lakes  
 2694 *Science* 308:1429-1429 doi:10.1126/science.1108142, 2005.
- 2695 266. Solomon, S. et al. (eds.), *Climate Change 2007: The Physical Science Basis.*  
 2696 *Contribution of Working Group I to the Fourth Assessment Report of the*  
 2697 *Intergovernmental Panel on Climate Change*, Cambridge Univ. Press, Cambridge,  
 2698 UK., 2007.
- 2699 267. Song C, Huang B, Ke L., Modeling and analysis of lake water storage changes  
 2700 on the Tibetan Plateau using multi-mission satellite data *Remote Sens Environ* 135:25-  
 2701 35 doi:10.1016/j.rse.2013.03.013, 2013.
- 2702 268. Spada G., Stocchi P., SELEN: A Fortran 90 program for solving the “sea-level  
 2703 equation”, *Computers & Geosciences* 33.4, 538-562, 2007.
- 2704 269. Spada G., Galassi G., New estimates of secular sea level rise from tide gauge  
 2705 data and GIA modelling, *Geophysical Journal International* 191(3): 1067-1094, 2012.
- 2706 270. Spada G., Galassi G., Spectral analysis of sea level during the altimetry era,  
 2707 and evidence for GIA and glacial melting fingerprints, *Global and Planetary Change*  
 2708 143:34-49, 2016.
- 2709 271. Spada G., Glacial isostatic adjustment and contemporary sea level rise: An  
 2710 overview. *Surveys in Geophysics* 38(1), 153-185, 2017.
- 2711 272. Spracklen DV, Arnold SR, Taylor CM., Observations of increased tropical  
 2712 rainfall preceded by air passage over forests *Nature* 489:282-U127  
 2713 doi:10.1038/nature11390, 2012.
- 2714 273. Sutterley T.C., Velicogna I., Csatho B., van den Broeke M., Rezvan-Behbahani  
 2715 S., Babonis G., Evaluating Greenland glacial isostatic adjustment corrections using  
 2716 GRACE, altimetry and surface mass balance data *Environmental Research Letters*  
 2717 9(1), 014004, 2014.
- 2718 274. Strassberg, G., B. R. Scanlon, and M. Rodell, Comparison of seasonal  
 2719 terrestrial water storage variations from GRACE with groundwater-level

- 2720 measurements from the High Plains Aquifer (USA), *Geophys. Res. Lett.*, 34, L14402,  
 2721 doi:10.1029/2007GL030139, 2007.
- 2722 275. Swenson S, Wahr J., Monitoring the water balance of Lake Victoria, East  
 2723 Africa, from space *J Hydro* 370:163-176, 2009.
- 2724 276. Syed, T. H., J. S. Famiglietti, D. P. Chambers, J. K. Willis, and K. Hilburn,  
 2725 Satellite-based global ocean mass balance reveals water cycle acceleration and  
 2726 increasing continental freshwater discharge, 1994–2006, *Proc. Natl. Acad. Sci. U. S.*  
 2727 *A.*, 107, 17,916–17,921, doi:10.1073/pnas.1003292107, 2010.
- 2728 277. Stammer, D., and Cazenave A., *Satellite Altimetry Over Oceans and Land*  
 2729 *Surfaces*, 617 pp., CRC Press, Taylor and Francis Group, Boca Raton, New York,  
 2730 London, ISBN: 13: 978-1-4987-4345-7, 2018.
- 2731 278. Tamisiea, M. E., Leuliette, E. W., Davis, J. L., and Mitrovica, J. X.,  
 2732 Constraining hydrological and cryospheric mass flux in southeastern Alaska using  
 2733 space-based gravity measurements. *Geophysical Research Letters*, 32:L20501,  
 2734 doi:10.1029/2005GL023961, 2005.
- 2735 279. Tamisiea M.E., Ongoing glacial isostatic contributions to observations of sea  
 2736 level change, *Geophysical Journal International* 186(3):1036, 2011.
- 2737 280. Tapley, B. D., S. Bettadpur, J. C. Ries, P. F. Thompson, and M. M. Watkins,  
 2738 GRACE measurements of mass variability in the Earth system. *Science* 305, 503–505,  
 2739 doi: 10.1126/science.1099192, 2004.
- 2740 281. Tapley, B. D., Bettadpur, S., Ries, J. C., Thompson, P. F., and Watkins, M. M.,  
 2741 The Gravity Recovery and Climate Experiment; Mission Overview and Early Results,  
 2742 *Geophys. Res. Lett.*, Vol. 31, No. 9, L09607, 10.1029/2004GL019920, 2004.
- 2743 282. Taylor, R. G., B. Scanlon, P. Döll, M. Rodell, R. van Beek, Y. Wada, L.  
 2744 Longuevergne, M. LeBlanc, J. S. Famiglietti, M. Edmunds, L. Konikow, T. R. Green,  
 2745 J. Chen, M. Taniguchi, M. F. P. Bierkens, A. MacDonald, Y. Fan, R. M. Maxwell, Y.  
 2746 Yechieli, J. J. Gurdak, D. M. Allen, M. Shamsudduha, K. Hiscock, P. J.-F. Yeh, I.  
 2747 Holman and H. Treidel, Groundwater and climate change, *Nature Clim. Change*, 3,  
 2748 322-329, doi:10.1038/nclimate1744, 2013.
- 2749 283. Thompson, P.R., and M.A. Merrifield, A unique asymmetry in the pattern of  
 2750 recent sea level change, *Geophys. Res. Lett.*, 41, 7675-7683, 2014.
- 2751 284. Tiwari, V. M., J. Wahr, and S. Swenson, Dwindling groundwater resources in  
 2752 northern India, from satellite gravity observations, *Geophys. Res. Lett.*, 36, L18401,  
 2753 doi:10.1029/2009GL039401, 2009.
- 2754 285. Tourian M, Elmi O, Chen Q, Devaraju B, Roohi S, Sneeuw N, A spaceborne  
 2755 multisensor approach to monitor the desiccation of Lake Urmia in Iran *Remote Sens*  
 2756 *Environ* 156:349-360, 2015.
- 2757 286. Turcotte DL, Schubert G, *Geodynamics*. Cambridge University Press,  
 2758 Cambridge, 2014.
- 2759 287. Valladeau, G., J. F. Legeais, M. Ablain, S. Guinehut, and N. Picot, “Comparing  
 2760 Altimetry with Tide Gauges and Argo Profiling Floats for Data Quality Assessment  
 2761 and Mean Sea Level Studies.” *Marine Geodesy* 35 (sup1):42–60.  
 2762 <https://doi.org/10.1080/01490419.2012.718226>, 2012.
- 2763 288. Van Den Broeke, M. R., Enderlin, E. M., Howat, I. M., Kuipers Munneke, P.,  
 2764 Noël, B. P. Y., Van De Berg, W. J., Van Meijgaard, E. & Wouters, B., On the recent  
 2765 contribution of the Greenland ice sheet to sea level change. *The Cryosphere*, 10, 1933-  
 2766 1946, 2016.
- 2767 289. Velicogna, I., Increasing rates of ice mass loss from the Greenland and  
 2768 Antarctic ice sheets revealed by GRACE. *Geophysical Research Letters*, 36, 2009.

- 2769 290. van der Werf GR et al., Global fire emissions and the contribution of  
 2770 deforestation, savanna, forest, agricultural, and peat fires (1997-2009) *Atmos Chem*  
 2771 *Phys* 10:11707-11735 doi:10.5194/acp-10-11707-2010, 2010.
- 2772 291. Van Dijk, A. I. J. M., L. J. Renzullo, Y. Wada, and P. Tregoning, A global  
 2773 water cycle reanalysis (2003–2012) merging satellite gravimetry and altimetry  
 2774 observations with a hydrological multi-model ensemble, *Hydrol. Earth Syst. Sci.*, 18,  
 2775 2955-2973, doi:10.5194/hess-18-2955-2014, 2014.
- 2776 292. Velicogna, I., Sutterley, T. C., & Van Den Broeke, M. R., Regional  
 2777 acceleration in ice mass loss from Greenland and Antarctica using GRACE time-  
 2778 variable gravity data. *Geophysical Research Letters*, 41(22), 8130-8137, 2014.
- 2779 293. Velicogna, I., Wahr, J., Measurements of Time-VARIABLE Gravity Show Mass  
 2780 Loss in Antarctica, *Science*, DOI: 10.1126/science.1123785, 2006.
- 2781 294. von Schuckmann, K., J.-B. Sallée, D. Chambers, P.-Y. Le Traon, C. Cabanes,  
 2782 F. Gaillard, S. Speich, and M. Hamon, Monitoring ocean heat content from the current  
 2783 generation of global ocean observing systems, *Ocean Science*, 10, 547-557,  
 2784 DOI:10.5194/os-10-547-2012, 2014.
- 2785 295. von Schuckmann K., Palmer M.D., Trenberth K.E., Cazenave A., D. Chambers,  
 2786 Champollion N. et al., Earth's energy imbalance: an imperative for monitoring, *Nature*  
 2787 *Climate Change*, 26, 138-144, 2016.
- 2788 296. Vörösmarty CJ, Sahagian D, Anthropogenic disturbance of the terrestrial water  
 2789 cycle *Bioscience* 50:753-765 doi:10.1641/0006-  
 2790 3568(2000)050[0753:Adottw]2.0.Co;2, 2000.
- 2791 297. Voss, K. A., J. S. Famiglietti, M. Lo, C. de Linage, M. Rodell, and S. C.  
 2792 Swenson, Groundwater depletion in the Middle East from GRACE with implications  
 2793 for transboundary water management in the Tigris-Euphrates-Western Iran region,  
 2794 *Water Resour. Res.*, 49, doi:10.1002/wrcr.20078, 2013.
- 2795 298. Watson, Christopher S., Neil J. White, John A. Church, Matt A. King, Reed J.  
 2796 Burgette, and Benoit Legresy, "Unabated Global Mean Sea-Level Rise over the  
 2797 Satellite Altimeter Era." *Nature Climate Change* 5 (6):565–68.  
 2798 <https://doi.org/10.1038/nclimate2635>, 2015.
- 2799 299. Wada, Y., L. P. H. van Beek, C. M. van Kempen, J. W. T. M. Reckman, S.  
 2800 Vasak, and M. F. P. Bierkens, Global depletion of groundwater resources, *Geophys.*  
 2801 *Res. Lett.*, 37, L20402, doi:10.1029/2010GL044571, 2010.
- 2802 300. Wada, Y., Modelling groundwater depletion at regional and global scales:  
 2803 Present state and future prospects, *Surv. Geophys.*, 37, 419-451, doi:10.1007/s10712-  
 2804 015-9347-x, Special Issue: ISSI Workshop on Remote Sensing and Water Resources,  
 2805 2017.
- 2806 301. Wada, Y., L. P. H. van Beek, and M. F. P. Bierkens, Nonsustainable  
 2807 groundwater sustaining irrigation: A global assessment, *Water Resour. Res.*, 48,  
 2808 W00L06, doi:10.1029/2011WR010562, Special Issue: Toward Sustainable  
 2809 Groundwater in Agriculture, 2012a.
- 2810 302. Wada, Y., L. P. H. van Beek, F. C. Sperna Weiland, B. F. Chao, Y.-H. Wu, and  
 2811 M. F. P. Bierkens, Past and future contribution of global groundwater depletion to sea-  
 2812 level rise, *Geophys. Res. Lett.*, 39, L09402, doi:10.1029/2012GL051230, 2012b.
- 2813 303. Wada, Y., M.-H. Lo, P. J.-F. Yeh, J. T. Reager, J. S. Famiglietti, R.-J. Wu, and  
 2814 Y.-H. Tseng, Fate of water pumped from underground causing sea level rise, *Nature*  
 2815 *Clim. Change*, doi:10.1038/nclimate3001, early online, 2016.
- 2816 304. Wada, Y., Reager, J. T., Chao, B. F., Wang, J., Lo, M. H., Song, C. and  
 2817 Gardner, A. S., Satellite Altimetry-Based Sea Level at Global and Regional Scales. In



- 2818 *Integrative Study of the Mean Sea Level and Its Components* (pp. 133-154). Springer  
 2819 International Publishing, 2017.
- 2820 305. Wang J, Sheng Y, Hinkel KM, Lyons EA, Drained thaw lake basin recovery on  
 2821 the western Arctic Coastal Plain of Alaska using high-resolution digital elevation  
 2822 models and remote sensing imagery *Remote Sensing of Environment* 119:325-336  
 2823 doi:10.1016/j.rse.2011.10.027, 2012.
- 2824 306. Wang J, Sheng Y, Tong TSD, Monitoring decadal lake dynamics across the  
 2825 Yangtze Basin downstream of Three Gorges Dam *Remote Sensing of Environment*  
 2826 152:251-269 doi:10.1016/j.rse.2014.06.004, 2014.
- 2827 307. Wahr J., Nerem R.S. and Bettadpur S.V., The pole tide and its effect on  
 2828 GRACE time-variable gravity measurements: Implications for estimates of surface  
 2829 mass variations. *Journal of Geophysical Research: Solid Earth* 120(6), 4597-4615,  
 2830 2015.
- 2831 308. Watkins, M. M., Wiese, D. N., Yuan, D.-N., Boening, C., and Landerer, F. W.,  
 2832 Improved methods for observing Earth's time variable mass distribution with GRACE  
 2833 using spherical cap mascons. *Journal of Geophysical Research (Solid Earth)*,  
 2834 120:2648–2671, doi:10.1002/2014JB011547, 2015.
- 2835 309. Wenzel M and J Schroter, Reconstruction of regional mean sea level anomalies  
 2836 from tide gauges using neural networks, *J. Geophys. Res.* 115.  
 2837 doi:10.1029/2009JC005630, 2010.
- 2838 310. Wessem J. M. et al., Modeling the climate and surface mass balance of polar  
 2839 ice sheets using RACMO2, part 2: Antarctica, *the Cryosphere*, 2017.
- 2840 311. Whitehouse, P. L., et al., A new glacial isostatic adjustment model for  
 2841 Antarctica: calibrating the deglacial model using observations of relative sea-level and  
 2842 present-day uplift rates, *Geophys Journal Int.*, 190, 1464-1482, 2012.
- 2843 312. Wiese, D. N., Landerer, F. W., and Watkins, M. M., Quantifying and reducing  
 2844 leakage errors in the JPL RL05M GRACE mascon solution. *Water Resources*  
 2845 *Research*, 52:7490–7502, doi:10.1002/2016WR019344, 2016.
- 2846 313. Willis, J.K., Chambers, D.T., Nerem, R.S., Assessing the globally averaged sea  
 2847 level budget on seasonal to interannual time scales, *J. Geophys. Res.* 113, C06015.  
 2848 doi:10.1029/2007JC004517, 2008.
- 2849 314. Wisser, D., S. Frolking, S. Hagen, and M. F. P. Bierkens, Beyond peak  
 2850 reservoir storage? A global estimate of declining water storage capacity in large  
 2851 reservoirs, *Water Resour. Res.*, 49, 5732–5739, doi:10.1002/wrcr.20452, 2013.
- 2852 315. Whitehouse, P.L., Bentley M.J., Milne G.A., King M.A., Thomas I.D., A new  
 2853 glacial isostatic adjustment model for Antarctica: calibrating the deglacial model using  
 2854 observations of relative sea-level and present-day uplift rates, *Geophysical Journal*  
 2855 *International* 190, 1464-1482, 2012.
- 2856 316. Wiese, D., Yuan, D., Boening, C., Landerer, F. & Watkins, M., JPL GRACE  
 2857 Mascon Ocean, Ice, and Hydrology Equivalent Water Height RL05M. 1 CRI Filtered,  
 2858 Ver. 2, PO. DAAC, CA, USA. Dataset provided by Wiese in Nov/Dec 2017, 2016.
- 2859 317. Wijffels, S. E., D. Roemmich, D. Monselesan, J. Church, J. Gilson, Ocean  
 2860 temperatures chronicle the ongoing warming of Earth. *Nature Climate Change*,  
 2861 (6),116-118, bdoi:10.1038/nclimate2924, 2016.
- 2862 318. Wöppelmann, G., and M. Marcos, Vertical land motion as a key to  
 2863 understanding sea level change and variability, *Rev. Geophys.*, 54, 64–92,  
 2864 doi:10.1002/2015RG000502, 2016.
- 2865 319. Wouters, B., Bamber, J. Á., Van den Broeke, M. R., Lenaerts, J. T. M., &  
 2866 Sasgen, I., Limits in detecting acceleration of ice sheet mass loss due to climate  
 2867 variability. *Nature Geoscience*, 6(8), 613, 2013.

- 2868 320. Wouters, B., R. E. M. Riva, D. A. Lavallée, and J. L. Bamber, Seasonal  
 2869 variations in sea level induced by continental water mass: First results from GRACE,  
 2870 *Geophys. Res. Lett.*, 38(3), doi:10.1029/2010GL046128, 2011.
- 2871 321. Wouters, B., Chambers, D. & Schrama, E., GRACE observes small-scale mass  
 2872 loss in Greenland. *Geophysical Research Letters*, 35, 2008.
- 2873 322. Wu X., Heflin M.B., Schotman H., Vermeersen B.L., Dong D., Gross R. S.,  
 2874 and .others, Simultaneous estimation of global present-day water transport and glacial  
 2875 isostatic adjustment. *Nature Geoscience* 3.9: 642-646, 2010.
- 2876 323. Yi, S., Sun, W., Heki, K., and Qian, A., An increase in the rate of global mean  
 2877 sea level rise since 2010. *Geophysical Research Letters*, 42:3998–4006,  
 2878 doi:10.1002/2015GL063902, 2015.
- 2879 324. Zawadzki L., M. Ablain, Estimating a drift in TOPEX-A Global Mean Sea  
 2880 Level using Poseidon-1 measurements, paper presented at the OSTST meeting, La  
 2881 Rochelle, 2016.
- 2882 325. Zhang G, Yao T, Xie H, Kang S, Lei Y, Increased mass over the Tibetan  
 2883 Plateau: From lakes or glaciers? *Geophys Res Lett*:1-6, 2013.
- 2884 326. Zemp, M., Frey, H., Gärtner-Roer, I., Nussbaumer, S., Hoelzle, M., Paul, F.,  
 2885 Haeberli, W., Denzinger, F., Ahlstrøm, A., Anderson, B., Bajracharya, S., Baroni, C.,  
 2886 Braun, L., Cáceres, B., Casassa, G., Cobos, G., Dávila, L., Delgado Granados, H.,  
 2887 Demuth, M., Espizua, L., Fischer, A., Fujita, K., Gadek, B., Ghazanfar, A., Hagen, J.,  
 2888 Holmlund, P., Karimi, N., Li, Z., Pelto, M., Pitte, P., Popovnin, V., Portocarrero, C.,  
 2889 Prinz, R., Sangewar, C., Severskiy, I., Sigurdsson, O., Soruco, A., Usubaliev, R. and  
 2890 Vincent, C., Historically unprecedented global glacier decline in the early 21st  
 2891 century, *Journal of Glaciology*, 61, 745–762, 2015.
- 2892 327. Zwally, J.H., J. Li, J.W. Robbins, J.L. Saba, D.H. Yi, A.C. Brenner, 2016,  
 2893 Mass gains of the Antarctic ice sheet exceed losses, *Journal of Glaciology*, 61, 1013-  
 2894 1036, doi :10.3189/2015JoG15J071.
- 2895
- 2896